Czech Technical University in Prague

Faculty of Nuclear Sciences and Physical Engineering

DISSERTATION

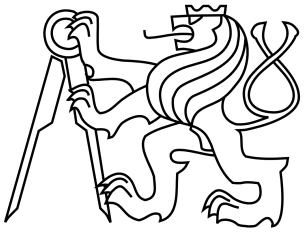

Prague 2020 Mgr. Michal Kozák

Czech Technical University in Prague

Faculty of Nuclear Sciences and Physical Engineering

DISSERTATION

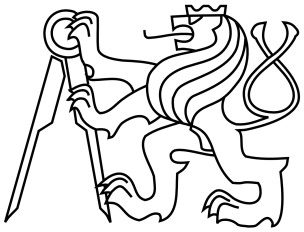

Robustness of Turing system

Prague 2020 Mgr. Michal Kozák

Bibliografický záznam

Autor	Mgr. Michal Kozák, České vysoké učení technické v Praze, Fakulta jaderná a fyzikálně inženýrská, Katedra matematiky
Název práce	Robustnost Turingova systému
Studijní program	Aplikace přírodních věd
Studijní obor	Matematické inženýrství
Školitel	Doc. Ing. Václav Klika, Ph.D., České vysoké učení technické v Praze, Fakulta jaderná a fyzikálně inženýrská, Katedra matematiky
Školitel specialista	Ing. Matěj Tušek, Ph.D., České vysoké učení technické v Praze, Fakulta jaderná a fyzikálně inženýrská, Katedra matematiky
Akademický rok	2019/2020
Počet stran	79
Klíčová slova	Turingův system, robustnost, advekce, prostorová závislost

Bibliographic Entry

Author	Mgr. Michal Kozák, Czech Technical University in Prague, Faculty of Nuclear Sciences and Physical Engineering, Department of Mathematics
Title of Dissertation	Robustness of Turing system
Degree Programme	Application of Natural Sciences
Field of Study	Mathematical Engineering
Supervisor	Doc. Ing. Václav Klika, Ph.D., Czech Technical University in Prague, Faculty of Nuclear Sciences and Physical Engineering, Department of Mathematics
Supervisor specialist	Ing. Matěj Tušek, Ph.D., Czech Technical University in Prague, Faculty of Nuclear Sciences and Physical Engineering, Department of Mathematics
Academic Year	2019/2020
Number of Pages	79
Keywords	Turing system, robustness, advection, spatial dependency.

Abstract

Předložená práce se zabývá Turingovým modelem, jedním z mechanismů popisující samovolné prostorové uspořádání, a jeho robustností, tj. mírou závislosti výsledných vzorů na malých změnách vstupních parametrů. Jsou provedeny dvě studie zkoumající vliv 1) konstatní advekce a 2) prostorové závislosti v kinetice. V prvním případě jsou uvažovány dva systémy mimo Turingův režim doplněné o několik okrajových podmínek; pro analýzu stability je využito Sturm-Liouvilleovy teorie a podmínky pro vznik vzoru prostřednictvím velikostí oblasti poháněné nestability jsou odvozeny z explicitního výpočtu vlastních čísel. V druhém případě je analyzován reakčně-difuzní systém s parametrem lineárního členu kinetiky ve formě skokové funkce a podmínky pro vznik vhodných vzorů jsou získány pomocí pečlivé kombinace analytických a numerických přístupů. Je ukázáno, že i malá advekce může podstatně změnit chování systému, a to v závislosti na volbě okrajových podmínek; a že přítomnost stability nebo nestability v Turingových modelech je lokální vlastností pro po částech konstantní parametry kinetik, a tedy že malá prostorová závislost tohoho tvaru významně nemění vznik Turingových vzorů.

The presented work deals with the Turing model, one of the possible mechanisms describing the self-organisation, and its robustness, i.e. the amount of a dependence of the resulting patterns on small changes in input parameters. Two studies examining the effect of 1) constant advection and 2) spatial dependence in kinetics are performed. In the former case, two systems outside Turing regime supplemented by various boundary conditions are considered, the Sturm-Liouville theory is incorporated into stability analysis and the conditions for pattern emergence via domain-size-driven instability are deduced from explicit calculation of eigenvalues. In the latter case, the reaction-diffusion system with a step function as a parameter at linear kinetics term is analysed and conditions for plausible pattern formation are obtained using a careful combination of analytical and numerical approaches. It is shown that even a small advection can substantially change a behaviour of the system depending on the choise of the boundary conditions; and that the presence of stability or instability in Turing models is a local property for piece-wise constant kinetic parameters and thus, small spatial dependency of such a form does not significantly change the emergence of Turing patterns.

Notation

$\mathbb{R}; \mathbb{R}_+$	real numbers; positive real numbers
$\mathbb{N}; \mathbb{N}_0$	natural numbers; natural numbers with zero
$L^2(\Omega)$	the space of all quadratic integrable functions with support inside Ω
Ω	an open connected bounded subset of $\mathbb{R}^n$
$\partial(\Omega)$	the boundary of Ω
L	positive constant representing the scale of the domain
$\dot{()}$	(time) derivative
$()'; ()''; ()^{(k)}$	(spatial) derivative of the first; the second; the k-th order
∂_i	(spatial) partial derivative with respect to i-th of element
∇, Δ	spatial gradient, Laplace operator
$\mathcal{L}$	linear spatial differential operator operates inside Ω
$\mathcal{L}^{bc}$	linear spatial differential operator operates on $\partial(\Omega)$
$\mathcal{L}_{dV}$	particular linear differential operator defined on the page 26
u, v	real functions representing morphogen concentrations
d, d_1, d_2	non-negative constants representing diffusion rates
V	non-negative constant representing advection rate
Pe	Péclet number defined as $\mathrm{Pe} = lV/d$
f, g	real functions representing kinetics
$\mathbf{A}, \mathbf{B}, \mathbf{J}$	matrices
$\operatorname{tr}\mathbf{B}$	a trace of a matrix $\mathbf{B}$
$\det\mathbf{B}$	a determinant of a matrix $\mathbf{B}$
$\operatorname{Re}\lambda$	the real part of the complex number λ
$T1 - T4$	standard conditions for Turing pattern formation, see section 1.1.1
κ_k	k-th eigenvalue of the Laplacian with Neumann's BC
C_k	k-th hyperbola, see section 1.1.3
C_E	an envelope of C_k for all $k \in \mathbb{N}$, see section 1.1.3
$\hat{u}$	prostorově konstantní, stacionární řešení
ξ	point from interval $(0, L)$ representing the point of a step
$\Theta_\xi(x); h(x)$	step functions at the point ξ with the step size 1; or s
$T1^L - T4^L$	modified Turing conditions belonging to interval $(0, \xi)$
$T1^R - T4^R$	modified Turing conditions belonging to interval (ξ, L)

Contents

1 Introduction

This thesis deals with an analysis of the Turing system, one of the models describing self-organizing pattern formation. Examples of such behaviour can be found in the thermal expansion of Rayleigh-Bénard convection cells [84], chemical reaction network dynamics as with the Belousov-Zhabotinskii system [99], cell responses to chemotactic gradients [32], mechanical stimuli of chemical reactions [37, 39, 36] and models of development [64, 101], the field of the biggest author's personal interest, therefore many other references of these examples shall be seen in the text below.

The fundamental model was proposed by Alan Turing in 1952 [101]. Based on his intuition he considered two substances, which diffuse and interact with themselves (so called morphogens) and showed that a small fluctuation of their concentration about a steady state (a ground state) together with diffusion can cause significant differences in the concentrations along the spatial axis, and hence spatially non-homogenous steady states can emerge, which we will call patterns. Mathematically, this symmetry breaking mechanism was described as a diffusion-driven instability (DDI) of the steady state in a reaction-diffusion system (RD system).

For many decades, one of the biggest issues for the plausibility of a Turing system in biological development was the lack of identification of morphogens and confirmation the molecular details matching those required for patterning. However, recent studies show extensive promise, as observed in experiments with pigmentation of zebrafish [42], formation of patterns on the skin of the wild cats [56], digit patterning [79], hair follicle localization [35, 74] or a tumor vascularization [9]. Furthermore, there is in addition the suggestion that the combination of Wolpert's positional information hypothesis [109, 29] with the Turing mechanism may increase the applicability of both [62, 17].

Many Turing systems have been proposed and analysed, both analytically and using numerical experiments. The majority of these studies consider only two species. Exemplar models are the Gierer-Meinhardt model [25] describing the growth of the hydra, the Schnakenberg model [89] describing a chemical reaction exhibiting limit-cycle behaviour or the Thomas model [97] describing chemical reaction of oxygen and uric acid in the presence of the enzyme uricase. Although many properties of the Turing system (in which this study is concerned mostly) are common independently on the choice of reaction kinetics, a particular choice determines the characteristics of resulting pattern and can influence the evolution behaviour. For a review of some models, see [64].

Since the Turing model is a very simple one, a more complex version should be taken into account if real phenomena are wanted to be described. Among possible extensions which can be incorporated are, for instance, a consideration of more substances, the effect of cross-diffusion, spatial dependency in parameters or a reformulation of the problem in a stochastic manner. Note that in many cases, the original idea of Turing patterns must be modified due to the change of settings. Usually, the correction is made following biological or chemical motivation, for instance domain-growth-induced patterns used in [40]. A short list of examples of the Turing model generalizations shall be seen in section 1.2.

In the context of the Turing model, the term "robustness" is associated with a dependency of resulting pattern on the initial state (mathematically represented by initial conditions). The robustness represents meeting the basal request from real situations that the qualitative characteristics of the resulting patterns are the same independently on small fluctuations in initial conditions, diffusion coefficients or kinetics parameters [58]. To illustrate this, the offspring of a jaguar should have coat with spots and rosettes but not stripes as a tiger; or that the number

of fingers on man's hand should always be five. Historically, the lack of robustness belonged among crucial failures of Turing models [2]. This type of robustness is also known as structural stability with an extreme but interesting example in ODEs being the universal differential equation – an equation possesing a solution arbitrarily close to any reasonable function [5].

An immediate question is which extensions of the Turing model affect the robustness of pattern formation. Examples of positive effects that have been studied include considering Dirichlet boundary conditions [15], growing domains [10, 57] or the addition of time delays [21]. Note that all there phenomena seem to be naturally present in real world, we can hypothesise that the observed lack of robustness of the Turing model can be linked to the simplicity of the original model.

On the other hand, there might be (neglected) phenomena which diminish robustness. When modelling the real world we try to include such processes which affect the described processes the most. Regardless of the degree of complexity of the events we model, there will always be a part of them that we neglect. The question then arises as whether these neglected phenomena do not affect the behaviour of the mathematical model more than would be apparent from the observations. That is, if the formulated model is sufficiently robust with respect to the choise of neglected phenomena.

For instance, in a model with more equations than two, we would investigate whether the results of a model with less number of equations do not differ substantially, and thus if the results of an analysis of the simpler model is suitable even for the original one. Or, if we consider a chemical process and the motion of molecules be the same in all directions as opposed to a situation where a small preference of one direction (represented by advection) is present; it depends on the analysis of the influence of a small advection, whether the zero preference for particle motion is realistic or not in the corresponding reaction networks.

The thesis consists of two main topics, one analysing the influence of small advection on pattern formation (section 2) and one investigating the classical Turing system but with a small spatial dependency in kinetics in the form of a step function (section 3). Since both procedures are already published [41, 47], the main purpose of this text is to be a guide to these articles. Besides giving an overview of the main results and conclusions, some interesting features are emphasized and a few technical parts are elucidated in a more detail. Certainly, we begin with introduction to the Turing system especially for readers who are not familiar with its concept and a short list of model generalizations is outlined there (section 1). Moreover, the alternative mechanism to the Turing's one, the domain-size-driven instability, is introduced and the relevant features of the Sturm-Liouville theory are presented in the same section; both suitable for general Turing systems as shown for the case of the system with advection in section 2.

In section 2 we consider a reaction-diffusion system with advection and we explore the effect of small advection on pattern formation. Since original Turing's diffusion-driven instability is not suitable for this case, an alternative mechanism, the domain-size-driven instability, is used instead. We will investigate whether patterning may occur for 1) two species with equal transport (i.e. a diffusion and an advection rate) and 2) one immobile and one mobile species with equal transport; both systems are supplemented by various boundary conditions and outside classical Turing regime. The Sturm-Liouville theory is used for stability analysis. The core of the procedure lies in the computation of eigenpairs of the appropriate systems and in following evalution of instability conditions; therefore this part is outlined in more detail than in the original article [41].

The influnce of a small spatial dependency in the form of a step function in the linear term of kinetics on Turing pattern formation is investigated in section 3. The whole procedure roughly follows the stability analysis of the classical Turing case, but with solving significant difficulties. The core of this section lies in the careful assembly of partilucar steps containing mixture of analytic and numeric approaches into a valid procedure to obtain usable conditions for formation of plausible patterns. Therefore, the concept of the whole procedure is presented in slightly different way than in the original article [47], the linear stability analysis is outlined for the case of spatial dependency in all kinetics terms (necessary for the application to the non-linear case) and a technical computation of the stationary solution to the linear problem is added to appendix (although not all possible final forms are explicitely outlined due to their high vastness).

The final section contains conlusions of obtained results separately for both examined cases, following by the consequences of obtained results for the robustness of the Turing system. The thesis is supplemented by already mentioned appendices and by a list of references.

1.1 Brief overview of Turing model

This subsection is designated for readers who are not familiar with the Turing system, since the thesis often refers to the model's analysis and its basic features. Such presentation can be found in many textbooks, theses or as introduction in many articles [64, 46, 111].

Turing's idea of reactable and diffusible chemicals can be mathematically described by a system of semi-linear parabolic differential equations (reaction-diffusion system). Let us consider the smallest system, where the diffusion-driven instability can be described, system formed by two equations

$$\begin{aligned} \partial_t u &= d_1 \Delta u + f(u,v) \\ \partial_t v &= d_2 \Delta v + g(u,v) \end{aligned} \qquad \text{in } (0,\infty)\times\Omega, \tag{1}$$

where u, v are morphogen concentrations, Ω is a bounded domain in $\mathbb{R}^N$ with $N \in \mathbb{N}$ spatial dimension, $\partial_t := \frac{\partial}{\partial t}$ denotes time partial derivative, Δ designates the Laplace operator (a sum of all N second spatial derivatives), f, g represents the reaction kinetics and d_1, d_2 are positive constants representing diffusion coefficients. This relation can be illustratively reformulated in the manner that in every point of the domain a change in the amount of morphogen in very small time interval (partial time derivative) corresponds to the sum of the amount of morphogens produced (or destroyd) by a reaction (reaction kinetics) and the amount of incoming or outcoming from the neighbourhood (the Laplace operator).

We asume that kinetics possesses a critical point (u^*, v^*), i.e. constansts fulfilling

$$f(u^*, v^*) = 0 \qquad \text{and} \qquad g(u^*, v^*) = 0, \tag{2}$$

and thus (u^*, v^*) is a steady solution (steady state) of system (1) without diffusion ($d_1, d_2 = 0$). This solution is an equilibrium, the original (ground) state from which we will initiate our considerations. If there is more than one solution to (2), only one of them is taken into account.

The equations (1) are supplemented by the boundary conditions (BC), i.e. conditions for morphogens on the boundary of Ω, most often by the homogeneous Neumann BC (zero-flux)

$$\frac{\partial u}{\partial n} = \frac{\partial v}{\partial n} = 0 \quad \text{on } \partial\Omega \tag{3}$$

and finally with initial conditions (IC) at time 0 describing the initial state of the system from which the system initiates:

$$u(0) = u_0, \quad v(0) = v_0 \quad \text{in } \Omega.$$

The most preferred BC are the mentioned one, homogeneous Neumann BC, i.e.

$$\frac{\partial u}{\partial n} = a, \qquad \frac{\partial v}{\partial n} = b \qquad \text{on } \partial\Omega$$

when taking $a = 0$ and $b = 0$. Not only they are suitable for various mathematical operations, they also have a very nice physical interpretation – the flow through the boundary is zero, nothing can leave or enter the domain and therefore such systems are described as independent of external phenomena.

Other frequently used BC conditions are Dirichlet BC

$$u = a, \qquad v = b \qquad \text{on } \partial\Omega,$$

which correspond to a situation when the concentration of substances on the boundary is prescribed to the specific value a, b. Particularly the choice $a, b = 0$, homogeneous Dirichlet BC, describes the setup with a border completely inhospitable to the population and the population dies out there. However, homogeneous Dirichlet BC are most often used in combination with a system that already has the steady state shifted to zero, while the physical explanation for such conditions is a homeostasis, when the system tries to keep the equilibrium (u^*, v^*) at the boundary, somehow advantageous for the particular object. For more examples and discussion of boundary conditions, see section 2.

The initial conditions are an important component of the whole process, since the solution of the evolution system (1) directly depends on it. However, due to the assumption of robustness stated in Introduction, the effect on the form of patterns should not be crucial, if the model will be assembled properly. In the following text, if it is not stated otherwise, the initial conditions (particularly functions u_0, v_0) describe small perturbation of concentrations about the equilibrium state (u^*, v^*) (meaning a small random noise) and they will not be explicitly mentioned.

Finally, at least a note about spaces of considered functions should be mentioned. Since we take many motivations from biological and chemical environment, it is natural to use mostly the "classical" formulation, i.e. we assume that all functions are smooth enough. The problem can be formulated even in weak sense (in [46, 52]) and it will be used implicitly using strong theorems (stability of PDE) or rarely explicitly, only if some special mathematical problem will be discussed (discussion about orthonormal bases of L^2 in section 2 or a linearization about a step function in a weak sense in section 3).

1.1.1 Fundamental conditions of Turing instability

We assume the existence of a stationary, spatially homogenous solution (u^*, v^*)[1] representing the original steady state (ground state, no-pattern), which is stable with respect to reaction kinetics (i.e. to the system without an effect of diffusion; $d_1 = 0, d_2 = 0$). And as Turing proposed, if the diffusion is added to the system, its effect will destabilize the homogeneous steady state and the consequent evolution will pass it to another steady state, mostly a spatially inhomogeneous one, the pattern. Mathematically, the ground state (u^*, v^*) is unstable with

[1] i.e. the solution to system (2) fulfilling selected boundary conditions

respect to system (1) with diffusion (ie. $d_1 > 0$, $d_2 > 0$). Alternatively, the whole idea can be paraphrased that the steady state is stable with respect to spatially homogeneous perturbations, but unstable with respect to spatially inhomogeneous ones.

Hence, for determination if DDI occurs, it is sufficient to analyse (linear) stability of the steady state. To proceed, we consider a system describing perturbation about the steady state obtained from (1) by substitution $\bar{u} = u - u^*$, $\bar{v} = v - v^*$ and Taylor expansion of kinetics about (u^*, v^*):

$$\begin{aligned} \partial_t \bar{u} &= d_1 \Delta \bar{u} + b_{11}\bar{u} + b_{12}\bar{v} + n_1(\bar{u}, \bar{v}) \\ \partial_t \bar{v} &= d_2 \Delta \bar{v} + b_{21}\bar{u} + b_{22}\bar{v} + n_2(\bar{u}, \bar{v}) \end{aligned} \qquad \text{in } (0, \infty) \times \Omega, \tag{4}$$

where $\mathbf{B} = (b_{ij})_{i,j=1,2}$ is Jacobian matrix of (f, g) and n_1, n_2 non-linear residues; supplemented with Neumann boundary conditions. From now on, we analyse stability of steady state $[0, 0]$ with respect to system (4).

First, stability of the homogenous steady state of system (4) with $d_1 = 0, d_2 = 0$ is required. Such system can be regarded as a continuum number of couples of ordinary differential equations ODE, since there is no spatial connection among the couples, therefore the conditions for (asymptotic) stability follow from standard theorem about linearized stability of ODEs, which requires that all eigenvalues of the matrix $\mathbf{B}$ have negative real parts.

The eigenvalues of the matrix $\mathbf{B}$ can be computed as the roots of the equation

$$\det(\mathbf{B} - \lambda \mathbf{I}) = 0,$$

which yields

$$\lambda_{1,2} = \frac{\operatorname{tr} \mathbf{B} \pm \sqrt{(\operatorname{tr} \mathbf{B})^2 - 4(\det \mathbf{B})}}{2},$$

and requiring negativity of their real parts is equivalent to require both following conditions

$$\operatorname{tr} \mathbf{B} = b_{11} + b_{22} < 0, \tag{T1}$$

$$\det \mathbf{B} = b_{11}b_{22} - b_{12}b_{21} > 0. \tag{T2}$$

To illustrate the meaning of these conditions see the example based on predator-prey model from [45] (the part of cited text about a limit cycle is not useful for our problem, but it is showed for completeness of the author's idea):

The condition $b_{11} + b_{22} < 0$ means that at least one of the substances u, v needs to be self-inhibiting in the sense that its 'diagonal' partial derivative be negative; such a substance has a stabilizing effect on itself near the equilibrium. This is self-evident in the predator-prey context.

Let us consider a region with an even distribution of two species, a predator and its prey, in an equilibrium state. If we, for simplicity, consider food to be the only factor affecting the occurrence of either species, then an equilibrium state means that the number of the prey is just sufficient to support the predators whose number, on the other hand, is just right to prevent a growth in the prey numbers. Imagine now that we do not allow for diffusion-like phenomena (a local increase in concentration in one place at the cost of a decline in its vicinity or vice versa) due to migration, i.e. we only admit uniform distributions of the species. Then it seems intuitive that the equilibrium state would be unstable if a slight (homogeneous) increase in the number of either of the species stimulated further growth. For instance, if the food capacity of the region for the prey was (hypothetically) infinite, any increase in its number would also enhance its reproduction; a greater number of the prey could in turn support more predators

and this spiral could continue forever, resulting in an ever-growing number of both species. That is certainly not what stability looks like. Note that nature has taken care of this in its very principles since an increase (decrease) in the occurrence of predators at an equilibrium state means more (less) competition, so the predator count will usually (but not always) be self-inhibiting rather than self-activating in the vicinity of an equilibrium state. But let us ignore this for a little while longer, for instance assuming that the sudden increase in prey concentration was large enough to neutralize the effect of competition (for food, at least). One could still be a little uneasy about the fact that we ignored the cross-dependence: the effect of predation. It seems reasonable that if the predator reproduced faster than the prey, even an infinite food capacity would not mean a boundless growth of the prey concentration: the predator-to-prey ratio would sooner or later increase beyond some threshold value, causing a reduction of the prey. Insufficient food supplies would then result in a drop in the predator numbers and one could naively hope that the equilibrium state might be restored. However, this would lead to a limit cycle rather than stability given that the non-linear terms do admit cyclic behaviour. We can observe such dynamics even if the predator is indeed self-inhibiting. An example of such dynamics is provided by the Lotka-Volterra model (see chapter 3.1 in [Murray2007]). Had we wished to avoid this discussion, instead of a predator-prey model we could have considered a parasite-host interaction or a chemical reaction, where two self-activating reactants intuitively seem more inclined to a chain reaction (e.g. nuclear fission) than towards stability. Based on all these examples, it (hopefully) appears intuitively clear that the self-inhibiting effects need to prevail for two substances/species to establish a stable equilibrium, in accordance with the first condition in (T1), (T2).

For exploring linearized stability of system (4) with diffusion, i.e. stability of system

$$\begin{aligned} \partial_t \bar{u} &= d_1 \Delta \bar{u} + b_{11}\bar{u} + b_{12}\bar{v} \\ \partial_t \bar{v} &= d_2 \Delta \bar{v} + b_{21}\bar{u} + b_{22}\bar{v} \end{aligned} \qquad \text{in } (0,\infty)\times\Omega, \tag{5}$$

we exploit the fact that the Laplace operator $-\Delta$ on a bounded (convex regular) domain with Neumann BC (even with Dirichlet or Robin BC) is self-adjoint, non-negative and its eigenvectors form an orthonormal basis of $\mathcal{L}^2(\Omega)$ (the space of all quadratic integrable functions with support inside Ω). Particularly, denoting (κ_n, φ_n) the eigenpair for $n \in \mathbb{N}$, the eigenvalues can be ordered to infinite (but countable) non-decreasing sequence

$$0 = \kappa_0 < \kappa_1 \leq \kappa_2 \leq \kappa_3 \leq \ldots$$

Since system (5) is linear, it is convenient to look for solutions in the separated form

$$\vec{u}(x,t) = A(x)B(t).$$

Then first, for fixed x the function in the form $B(t) = \mathrm{e}^{\lambda t}$ for some λ will solve the system with respect to t, and second, since we have orthonormal basis $\{\varphi_k\}_{k=0}^{+\infty}$, the function can be expanded into Fourier series and in summary, we are looking for solution of the form

$$\vec{u}(x,t) = \mathrm{e}^{\lambda t} \sum_{k=0}^{\infty} c_k \varphi_k(x). \tag{6}$$

Note that this standard approach disregards any transition effects like transient growth, which is not governed by spectral properties of the operator corresponding to system (5). The reason

for this is that we do not view the whole problem as a single linear operator, which would be typically non-normal and subsequently transition effects would be frequent. However, it can be shown that for such behaviour to be significant fine parameter tuning is required [104](e.g. significant transient growth, which is captured by non-linearities and hence invalidates linear stability based on the spectrum of the Laplacian). After substitution to system (5) we get

$$\lambda\varphi_k = \mathbf{B}\varphi_k - \mathbf{D}\kappa_k\varphi_k.$$

Since we are searching for a non-trivial solution of the later equation, we obtain the conditions for that to occur, the so-called dispersion relation:

$$\det\left(\lambda\mathbf{I} - \mathbf{B} + \mathbf{D}\kappa_k\right) = 0, \tag{7}$$

which can be rewritten into quadratic equation

$$0 = \lambda^2 + (\kappa_k d_1 + \kappa_k d_2 - b_{11} - b_{22})\lambda + H_d(\kappa_k) \tag{8}$$

with a denotation

$$H_d(\kappa_k) = (\kappa_k d_1 - b_{11})(\kappa_k d_2 - b_{22}) - b_{12}b_{21} \tag{9}$$

and the resulting root λ_k[2] is of the form

$$\lambda_{1,2}^{(k)} = \frac{b_{11} + b_{22} - (d_1 + d_2)\kappa_k \pm \sqrt{[b_{11} + b_{22} - (d_1 + d_2)\kappa_k]^2 - 4H_d(\kappa_k)}}{2}, \tag{10}$$

Due to the form (6) of $\vec{u}$, there should exists at least one real part of λ in order to small perturbations about ground state to grow fast enough to form a inhomogeneous steady state.[3] Evidently, $\kappa_k(d_1 + d_2)$ is positive and together with condition (T1) yields

$$b_{11} + b_{22} - (d_1 + d_2)\kappa_k < 0$$

and therefore $\lambda_2^{(k)}$ has negative real part for all k. Consequently, we need at least one $k \in \mathbb{N}$ fulfilling $\operatorname{Re}\lambda_1^{(k)} > 0$, thus from (10) we need validity of

$$H_d(\kappa_k) = d_1 d_2(\kappa_k)^2 - (b_{11}d_2 + b_{22}d_1)\kappa_k + b_{11}b_{22} - b_{12}b_{21} < 0. \tag{11}$$

From the expression (11) the following necessary condition is clearly obtained

$$b_{11}d_2 + b_{22}d_1 > 0. \tag{T3}$$

The fourth Turing condition, and the sufficient condition for (11), arises from the analysis of H_d. Clearly, this function is convex, therefore we demand that the function at the point of its minimum reaches below zero. Thus, step by step, we find a minimum:

$$0 = \frac{\partial H_d(\kappa)}{\partial\kappa} = 2\kappa d_1 d_2 - (b_{11}d_2 + b_{22}d_1),$$

[2] λ_k is for $k \in \mathbb{N}_0$ an eigenvalue of the operator corresponding to system (5). That can be shown straightforwardly using proper formulation in weak sense, for instance outlined in [46]. Both approaches are based on theory of semigroups, the exponential solution here or the Theorem about stability in linear reaction-diffusion system there.

[3] Or using Theorem about stability mentioned above, at least one eigenvalue λ_k should have positive real part for the steady state be unstable.

$$\kappa_{\min} = \frac{b_{11}d_2 + b_{22}d_1}{2d_1d_2}.$$

Note that $\kappa_{\min} > 0$ holds. The value of H_d at the minimum is

$$H_d(\kappa_{\min}) = -\frac{(b_{11}d_2 + b_{22}d_1)^2}{4d_1d_2} + b_{11}b_{22} - b_{12}b_{21}.$$

Thus we get the last Turing condition

$$\frac{(b_{11}d_2 + b_{22}d_1)^2}{4d_1d_2} > \det B. \tag{T4}$$

1.1.2 Corollaries of essential Turing conditions

Now we continue with some corollaries. Combining conditions (T1) and (T3) we obtain that b_{11} and b_{22} have opposite signs and diffusion coefficients d_1, d_2 are forced to be unequal. In addition with (T2) we get that $b_{12}b_{21}$ is negative, therefore b_{12} and b_{21} are forced to have opposite signs. In summary, the matrix $\mathbf{B}$ can be (except for relabelling of morphogens) only one of two following forms

$$\begin{pmatrix} + & - \\ + & - \end{pmatrix}, \qquad \begin{pmatrix} + & + \\ - & - \end{pmatrix}.$$

In the former case, u is denoted as an activator (its positive values cause an increase of both morphogens) and v as in inhibitor (its positive values cause their decrease), whereas the latter case is called positive feedback or substrate depletion. In both cases, from Turing conditions follows $d_1 < d_2$. For illustration let us again mention some examples from [45]:

In the predator-prey context, as long as we still consider food to be the decisive element, the latter scenario with $g_u > 0$ means that u represents prey in a region sufficiently abundant in vegetation ($f_u > 0$) whereas v stands for a predator competing for food (and/or, quite commonly, territory; since $g_v < 0$). In this case an inhomogeneous steady state thus requires that the dispersion of the predator be faster than that of the prey. A local (random) increase in prey density is autocatalytic but also stimulates local growth of predator numbers. Due to faster dispersion, predators will then spread into neighbouring areas (before the prey does) where increased predator density will cause a drop in both predator and prey count ($f_v, g_v < 0$) so the pattern we expect should display a correlation between high (and low) densities of both the predator and its prey. Note that if it were the prey that dispersed faster, no such pattern would be possible; instead we could expect to see a 'wave' of increased prey density spreading from our 'source' area, stimulating a wave of predator abundance that would (possibly) restore the equilibrium.

On the other hand, the former case with $f_v > 0$ makes v count the prey while u counts the predator. We can assume that an increase in the prey numbers results in food shortages as $g_v < 0$, whereas higher concentration of predators has a positive effect on their hunting and/or reproductive effectiveness ($f_u > 0$). This time the prey needs to disperse faster for anything 'interesting' to happen. Now a locally higher prey density will provoke a local rise in predator numbers as well ($f_v > 0$), but will eventually drop naturally due to insufficient food supplies as well as predation ($g_v, g_u < 0$). Given that these effects are strong enough (note that the impact of cross-dependence has to 'prevail' since $|f_v g_u| > |f_u g_v|$ by (T1), (T2)), it will drop well below the equilibrium level, inducing net influx of prey from the vicinity of the 'outbreak'. If the flow of the prey is fast enough, it will provide the higher number of

predators with sufficient amount of food so that the latter can persist at their above-equilibrium concentration. On the contrary, predator count will drop in the neighbouring areas due to the outflow of prey, which in turn enables the prey to achieve higher density there. The flux of the prey from this high density areas into low prey/high predator density territories takes care of the self-inhibiting effect of increased prey numbers (e.g. local food shortages). Hence, we expect that high predator density should correlate with low prey concentration and vice versa should a permanent pattern be established. Note that in both cases the self-inhibiting species had to diffuse faster than the self-activating one. This is one of the well-known features of DDI and is often referred to as short-range activation, long-range inhibition.

In the biological setting, diffusion could not be experimentally controlled as easily as it is required in DDI and therefore, such process lacks a direct biological motivation. A following observation is useful. Consider the domain of the form $\Omega = L\Omega_0$ with positive L representing a scaling of the initial domain Ω_0. Using substitution $\tilde{x} = x/L$ in system (1) we obtain

$$\begin{aligned} \partial_t u &= \frac{d_1}{L^2}\tilde{\Delta}u + f(u,v) \\ \partial_t v &= \frac{d_2}{L^2}\tilde{\Delta}v + g(u,v) \end{aligned} \qquad \text{in } (0,\infty)\times\Omega_0, \tag{12}$$

where $\tilde{\Delta}$ represents Laplace operator with respect to spatial variable $\tilde{x}$. Hence we can see that the diffusion coefficients scale as $1/L^2$ and therefore DDI can be interpreted as a self-organisative process with the pattern emergence driven by the size of the domain.

Thus the analysis of the pattern emergence by diffusion can be expressed as a finding a critical size of the domain, starting from which the system can exhibit a pattern, while the steady state remains homogeneous for smaller domains than the critical one. Such explanation of the DDI can be more familiar to the biological applications, and alternatively, it gives us a reformualtion not dependent on specified movement of substances and hence, more suitable for system with additions effect (f.e. with advection). Let us denote this procedure as domain-size-driven instability, which will be discussed in more detail in section 1.2.2.

1.1.3 Turing space and areas of stability or instability

Now, we are concerned, for which parameters the problem (4) exhibits Turing patterns. The set of such parameters is called the Turing space. A particular choice of the parameters can be motivated by an application (for instance biologically motivated coefficients of kinetics, as a, b in section 3) or by a need for further analysis (diffusion coefficients). Let us describe the latter case in more detail and describe the set of diffusion coefficients (d_1, d_2) for which system (4) fulfils Turing conditions. Notation follows [52, 46].

Following the derivation of Turing conditions involving the diffusion coefficients it is clear that the state-changing condition is a sign of $H_d(\kappa_k)$ defined in (9). If we denote the set of diffusion coefficients vanishing the term $H_d(\kappa_k)$ in following way

$$C_k = \left\{ [d_1, d_2] \in \mathbb{R}^2_+ \colon d_2 = \frac{1}{\kappa_k}\left(\frac{b_{12}b_{21}}{d_1\kappa_k - b_{11}} + b_{22}\right)\right\}$$

and if we plot the set in a graph with d_1, d_2 on the axes (see fig. 1), we see that C_k are parts of hyperbolas with asymptotes $d_1 = \frac{b_{11}}{\kappa_k}$ and $d_2 = \frac{b_{22}}{\kappa_k}$. It can be shown that all hyperbolas have

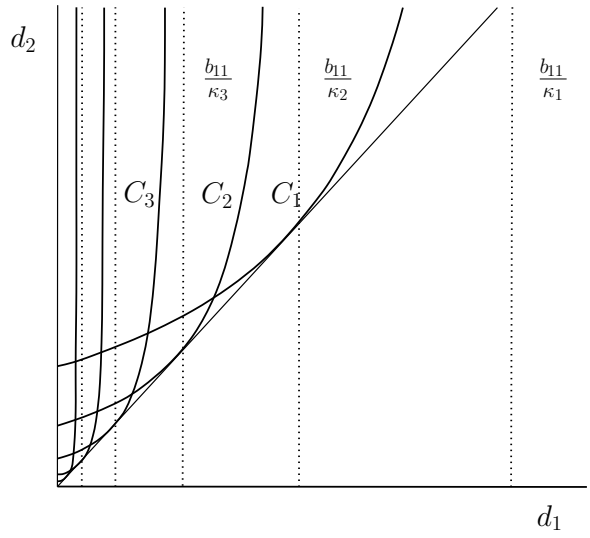

Figure 1: An illustration of hyperbolas C_k representing a critical diffusion coefficients for which the steady state (u^*, v^*) changes a stability with respect to full system (4) with appropriate tangent lines. Furthemore, $\mathbb{R}^2_+$ is divided by the "envelope" C_E into an area of stability (the right-bottom section) and an area of instability (the left-top section).

one common tangent line [68]

$$d_2 = \frac{b_{11}b_{22} + 2\sqrt{-b_{12}b_{21}\det B}}{b_{11}^2} d_1.$$

Further characteristics follow from the properties of eigenvalues of Laplacian (eigenvalues κ_k can be ordered into a countable infinite non-decreasing sequence): from the form of C_k follows that C_k tends to $d_1 = 0$ for $k \to +\infty$. Moreover, if the eigenvalues of Laplacian are simple, i.e. $\kappa_k < \kappa_{k+1}$ for every $k \in \mathbb{N}_0$ (for instance, this applies to $\Omega \subset \mathbb{R}$), then $C_j \neq C_k$ for all unequal $j, k \in \mathbb{N}$. If, on the contrary, the eigenvalue κ_k has multiplicity $j_k \in \mathbb{N}$, then following holds

$$C_{k-1} \neq C_k = C_{k+1} = \cdots = C_{k+j_k-1} \neq C_{k+j_k}.$$

The beauty of hyperbolas C_k can be summarized into the following proposition: Assume that conditions put on matrix $\mathbf{B}$ (T1), (T2), (T3) hold. Then for every $\lambda_1^{(k)}$ ($\lambda_2^{(k)}$ has negative real part) fulfilling (7) holds:

$$\begin{cases} \operatorname{Re}\lambda_1^{(k)} < 0 & \text{for } (d_1, d_2) \in \mathbb{R}^2_+ \text{ lying to the right from } C_k, \\ \lambda_1^{(k)} = 0 & \text{for } (d_1, d_2) \in \mathbb{R}^2_+ \text{ lying on } C_k, \\ \operatorname{Re}\lambda_1^{(k)} > 0 & \text{for } (d_1, d_2) \in \mathbb{R}^2_+ \text{ lying to the left from } C_k. \end{cases}$$

Finally, if we denote the "envelope" of all hyperbolas as a set

$$C_E = \left\{ [d_1, d_2] \colon d_1 \in \mathbb{R}_+,\ d_2 = \min\left\{ z \colon [d_1, z] \in \bigcup_{k \in \mathbb{N}} C_k \right\} \right\}, \tag{13}$$

then C_E separates the $\mathbb{R}^2_+$ into two parts, an area of stability, i.e. the set of $(d_1, d_2) \in \mathbb{R}^2_+$ for which the steady state is stable; and an area of instability, the Turing space if (T1), (T2), (T3) hold, the set of the pairs of diffusion coefficients for which the steady state is unstable.

From this point, an investigation which pairs of diffusion coefficients there exists at least one non-homogeneous stationary solution can start. Even unbounded connected sets of such point can be found using Global Rabinowitz Theorem [78] or its generalized version [105]. For instance, the existence of such set was shown in the area of instability for Thomas model [46] or even generally in the area of stability [53]. Such results, together with appropriate a priori estimates of steady solutions, are helpful for determining where the steady states of numerical evolution experiments or the expectations of real applications could be located.

1.2 Generalizations of Turing system

Since the original Turing model is very simple, many investigations of the reaction-diffusion system with various additional phenomena were made for the sake of achieving an exhibition of wider class of resulting solutions or due to an increase of robustness of the whole problem. First in this section, a few such investigations of some generalizations of the Turing system are listed, with a particular emphasize on the main topics of this thesis – the influence of advection and spatial dependency.

Secondly, an alternative mechanism to Turing's one, which we call domain-size-driven instability, is introduced. Such mechanism follows more affable description using domain growth as a force to change a stability and can be used for some enhanced reaction-diffusion systems. And finally, to proceed with the stability analysis in some diverse model extensions, the use of Sturm-Liouville theory can be adopted, therefore we briefly present the relevant features of Sturm-Liouville theory. This theory will be used to analyse domain-size-driven instability for the system with advection in section 2.

1.2.1 Examples of generalized Turing systems

The author is aware of his abilities that he is not capable to cover such a topic in a full comprehensive range. Rather than that, this list could serve as a stepping-stone for a study of the particular fields.

Growing domains. As was presented in section 1.1.2, the main biological interpretation of diffusion-driven instability is a transformation of change in diffusion to change in a domain size, and thus taking a domain size only as a bifurcation parameter [70, 10]. Such formulation of the domain growth influence on the condition of the Turing instability neglects the system non-autonomy. In spite of that, it was observed in [10] that exponential growth causes so-called doubling effect – regular periodic doubling of the number of peaks with high and low concentrations following the exponential domain growth. Such process decreases dependency of the resulting pattern on the initial conditions and thus increasing robustness of the model.

The proper description was firstly solved numerically, for instance the growth of teeth [50] or stripe formation in juvenile fish Pomacanthus [73] using exponential growth, lately it was analysed explicitly considering domain growth dynamics [11, 57]. The various growth functions (linear, logistic and exponential) are analysed with diverse effects on conditions on pattern emergence, in some cases the patterns are called domain-growth-induced, since the growth alone is the force to create such patters and it is shown that such patterns can be obtained even for system of type activator-activator. In [40] the investigation of the effect of the domain growth is more thorough considering the history of the evolution following the growth. Then, the conditions to pattern formation are weakened even more, although their high complexity

requires numerical evaluation. Note that on faster growing domains, there is a total breakdown of the continuum description as modes of arbitrarily high wavenumber modes are excited, leading to the growth of fluctuations on smaller scales than that of an individual and thus a loss of self-consistency of the modelling assumptions.

Let us note here the opposite effort. Motivated by a regeneration of flatworm, authors in [108] sought such an adjustment of the Turing system so that the pattern scales proportionally to the size of the domain. Similar phenomenon can be seen observing the emergence of exactly the same number of five fingers independently of their distal growth [17].

Three and more equations. The motivation for utilization of more than two substances are apparent and was mentioned even in Turing's original work [101]. In every biological or chemical process, there is a vast of substances, from which only the most important are necessary to take account. And certainly, if we consider more than two equations, the results of the mathematical model will corresponds more to the reality. However, with regards to analysis procedures, its difficulty increases with higher number of equations n, which coincides most with the eigenvalue problem of n-dimensional Hurwitz matrix. Necessary and sufficient conditions for the Turing instability for n equations were derived in [88].

It is clear that requirements on characteristics of substances are relaxed in the presence of more than two substances. Even for the case of three equations, which is the case often used in applications nowadays [79], it is not necessary that 1) all diffusion coefficients have to be non-zero (an immobile substance) [35, 43, 59] or 2) non-equal [60] or 3) steady states are only solutions (travelling waves [18]). It follows that substances involved in the mechanism are not only identified as pure activators or pure inhibitors, however still, the substances can be divided in two logical subsystems interacting like activator or inhibitor, respectively; thoroughly analysed in [88] or in [60].

With the possibility of interactions of more substances, the system is applicable particularly to situations where two main substances were not clearly determined as in the development of cyanobacterial organism [14] or digit patterning [79].

A particular example of three considered equations is a realistic situatino of two interacting substances, where one of them has two distinct stages, different in diffusion or reaction rates – for instance if the substance can bind to a substrate and hence has zero diffusion rate [43, 65]. From the point of view of the robustness issue it follows that not only mobile substances (ones with nontrivial diffusion) should be taken account, but also the immobile ones since such additional interaction can crucially change the behaviour of the system [35].

Equations with time delays. A possible biological motivation for introducing a time delay in reaction diffusion systems is the situation when reaction delays are particularly important when dealing with the production of crucial proteins as a cascade of time-consuming biological processes must occur in order for a single protein to be produced [111]. Delayed equations are difficult to analyse even in the case of ordinary equations, therefore numerical simulations are mainly performed while being supported by an analysis of a specific system. In [21, 93] it is illustrated that behaviour of linearized system does not coincide with the full system, thus linearized stability does not reflect the behaviour of the full model. Numerical experiments indicate that except for a higher sensitivity to initial conditions, there is not much to say generally about the behaviour of the full system as the behaviour differs according to various kinetics. For instance, a prolongation of the evolution time is caused in the case of Schnakenberg kinetics resulting in solutions without any oscillations [21], whilst in the cases

of various versions of Gierer-Meinhardt kinetics the delay can cause oscillations or blow-ups, depending on the exact combinations of kinetics and sub-cellular dynamics [93]. For these two kinetics cases the conditions for different mechanism of pattern formation are obtained [116] and the influence of growing domains is studied [21, 91, 92] – the effect of growth is not so significant in comparison to undelayed models, the lack of robustness with respect to initial conditions preserves and if, in addition, the growth contains the delay itself, the possibilities of behaviour seems to be unbounded [92].

Cross-diffusion. Non-triviality of non-diagonal diffusion coefficients D_{jk} models a dependence of a movement of the first substance on a concentration of the second one. This phenomenon can be seen as a bacterial chemotaxis [100], development of vegetation patterns [94], in plasma physics [13] or predator-prey models [103]. The analysis of Turing patterns was carried out for constant D_{jk} first [1, 44, 103], then for more relevant diffusion coefficients satisfying

$$D_{jk}(\mathbf{u}) \to 0 \quad \text{as} \quad u_k \to 0, \quad k \neq j$$

since there can be no flux of species k if concentration of such species falls to zero (i.e. $u_k \equiv 0$) [51]. The resulting solutions of the Turing instability are not only stationary solutions ([98] for more general diffusion coefficients), but even travelling fronts [23, 22].

Stochasticity. Original (deterministic) model assumes continuity of species concentration (rather than a number of species), which decently approximate real situation with high number of species representatives (e.g. molecules). But that is not the case in all real systems, some populations have numbers in dozens, for instance the number of the lac repressor in *Escherichia coli*, which is involved in the regulation of gene expression, is only in 10-30 [30, 113]. In such a situation, the incorporation of stochastic processes is necessary. According to [113, 102] two different types of biological noise can be considered (and a proposed model should follow it) 1) intrinsic, emanating from random fluctuations in the population interactions, and 2) extrinsic (environmental), describing noise with source from outside. A great progress was achieved in the latter case using approximations or simulations of appropriate stochastic differential equations (see [24] for a review). As presented in [102], standard approach in the former case begins with a transcription of the problem into a chemical master-equation formalism and follows by a derivation of a Fokker-Planck equation, which is then analysed. Stochastic Turing patterns, which is a designation of steady solutions of appropriate stochastic system and induced by diffusion or noise, are studied e.g. in [6, 115, 4].

Stochasticity is such a result-changing phenomenon that large focus lies on its effect on the generalized system presented above. Therefore we can find studies of interaction between stochasticity and growing domains [112, 110], cross-diffusion [19], delays [114] or more equations [14]. For clear and summarizing comparison of stochastic and deterministic Turing system, see [90, 7].

An **advection** flux is readily motivated in eco-hydrological systems, such as river based ecological systems [31, 96]. Additional examples include the impact of a bias in the random motility underlying diffusion, which is relevant for systems where the species are at larger scale than molecular; a further example at the cellular scale concerns the Turing systems in synthetic biology, with interacting cells and signalling molecules together with a background chemotactic field [16]. One can also consider the introduction of background flows to chemical Turing systems, such as the CIMA-starch reaction [69, 8], or even chemical systems that may

not exhibit a Turing instability given the weaker self-organisation constraints. As a further prospective biological example, we mention the proposed Turing instability hypothesised for the interaction of tumour growth factors [9], which would also be subject to a weak advective flux due to interstitial flows.

As a final example, if we subject Fick's law of diffusion to scrutiny, specifically if we derive the evolution equations for reacting mixtures using the framework of non-equilibrium thermodynamics [34, 54, 38], we observe that advection can appear as a consequence of chemical reactions among constituents. Particularly, from a careful formulation of mixture theory of fluids it follows that chemical kinetics need not only be driven by chemical affinity – as would be the case with Fick's or Maxwell-Stefan law – but can also be driven by diffusive flux [75]. This not only entails that it is consistent for diffusion to drive chemical reactions but that the converse also applies and chemical reactions alone can consistently induce diffusion flux, with gradients of chemical reactions thus inducing advective terms. Hence introducing and studying a new concept of self-orchestrated pattern formation in the presence of flows, induced by gradients of chemical reactions, is thermodynamically consistent and thus not unreasonable with analogous remarks also applying for thermal gradients in chemical systems.

The idea of considering advection as a generalisation of the Turing instability dates back to the work of Rovinsky and Menzinger who, inspired by the Belousov-Zhabotinsky reaction, proposed the so-called differential-flow-induced chemical instability (DIFICI) for self-organisation [81, 82]. Here, advection is added to the Turing reaction diffusion system in the same manner as in section 2; with DIFICI, there is a resulting non-steady chemical instability outside the Turing regime, characterised by periodic travelling waves [83, 88, 86]. This mechanism was also generalised by Satnoianu et. al. [88] to systems possessing both differential flow and diffusive transport, analogously to the need for differential diffusion in the Turing instability, which led to the prospect of the so-called flow-and-diffusion structures. Other studies on the stability of reaction-diffusion and advection systems have also been conducted by Nekhamkina, Sheintuch and Smagina [66, 67, 95].

Results in these previous studies are typically based on results for infinite domains. However, Reddy and Trefethen [80] have pointed out that spectral analysis on the real line may be of limited value in the reaction-diffusion-advection problem since the similarity of the spectrum on infinite and finite domains, and thus the similarity in stability behaviour, is dependent on the magnitude of the Péclet number, $\mathrm{Pe} = LV/d$, which we shall explicitly explore. Hence for large domains there is not a continuous transition of spectral properties from infinite domains and thus we cannot rely on insight from the previous studies on infinite domains, especially given our interest in diverse choices of boundary conditions, as further confirmed by studies of Davies [12].

An addition of **Spatial dependency** into parameters of the Turing system could break a high degree of periodicity of the resulting patterns and such system could be capable to capture key features of many real systems, where the patterns significantly change in space as illustratively shown in [20]. The Gierer-Meinhardt model [25], for example, is originally based on a source with a gradient; even Turing in his paper [101] discussed that "Most of an organism, most of the time, is developing from one pattern into another, rather than from homogeneity into a pattern", suggesting significant spatial dependency may be initially present before the impact of the Turing instability.

There are many examples of spatial irregularity in patterns where wavelength variation is manifested and such heterogeneous pattern modulation has a crucial impact on both the real

product and self-organization process. For instance a distribution of mouse or cat whiskers [74], alternating thin and thick stripes of Lionfish [72], emergence of fingers [17] or the heterogeneity of the environment in landscape ecology [77]. Such ubiquitous examples emphasize the critical importance of studying the impact of heterogeneity and its effects on the properties of self-organizing systems.

However, the standard procedure of stability analysis is not easily extendable to the case with spatially dependent coefficients as, for example, a homogeneous steady state does not exist in general given spatially dependent kinetics. Probably the most well understood effect of heterogeneity comes from the shadow limit in Gierer-Meinhardt kinetics using spike solutions [33, 107, 106] but note that this requires the applicability of the infinite or arbitrarily large diffusion coefficient in one of the species. Further the case of spatially dependent diffusion coefficient was analysed in [3] with a step function representing the dependency. Heterogeneity in the reaction kinetics was analysed numerically [72] and limited analytical progress in stability analysis has been established with spatial dependency in the kinetics. Examples include asymptotically small, spatially dependent, linear gradients of morphogen source [26, 28, 27], a cosine spatial dependence in a coefficient of the kinetics [61] and a step function, independent of morphogen concentration, added to the kinetics [71]. Finally, very recently a rather general stability analysis with spatial heterogeneity in reaction kinetics was successfully proposed including a transition from one pattern into another [49]. Essentially the only situation this approach using WKBJ asymptotics does not cover is when the spatial oscillations are rapid, which is a fundamental feature induced by the jump discontinuity in the kinetics that we consider in section 3.

1.2.2 Domain-size-driven instability

At the end of section 1.1.2 it was shown that the assessment of critical diffusion coefficients, with which system (1) exhibits Turing patterns, can be reformulated into a finding of critical domain sizes. Thus, instead of the principle based on a change of diffusion rates, the cause of pattern formation can be described as a domain growth. This idea is discussed in more detail in this section with the goal of a statement of an alternative mechanism to Turing's one, which can be moreover used in more general settings.

Note that the Turing instability is typically highly constrained with demanding constraints for its presence, as documented by Murray [64], and hence there are often only small regions of parameter space where an instability may occur. As one example, for the standard model based on diffusive transport, the system must be stable in the absence of diffusion, otherwise the homogeneous steady state is destabilised by homogeneous perturbations on a small domain. Given the common choice of zero diffusive flux conditions, which do not preclude spatially homogeneous perturbations, this becomes a stringent constraint on the kinetics.

However, consider a model generalisation, even a weak one, which entails that a homogeneous perturbation cannot be supported, for example due to incompatibility with the boundary conditions. Then homogeneous perturbations are prevented from growing on small domains by the boundary conditions without appeal to a stability constraint and hence there is stability on small domains without the usual restrictions on the kinetics of the standard Turing instability. In turn, the extent of the constraints on the model kinetics and transport that are required for self-organisation can be substantially less stringent and yet the mechanism can still exhibit domain size control, with a bifurcation to instability if the domain size becomes too large.

One example of such a model generalisation from a standard Turing model with zero diffusive

flux boundary conditions is the imposition of a Dirichlet boundary condition that is consistent with the homogeneous steady state. In turn, this suggests that a simple change in the boundary conditions may substantially weaken the constraints required for domain size controlled self-organisation to occur. As a second example, consider the presence of advection, where the flux of a species u is $-d\nabla u + \mathbf{V}u$, and d is the diffusion coefficient, with $\mathbf{V}$ the advective velocity field. The flux condition consistent with a homogeneous steady state value of u^* is given by

$$\mathbf{n} \cdot (-d\nabla u + \mathbf{V}u) = \mathbf{n} \cdot \mathbf{V}u^*$$

and this does not support a homogeneous perturbation away from the steady state. Hence even weak advection may substantively alter the conditions for system self-organisation.

Final constraint is that the most unstable mode(s) are of bounded wavenumber, so that there is a well-defined spatial lengthscale of the patterns induced by the instability; if this is violated then patterning occurs on arbitrarily small lengthscales, which results in the breakdown of the continuum approximation [35].

Thus in summary, we propose that **domain-size-driven instability** can be characterised by: one, the existence of a critical size below which the system is stable to small perturbations and above which instability generally occurs (which particularly means that the stability of homogeneous steady state with respect to homogeneous pertubrations is required if such perturbations can be supported); two, the existence of only a finite number of unstable modes as otherwise the continuum description would break down (and no structure in spatial organisation would appear except salt-and-pepper pattern).

As was already discussed, such mechanism shows to be identical with Turing's idea in the classical case with Neumann BC, but 1) in the case of Dirichlet BC they differ, particularly the former mechanism gives an enlargement of the Turing space; and 2) the proposed mechanism can be suitable even for some generalizations of classical case where these two concept diverge, for example with a presence of small advection, as presented in section 2.

1.2.3 Sturm-Liouville theory

Let us consider the following problem that is a generalisation of a reaction diffusion system considered by Turing for morphogenesis. For simplicity we restrict the analysis to a 1D domain $\Omega = [0, L]$ and consider

$$\frac{\partial}{\partial t}\begin{pmatrix} r(x)\ u \\ r(x)\ v \end{pmatrix} = \begin{pmatrix} d_1\ \mathcal{L}(u) \\ d_2\ \mathcal{L}(v) \end{pmatrix} + r(x)\begin{pmatrix} f(u,v) \\ g(u,v) \end{pmatrix},$$

where $r(x)$ is a non-zero function, $\mathcal{L}u := \frac{\partial}{\partial x}\left(p(x)\frac{\partial}{\partial x}u\right)$ is a linear operator with d_1, d_2 two positive diffusion constants and u, v represent the concentrations of two morphogens.

First, note that stability analysis of a stationary solution that is spatially dependent is beyond the scope of this paper. Hence, we restrict ourselves to the standard case when the existence of a homogeneous stationary solution u^*, v^* is required. Thus

$$\mathbf{0} = \begin{pmatrix} f(u^*, v^*) \\ g(u^*, v^*) \end{pmatrix}.$$

With y representing u or v, and y^* the homogeneous steady state value, we consider the above equations subject to inhomogeneous Robin boundary conditions,

$$\alpha_1 y(0) + \alpha_2 y'(0) = \alpha_1 y^*,\ \beta_1 y(L) + \beta_2 y'(L) = \beta_1 y^*,$$
$$\alpha_i \in \mathbb{R},\ \beta_i \in \mathbb{R},\ |\alpha_1| + |\alpha_2| > 0,\ |\beta_1| + |\beta_2| > 0.$$

The spatial operator $\mathcal{L} = \frac{\partial}{\partial x}\left(p(x)\frac{\partial}{\partial x}\right)$ with the homogeneous analogues of these boundary conditions is a fully self-adjoint Sturm-Liouville operator. Hence, for the function space $L^2([0, L])$ its set of its eigenfunctions form a complete basis set of orthonormal square-integrable functions.

To proceed in our consideration of Sturm Liouville theory, let γ_n solve

$$(\mathcal{L}\gamma_n)(x) = \frac{\partial}{\partial x}\left(p(x)\frac{\partial}{\partial x}\gamma_n(x)\right) = -\lambda_n r(x)\gamma_n(x)$$

where n labels the eigenpair $(\lambda_n, \gamma_n(x))$ of the operator. With the expansion

$$\begin{pmatrix} u \\ v \end{pmatrix} = \begin{pmatrix} u^* \\ v^* \end{pmatrix} + \begin{pmatrix} \alpha \\ \beta \end{pmatrix}, \quad \begin{pmatrix} \alpha \\ \beta \end{pmatrix} = \sum_n \mathbf{w}_n \gamma_n, \quad \mathbf{w}_n = \begin{pmatrix} w_n^1 \\ w_n^2 \end{pmatrix}$$

we take advantage of the fact that the set of γ_n form an othonormal basis of $L^2([0, L])$. Linearising about $(u^*, v^*)^T$, and therefore assuming $|\alpha| \ll 1$, $|\beta| \ll 1$, yields

$$\sum_n r(x)\gamma_n(x)\left(\dot{\mathbf{w}}_n + \begin{pmatrix} d_1\lambda_n w_n^1 \\ d_2\lambda_n w_n^2 \end{pmatrix} - \mathbf{J}\mathbf{w}_n\right) = \mathbf{0},$$

where $\mathbf{J} = (J_{ij})_{i,j\in\{1,2\}}$ denotes the Jacobian of the reaction kinetics evaluated at the homogeneous steady state, (u^*, v^*), with the dot $\dot{()}$ denoting a time derivative. As the eigenfunctions γ_n form an orthonormal basis, we have that

$$\dot{\mathbf{w}}_n = -\left(\lambda_n \begin{pmatrix} d_1 & 0 \\ 0 & d_2 \end{pmatrix} - \mathbf{J}\right)\mathbf{w}_n$$

and hence the dispersion relation is given by

$$\det\left(\sigma_n \mathbf{I} + \lambda_n \begin{pmatrix} d_1 & 0 \\ 0 & d_2 \end{pmatrix} - \mathbf{J}\right) = 0,$$

where its roots σ_n correspond to eigenvalues of the linearised system. These consequently determine the linear stability of the homogeneous steady state. Potential difficulties in dealing with this additional generality compared to textbook analyses [64] are, of course, subsumed in the eigenvalue problem of the Sturm-Liouville operator $\mathcal{L}$.

To illustrate the above ideas in a concrete setting, we consider an example with heterogeneous transport, with $p(x) = e^{-x}$ and $r(x) = 1$, as would be relevant for an effective theory of interacting chemical species in a porous medium with an exponential spatial dependence in the porosity. Then, in particular, we have

$$\frac{\partial}{\partial t}\begin{pmatrix} u \\ v \end{pmatrix} = \begin{pmatrix} d_1\frac{\partial}{\partial x}(e^{-x}\frac{\partial}{\partial x}u) \\ d_2\frac{\partial}{\partial x}\left(e^{-x}\frac{\partial}{\partial x}v\right) \end{pmatrix} + \begin{pmatrix} f(u,v) \\ g(u,v) \end{pmatrix}$$

with $\frac{\partial}{\partial x}u = \frac{\partial}{\partial x}v = 0$ at $x \in \{0, L\}$. The corresponding eigenfunctions of the spatial operator $\mathcal{L} = \frac{\partial}{\partial x}\left(e^{-x}\frac{\partial}{\partial x}\right)$ with the zero-flux boundary conditions are

$$\gamma_n(x) = e^{x/2}\Big[Y(0, 2\sqrt{\lambda_n})J(1, 2\sqrt{\lambda_n}e^{x/2}) - J(0, 2\sqrt{\lambda_n})Y(1, 2\sqrt{\lambda_n}e^{x/2})\Big],$$

where J and Y denote Bessel functions of the first and second kind and its spectrum is equal to the pure point spectrum, with the eigenvalue λ_n denoting the n-th root of the term in the

square brackets. Algebraic conditions for the linear stability of the homogeneous steady state, whether in the context of a Turing instability, or more generally a domain-size-driven instability, directly follow from the general treatment above.

In this way, the use of Sturm-Liouville theory enables the analysis of problems that go beyond the textbook theory of the Turing instability and these techniques could also be used to study the impact of spatial variation in other contexts. One example is the impact of extracellular matrix heterogeneity on the Turing instability given Lengyel and Epstein's effective theory [55, 43]. A second example would be to examine the impact of a background, spatially heterogeneous, chemotactic field c influencing a cell density n via the model

$$\frac{\partial}{\partial t}u = d\nabla^2 u - \chi\nabla c\nabla u + f(u),$$

with ∇ denoting the spatial gradient. However, instead, below we will exploit this framework to analyse different boundary conditions and reaction-diffusion-advection problems, in particular to assess whether there is a prospect of a domain-size-driven instability without the constraining necessity of a stable homogeneous steady state.

2 RD system with advection

2.1 Statement of the problem

We shall consider the more general concept of a domain-size-driven instability in the presence of constant advection and other boundary conditions, to assess for instance whether this can relax the requirement of short-range activation and long-range inhibition characterising the Turing instability. As such, we focus on systems that are not associated with the Turing instability, to see whether they nonetheless exhibit a domain-size-driven instability.

Thus two particular cases for the bulk behaviour of a two-species reaction-diffusion-advection system will be considered in a one-dimensional domain $\Omega = [0, L]$, one case with equally transporting species and the other case with an immobile species. Both systems are outside the regime of a classical Turing mechanism in that if advection is neglected, and Neumann boundary conditions enforced, the system still does not exhibit a Turing instability [64]. Furthermore, the above Sturm-Liouville theory can be applied with $r(x) = p(x) = e^{-xV/d}$ for a constant advection V, and also $d = d_1 = d_2$ when both species are mobile and $d = d_1, d_2 = 0$ when one of the species is immobile.

Four types of boundary conditions are considered that are relevant for reaction-diffusion-advection problems. Noting (u^*, v^*) defines the homogeneous steady state about which linear stability is of interest, we explore the following conditions for $V > 0$:

Dirichlet BC $u(x) = u^*$ at $x \in \{0, L\}$,

Fixed flux BC $-d_1 \frac{\partial}{\partial x} u(x) + Vu(x) = Vu^*$ at $x \in \{0, L\}$,

Danckwert's BC $-d_1 \frac{\partial}{\partial x} u(0) + Vu(0) = -d_1 \frac{\partial}{\partial x} u^* + Vu^* = Vu^*$ and $\frac{\partial}{\partial x} u(L) = 0$,

Periodic BC $u(0) = u(L)$ and $\frac{\partial}{\partial x} u(0) = \frac{\partial}{\partial x} u(L)$,

which are all consistent with the homogeneous steady state. The same boundary condition is also imposed on both species if the v species is mobile.

The physical meaning of the first three boundary conditions is clear. The Danckwert's boundary condition is commonly used in plug flow reactors. The boundary condition at the inlet, which is at $x = 0$ for $V > 0$, follows from the balance of mass at the boundary where the influx is considered to be well-controlled and with a defined composition at the homogeneous steady state, u^*. Hence diffusion in the inlet tube is considered to be negligible as there is no spatial variation of concentration in the inlet tube. In the bulk of the reactor, mixing and reactions of the chemicals takes place, with the possibility of pattern formation. Finally, the second boundary condition assumes that the concentration is effectively constant at the point where the flow leaves the plug flow reactor, $x = L$, with mass balance automatically satisfied. For more details we refer the reader to citation [76] for example. Please note here that as the boundary conditions are asymmetric one has to specify the inlet and outlet unambiguously by fixing the sign of $V > 0$, corresponding to transport along the x axis in our notation. Considering $V < 0$ requires a swap in the boundary conditions and hence recalculating the spectrum.

2.2 Stability analysis without BC specified

In this subsection, we present steps of the procedure, which are common for all BCs, that means: a statement of the problem and stability analysis for both, with and without differential

transport; the first steps of computing eigenvalues λ_n. For ilustration of the presentation, we use fixed-flux BC.

2.2.1 The absence of differential transport

We consider a system of two interacting species u, v where both species are diffusing and advecting with the same transport rates, so that $d = d_1 = d_2$ with the same advection for both species. Hence,

$$\begin{aligned}\frac{\partial}{\partial t}\begin{pmatrix}u\\v\end{pmatrix} &= \begin{pmatrix}d\frac{\partial^2}{\partial x^2}u - V\frac{\partial}{\partial x}u\\ d\frac{\partial^2}{\partial x^2}v - V\frac{\partial}{\partial x}v\end{pmatrix} + \begin{pmatrix}f(u,v)\\g(u,v)\end{pmatrix} \\ &\overset{def}{=} \mathcal{L}_{dV}\begin{pmatrix}u\\v\end{pmatrix} + \begin{pmatrix}f(u,v)\\g(u,v)\end{pmatrix} \\ &= d\frac{1}{r(x)}\underbrace{\frac{\partial}{\partial x}\left(p(x)\frac{\partial}{\partial x}\right)}_{\mathcal{L}}\begin{pmatrix}u\\v\end{pmatrix} + \begin{pmatrix}f(u,v)\\g(u,v)\end{pmatrix}\end{aligned} \tag{14}$$

where the functions f, g describe the reaction kinetics and a linear operator with constant coefficients $\mathcal{L}_{dV} = d\frac{\partial^2}{\partial x^2} - V\frac{\partial}{\partial x}$ has been introduced for simplicity, whilst a connection to previously discussed Sturm-Liouville theory is stated in the last equation with $p(x) = r(x) = \exp(-xV/d)$.

The bulk equations (14) are accompanied by the appropriate boundary conditions, f.e. use fixed-flux boundary conditions, for both species u, v, that is $\mathcal{L}^{bc}u := Vu(x) - d\frac{\partial}{\partial x}u(x) = Vu^*$ and $\mathcal{L}^{bc}v = Vv^*$ for $x \in \{0, L\}$. Thus an initial condition with a small perturbation of the homogeneous steady state, of the form

$$u(t=0,x) = u^* + u_0(x),\ v(t=0,x) = v^* + v_0(x),$$

with $|u_0| \ll u^*$, $|v_0| \ll v^*$, requires the zero flux homogeneous boundary condition

$$Vu_0(x) - d\frac{\partial}{\partial x}u_0(x) = 0$$

at each boundary for compatibility with the initial conditions, and similarly for species v.

Linearisation about the homogeneous steady state, (u^*, v^*), with $(\bar{u}, \bar{v}) = (u, v) - (u^*, v^*)$ yields the bulk equations

$$\frac{\partial}{\partial t}\begin{pmatrix}\bar{u}\\\bar{v}\end{pmatrix} - \mathcal{L}_{dV}\begin{pmatrix}\bar{u}\\\bar{v}\end{pmatrix} = \mathbf{J}\begin{pmatrix}\bar{u}\\\bar{v}\end{pmatrix}, \tag{15}$$

where the matrix of linearised kinetics, $\mathbf{J}$, is evaluated at the homogeneous steady state (u^*, v^*) and small perturbations have been assumed, thus allowing the neglect of higher order terms, with a view to linear stability analysis below. The initial conditions are $\bar{u}(t=0,x) = u_0(x)$, $\bar{v}(t=0,x) = v_0(x)$ and are assumed to be compatible with the zero-flux boundary conditions.

With γ_n and λ_n respectively denoting the n^{th} eigenmode and eigenvalue, note that the eigenvalue problem $-\mathcal{L}_{dV}\gamma_n = \lambda_n\gamma_n$, is the same as $-d\mathcal{L}\gamma_n = r(x)\lambda_n\gamma_n$. Furthermore, when supplemented with the homogeneous boundary conditions $\mathcal{L}^{bc}\gamma_n = 0$, the latter is a fully self-adjoint Sturm Liouville problem and thus possesses an orthonormal basis of eigenmodes in the function space $L^2([0, L])$, albeit with a weighting function of $r(x)$ in the inner product and thus the norm as well. Hence, we also have a orthonormal basis of eigenmodes of $-\mathcal{L}_{dV}$ on $(0, L)$ for an appropriate choice of inner product.

Note that for the case of periodic boundary conditions, Sturm-Liouville theory does not apply, since the operator lacks full self-adjointness due to the fact $p(x)$ is not periodic. However for the examples considered below, explicit calculation of the eigenfunctions for periodic boundary conditions reveals that they are Fourier mode harmonics (see section 2.3.1) and hence constitute a complete orthonormal basis of square integrable functions. Nonetheless the associated eigenvalues are not required to be real as Sturm Liouville theory does not apply.

Hence, the stability of the homogeneous steady state, (u^*, v^*), can be assessed from whether there is growth or decay for the amplitudes of these eigenmodes on substituting the expansion

$$\bar{u} = \sum_n w_n^u(t)\gamma_n(x), \quad \bar{v} = \sum_n w_n^v(t)\gamma_n(x)$$

into equation (15). With this substitution we thus have

$$\sum_n \left[\begin{pmatrix} \dot{w}_n^u \\ \dot{w}_n^b \end{pmatrix} + (\lambda_n \mathbf{I} - \mathbf{J}) \begin{pmatrix} w_n^u \\ w_n^v \end{pmatrix} \right] \gamma_n = 0.$$

and the homogeneous steady state is stable if all roots $\sigma_\pm$ of the dispersion relation

$$\det\left(-\sigma_\pm \mathbf{I} - (\lambda_n \mathbf{I} - \mathbf{J})\right) = 0 \tag{16}$$

have negative real parts; conversely it is unstable if at least one of the roots has a positive real part.

Except for parameter fine-tuning, which would be hard to justify due to the requirement of robustness, we have there exists an invertible matrix $\mathbf{U}$ such that matrix $\mathbf{J}$ can be characterised by its eigenvalues $\mu_\pm$

$$\mathbf{J} = \mathbf{U}^{-1} \begin{pmatrix} \mu_+ & 0 \\ 0 & \mu_- \end{pmatrix} \mathbf{U}$$

and hence the dispersion relation (16) can be rewritten as

$$\det\left[\mathbf{U}^{-1}\left(-\sigma_\pm \mathbf{I} + \begin{pmatrix} \mu_+ - \lambda_n & 0 \\ 0 & \mu_- - \lambda_n \end{pmatrix}\right)\mathbf{U}\right] = 0,$$

with roots $\sigma_\pm = \mu_\pm - \lambda_n$. Under such circumstances, we may conclude that the homogeneous steady state (u^*, v^*) is linearly stable if and only if

$$\mathrm{Re}(\sigma_\pm) = \mathrm{Re}(\mu_\pm - \lambda_n) > 0, \tag{17}$$

where λ_n are eigenvalues of the spatial operator $-\mathcal{L}_{dV}$, subject to the boundary conditions $\mathcal{L}^{bc}\gamma_n = 0$ at $x \in \{0, L\}$ and $\mu_\pm$ are two eigenvalues of the linearised kinetics Jacobian matrix $\mathbf{J}$. Furthermore it can be easily shown that the conclusion also holds when $\mathbf{J}$ is not diagonalisable via the use of Jordan normal forms. On the other hand, if the matrix $\mathbf{J}$ is diagonalisable, by rotation of u, v into eigenvectors of $\mathbf{J}$ one arrives at two uncoupled one species problem with the same boundary conditions and linear kinetics with coefficients equal to the eigenvalues $\mu_\pm$. Therefore all the results below for pattern formation without differential transport hold for a single species system provided $\mathbf{J}$ is diagonalisable (almost always is in the sense of natural measure on 2D matrices) further strengthening the significance of these results.

To conclude the stability analysis it suffices to identify eigenvalues of the spatial operator $-\mathcal{L}_{dV}$ and thus solve the eigenvalue problem,

$$-\mathcal{L}_{dV}\gamma_n = -\left(d\frac{\partial^2}{\partial x^2} - V\frac{\partial}{\partial x}\right)\gamma_n = \lambda_n \gamma_n \tag{18}$$

subject to particular boundary conditions.

2.2.2 Differential transport

In this subsection we once more consider a system of two interacting species u, v but now with one species transporting via diffusion and advection, while the other species is bound to a fixed substrate. Hence we have

$$\frac{\partial}{\partial t}\begin{pmatrix} u \\ v \end{pmatrix} = \begin{pmatrix} d\frac{\partial^2}{\partial x^2}u - V\frac{\partial}{\partial x}u \\ 0 \end{pmatrix} + \begin{pmatrix} f(u,v) \\ g(u,v) \end{pmatrix}, \tag{19}$$

where functions f, g describe the reaction kinetics. Hence, the appropriate boundary conditions (fixex flux BC in our case) apply just for species u, with $\mathcal{L}^{bc}u = Vu^*$ and a small perturbation of the homogeneous steady state is considered as an initial condition, that is

$$u(t=0,x) = u^* + u_0(x), \quad |u_0| \ll u^*.$$

The compatibility constraints for the consistency of the boundary and initial conditions of species u are the same as in the previous case.

Using $\bar{u} = u - u^*, \bar{v} = v - v^*$, we once more linearise the equations to find

$$\frac{\partial}{\partial t}\begin{pmatrix} \bar{u} \\ \bar{v} \end{pmatrix} - \mathcal{L}_{dV}\begin{pmatrix} \bar{u} \\ 0 \end{pmatrix} = \mathbf{J}\begin{pmatrix} \bar{u} \\ \bar{v} \end{pmatrix}, \tag{20}$$

with $\bar{u}$ satisfying homogeneous boundary conditions.

Before proceeding, we demonstrate that apart from a degenerate case requiring mathematical precision in the reaction rate constants, the bulk equations and boundary conditions of the linearised problem guarantee that even the perturbation $\bar{v}$ can be spanned by the Sturm-Liouville eigenfunctions. In particular, working in the L^2 function space, albeit inheriting the inner product and corresponding norm associated with Sturm-Liouville eigenfunctions, we decompose $\bar{v} = \bar{v}_\gamma + v_{\gamma\perp}$, where $\bar{v}_\gamma$ is in the sub-space of $L^2([0,L])$ spanned by the Sturm-Liouville eigenfunctions, and $v_{\gamma\perp}$ is perpendicular to this subspace. Then with the expansions

$$\bar{u} = \sum_n w_n^u(t)\gamma_n(x), \quad \bar{v}_\gamma = \sum_n w_n^v(t)\gamma_n(x),$$

equation eq. (20) becomes

$$\sum_n \left[\begin{pmatrix} \dot{w}_n^u \\ \dot{w}_n^v \end{pmatrix} + \left(\begin{pmatrix} \lambda_n & 0 \\ 0 & 0 \end{pmatrix} - \mathbf{J}\right)\begin{pmatrix} w_n^u \\ w_n^v \end{pmatrix}\right]\gamma_n + \begin{pmatrix} -J_{12}v_{\gamma\perp} \\ \dot{v}_{\gamma\perp} - J_{22}v_{\gamma\perp} \end{pmatrix} = 0.$$

We neglect the degenerate case when the upper off-diagonal Jacobian coefficient at the homogeneous steady state J_{12} is zero, since this requires mathematical precision and we focus on systems that are robust to small parameter variations. Hence, we have $v_{\gamma\perp} = 0$ as this is, by construction, orthogonal to the span of the Sturm-Liouville eigenfunctions and thus cannot be balanced by Sturm-Liouville functions in the upper row of the above equation, giving $\mathcal{L}^{bc}\bar{v}|_{0,L} = 0$. Note that although species v is not directly transported, spatial variations will develop as a consequence of the interactions with species a mediated by kinetics $\mathbf{J}$.

Insisting on continuous solutions also requires consistency between the initial and boundary conditions, such that

$$\mathcal{L}^{bc}v(t=0)|_{0,L} = \mathcal{L}^{bc}\bar{v}(t=0)|_{0,L} + \mathcal{L}^{bc}v^* = Vv^*,$$

after which the species concentration v satisfies the same identity for all later times from the dynamics of the system enforcing the constraint

$$\mathcal{L}^{bc}\bar{v}|_{0,L} = 0.$$

Henceforth, we proceed with

$$\bar{v} = \overline{v}_{\gamma},$$

and thus

$$\sum_n \left[\begin{pmatrix} \dot{w}_n^u \\ \dot{w}_n^v \end{pmatrix} + \left(\begin{pmatrix} \lambda_n & 0 \\ 0 & 0 \end{pmatrix} - \mathbf{J} \right) \begin{pmatrix} w_n^u \\ w_n^v \end{pmatrix} \right] \gamma_n = 0.$$

Consequently, linear stability is guaranteed if the matrix

$$-\left(\begin{pmatrix} \lambda_n & 0 \\ 0 & 0 \end{pmatrix} - \mathbf{J} \right)$$

has eigenvalues $\sigma_{\pm}$

$$\sigma_{\pm} = \frac{\operatorname{tr}\mathbf{J} - \lambda_n}{2} \left(1 \pm \sqrt{1 - 4\frac{\det\mathbf{J} - J_{22}\lambda_n}{(\operatorname{tr}\mathbf{J} - \lambda_n)^2}} \right) \tag{21}$$

with negative real parts $\forall n \in \{1, 2, 3 \ldots\}$, where the eigenvalues of $-\mathcal{L}_{dV}$, denoted λ_n, are inherited from the previous example.

2.2.3 Computing of the eigenvalues

Both previous subsections ended with the requirement of computing the eigenpairs (λ_n, γ_n) of the problem (18), i.e. of the linear diffusion-advection operator

$$-\mathcal{L}_{dV} = \left(V\frac{\partial}{\partial x} - d\frac{\partial^2}{\partial x^2} \right), \tag{22}$$

with various boundary conditions mentioned in the introduction of section 2. In this subsection we outline the common beginning of the computation. The following procedure is straightforward, although not technically trivial.

Since we will operate in one dimensional space, we rewrite system (22) in the standard notation for that case. Thus we solve a system of equations

$$-\mathcal{L}_{dV}\gamma_n \equiv -d\gamma_n'' + V\gamma_n' = \lambda_n\gamma_n, \tag{23}$$

where $[\lambda_n, \gamma_n]$ denotes an eigenpair for each $n \in \mathbb{N}_0$ to the problem (22) with boundary conditions, since we know that spectra of operators belonging to all the considered boundary conditions are countable.

First, a standard substitution $\gamma_n = \mathrm{e}^{\frac{V}{2d}x}\psi_n$, $n \in \mathbb{N}_0$, is used to transform the equations (23) to the normal form

$$-d\psi_n'' = \left(\frac{V^2}{4d} - \lambda_n \right) \psi_n$$

and using designation $\nu_n := \frac{\lambda}{d} - \frac{V^2}{4d^2}$ we obtain the following equivalent problem

$$-\psi_n'' = \nu_n\psi_n \tag{24}$$

with boundary conditions

Dirichlet BC $\psi_n(x) = 0$ at $x \in \{0, L\}$,

Fixed flux BC $\psi_n'(x) = \frac{V}{2d}\psi_n(x) = 0$ at $x \in \{0, L\}$,

Danckwert's BC $\psi_n'(0) = \frac{V}{2d}\psi_n(0)$ and $\psi_n'(L) = -\frac{V}{2d}\psi_n(L)$,

Periodic BC $\psi_n^{(k)}(0) = \mathrm{e}^{\frac{V}{2d}L}\psi_n^{(k)}(L)$ for $k \in \{0, 1\}$.

In the first three cases the eigensystem is real, thus the solutions of the following form will be assumed

$$\nu_n = 0: \ \psi_n(x) = Ax + B,$$

$$\nu_n > 0: \ \psi_n(x) = A\sin\sqrt{\nu}x + B\cos\sqrt{\nu}x,$$

$$\nu_n < 0: \ \psi_n(x) = A\mathrm{e}^{\sqrt{-\nu}x} + B\mathrm{e}^{-\sqrt{-\nu}x}$$

with $A, B \in \mathbb{R}$; whereas the eigenvalues of the system with periodic (the last mentioned) boundary conditions are generally complex, therefore we will be looking for the solutions in the form

$$\psi_n(x) = A\mathrm{e}^{i\sqrt{\nu_n}x} + B\mathrm{e}^{-i\sqrt{\nu_n}x} \tag{25}$$

with $A, B \in \mathbb{C}$.

The procedure will continue separately for each boundary condition in following subsection.

2.3 Results for particular BC

2.3.1 Fixed flux BC

Let start with the case of zero flux BC.

$\nu_n = 0:$ The first case leads only to a trivial solution, since system

$$\begin{aligned} 0 &= -dA + \frac{V}{2}(AL + B), \\ 0 &= -dA + \frac{V}{2}B \end{aligned}$$

has only $(A, B) = (0, 0)$ as a solution.

$\nu_n > 0:$ The substitution yields a system

$$\begin{aligned} 0 &= -dA\sqrt{\nu} + B\frac{V}{2}, \\ 0 &= \left(A\frac{V}{2} + dB\sqrt{\nu}\right)\sin\sqrt{\nu}L + \left(-dA\sqrt{\nu} + B\frac{V}{2}\right)\cos\sqrt{\nu}L. \end{aligned}$$

Inserting latter equation into the former we get an equation

$$\left(\frac{V}{2} + \frac{2d^2}{V}\nu_n\right)A\sin\sqrt{\nu}L = 0$$

and since d, V, ν_n are strictly positive real numbers, the only solution arises from the second term of the equation and it is of the form $\nu_n = \left(\frac{n\pi}{L}\right)^2$ for $n \in \mathbb{N}$.

$\nu_n < 0$: The last case yields one more solution. After substitution we obtain a system

$$0 = \left(\frac{V}{2} - d\sqrt{-\nu}\right)A + \left(d\sqrt{-\nu} + \frac{V}{2}\right)B,$$
$$0 = \left(\frac{V}{2} - d\sqrt{-\nu}\right)A\mathrm{e}^{\sqrt{-\nu}L} + \left(d\sqrt{-\nu} + \frac{V}{2}\right)B\mathrm{e}^{-\sqrt{-\nu}L}.$$

Adding $-\mathrm{e}^{-\sqrt{-\nu}L}$-multiple of the second equation to the first equation we get an equation

$$\left(\frac{V}{2} - d\sqrt{-\nu}\right)A\left(\mathrm{e}^{2\sqrt{-\nu}L} - 1\right)\mathrm{e}^{-\sqrt{-\nu}L} = 0,$$

which holds only if $\nu_n = -\left(\frac{V}{2d}\right)^2$.

In summary, in the case of the fixed-flux boundary conditions the eigensystem consists of

$$\lambda_0 = 0, \qquad \lambda_n = \frac{d}{L^2}\left((n\pi)^2 + \frac{1}{4}\mathrm{Pe}^2\right),$$
$$\gamma_0(x) = \mathrm{e}^{\mathrm{Pe}\frac{x}{L}}, \qquad \gamma_n(x) = \mathrm{e}^{\frac{\mathrm{Pe}}{2}\frac{x}{L}}\left(\sin\left(n\pi\frac{x}{L}\right) + \frac{2n\pi}{\mathrm{Pe}}\cos\left(n\pi\frac{x}{L}\right)\right).$$

The domain-size-driven instability requires

$$\lim_{L\to 0}\mathrm{Re}(\sigma_\pm) < 0 \text{ while } \exists L^* > 0, \quad \mathrm{Re}(\sigma_+(L^*)) > 0 \tag{26}$$

but as $\lambda_0 = 0$ does not scale with the domain size L, $\lim_{L\to 0}\mathrm{Re}(\sigma_\pm) = \mathrm{Re}(\mu_\pm)$, we observe that stability of the kinetics is required as in the classical Turing instability although not being linked to a homogeneous perturbation. Further no instability can appear as

$$\mathrm{Re}(\sigma_\pm) = \underbrace{\mathrm{Re}(\mu_\pm)}_{\leq 0} - \underbrace{\lambda_n}_{\leq 0}.$$

Hence, the domain-size-driven instability is equivalent to a Turing instability with or without the presence of advection in a two species system with equal transport and fixed flux boundary conditions. In particular, no self-emergent pattern can be expected despite the fact that homogeneous perturbation is not permitted by the boundary conditions in a system with advection.

In the case with differential transport, we may conclude that for a prospective Turing instability, where stability of the homogeneous steady state is required so that $\mathrm{tr}\,\mathbf{J} < 0, \det\mathbf{J} > 0$, the subsequently required linear instability with respect to inhomogeneous perturbations requires

$$(-J_{22}\lambda_n + \det\mathbf{J}) < 0.$$

As $\lambda_n > 0$ and increases with n, instability firstly requires $J_{22} > 0$. However, once this holds, the number of unstable modes is unbounded, with the concomitant prediction of salt and pepper patterning, and ultimately a breakdown of the continuum approximation, rather than a Turing instability, in accordance with our previous findings about large wave-number behaviour [35]. Hence a Turing instability cannot be supported by this system. Further note that using calculus one can show that unless $J_{12}J_{21} = 0$ the dependence of $\sigma_\pm(\lambda_n)$ is monotonous once $J_{22} < 0$ as required by the finite number of unstable modes.

As the fixed-flux boundary condition allows for a zero eigenvalue (although not corresponding to a constant homogeneous steady state solution), inspection of (21) reveals that again the stability of the zero eigenvalue state is required and thus the DSDI coincides with the TI, and hence there is no prospect of self-emergent pattern formation neither for Turing nor domain-size-driven instability.

2.3.2 Dirichlet BC

The case of Dirichlet BC is truly straightforward, the conclusions are obtained immediately after substitutions.

$\nu_n = 0$: From obtained system $B = 0$ and $AL + B = 0$ is clear that there is no solution for this case.

$\nu_n > 0$: From $B = 0$ and $0 = A \sin \sqrt{\nu_n} L$ a solution $\nu_n = \left(\frac{n\pi}{L}\right)^2$ arises for all $n \in \mathbb{N}$.

$\nu_n < 0$: There is no non-trivial solution for this case, since system $A + B = 0$ and $A\mathrm{e}^{\sqrt{-\nu}L} + B\mathrm{e}^{-\sqrt{-\nu}L} = 0$ has solution if and only if equation $\mathrm{e}^{2\sqrt{-\nu}L} = 1$ has solution.

Using backward substitution we obtain the resulting eigenpairs with $n \in \mathbb{N}$

$$\lambda_n = d\left(\frac{n\pi}{L}\right)^2 + \frac{1}{4}\frac{V^2}{d} = \frac{d}{L^2}\left((n\pi)^2 + \frac{1}{4}\mathrm{Pe}^2\right),$$
$$\gamma_n(x) = e^{\frac{V}{2d}x} \sin\left(\frac{n\pi}{L}x\right) = e^{\frac{\mathrm{Pe}}{2}\frac{x}{L}} \sin\left(n\pi\frac{x}{L}\right).$$

Note that the eigenvalues of the Dirichlet case are the same as those for Neumann boundary conditions but with the crucial exception of the zero eigenvalue. As a result, the stability of the homogeneous steady state is no longer required and thus the conditions for a domain-size-driven instability are much less restrictive and when such an instability occurs, it is accompanied by an exponential modulation of the eigenmodes when the advection is non-zero.

Particularly, for a sufficiently small domain, one always has

$$\mathrm{Re}(\sigma_\pm) = \mathrm{Re}(\mu_\pm) - \lambda_n(L) < 0$$

as $\lim_{L\to 0} \lambda_n(L) = +\infty$ and the system is always stable. As the domain increases, λ_n drops. If v is not too large and the kinetics are inherently unstable, that is $\mathrm{Re}(\mu_+) > 0$, one can have a bifurcation to instability with larger domains, inducing self-organisation, but not via a Turing instability which requires $\mathrm{Re}(\mu_\pm) < 0$. We numerically verify this finding in fig. 2.

For differential transport as considered above, again the stability of the homogeneous steady state is not required, as in the example with equal transport or explicitly by the inspection of (21). Then, if $J_{22} < 0$, there is only a finite number of unstable modes that can manifest as $\lambda_n > 0$, with λ_n growing with increasing n and subsequently $\mathrm{Re}(\sigma_\pm) < 0$ for large enough n. The prospect for instability of the first few modes follows from the possibility of satisfying $\mathrm{tr}\,\mathbf{J} - \lambda_n > 0$ or $\det \mathbf{J} - J_{22}\lambda_n < 0$ and this applies for arbitrarily small advection V for the same reasons as above in the case without differential transport.

In summary, the standard Turing mechanism requires both species are motile, with differential transport. However, this is not the case for a domain driven instability, with the emergence of self-organisation for sufficiently large domains, and patterning can occur even with a bound, immobile species or in a two species system with equal transport when the Dirichlet boundary condition is appropriate (and which for diagonalisable $\mathbf{J}$ reduces to a single RDA problem). Note that this is in line with the observation that a bifurcation from the steady state can occur for a single reacting diffusing species with Dirichlet boundary conditions [64], and the introduction of DSDI puts this result in a more general context. In particular, only an instability of the homogeneous steady state is required, which is much simpler and less constraining than the demands of the Turing instability with its concomitant requirement of short-range activation and long-range inhibition.

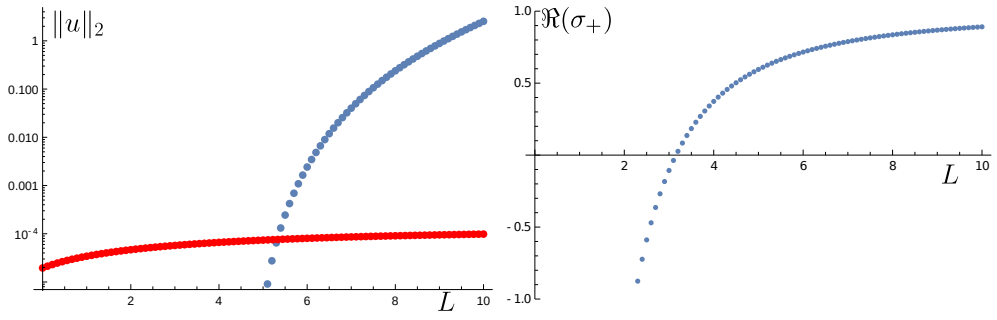

Figure 2: Illustration of the domain-size-driven instability for a single species reaction-diffusion-advection system, with linear unstable kinetics $f(u) = u$ and Dirichlet boundary conditions. A typical example was considered with: $d = 1, V = 0.2$. The analysis predicts that the critical domain length is $L_{cr} = \pi\sqrt{d/(\mu - V^2/(4d))} = 3.16$, above which instability should appear. An initial condition has been chosen such that it is a random perturbation with peak amplitude 0.01 and stretched to the changing domain size L. Figure A) plots the L^2 norm with the weighting function $r(x) = e^{-xV/d}$ of the solution at time $t = 10$ as a function of domain size L while the red dashed line denotes the weighted L^2 norm of the initial condition; B) A plot of the analytical values for $\mathrm{Re}(\sigma_+)$ versus domain size, highlighting the critical domain size L_{cr}. The slight mismatch between the analytical prediction and numerical solution, figs. A) and B), is likely because L_{cr} is determined from a condition where only the first eigenmode does not decay but all the others do; hence when starting from a random initial condition, the remaining eigenmodes have to decay and therefore reduce the norm.

2.3.3 Danckwert's BC

$\nu_n = 0$: We clearly obtain a system

$$A = -\frac{V}{2d}(AL + B),$$
$$A = \frac{V}{2d}B.$$

After summing both equations we get $0 = A(\frac{VL}{4d} + 1)$, which cannot be fulfilled if all parameters are positive, thus there is no permissible solution.

$\nu_n < 0$: We get a system

$$A\left(\sqrt{-\nu_n} - \frac{V}{2d}\right) = B\left(\sqrt{-\nu_n} + \frac{V}{2d}\right),$$
$$A\mathrm{e}^{\sqrt{-\nu_n}L}\left(\sqrt{-\nu_n} + \frac{V}{2d}\right) = B\mathrm{e}^{-\sqrt{-\nu_n}L}\left(\sqrt{-\nu_n} - \frac{V}{2d}\right).$$

Expressing B from the former equation and inserting into the latter we obtain an equation

$$\mathrm{e}^{\sqrt{-\nu_n}L} = \frac{(\sqrt{-\nu_n} - \frac{V}{2d})^2}{(\sqrt{-\nu_n} + \frac{V}{2d})^2}\mathrm{e}^{-\sqrt{-\nu_n}L}.$$

Using a notation of Péclet number $\mathrm{Pe} = LV/d$ and a designation $\sqrt{\tilde{\zeta}_n} = \sqrt{-\nu_n}L$ we get

another form of the previous equation

$$\mathrm{e}^{2\tilde{\zeta}_n} = \left(\frac{2\tilde{\zeta}_n - \mathrm{Pe}}{2\tilde{\zeta}_n + \mathrm{Pe}}\right)^2. \tag{27}$$

Since $\tilde{\zeta}_n$ is strictly positive, the left-hand side of the equation is greater than 1 and the argument of the quadratic function is strictly less than 1, therefore there is no positive root of the equation (27) and thus there is no additional solution to the equation (24) in this case.

$\nu_n > 0$: We get a system

$$0 = -A\sqrt{\nu} + B\frac{V}{2d},$$
$$\left(A\frac{V}{2d} - B\sqrt{\nu}\right)\sin\left(\sqrt{\nu_n}L\right) = \left(-A\sqrt{\nu} - B\frac{V}{2d}\right)\cos\left(\sqrt{\nu_n}L\right).$$

After substituting the former equation to the latter we get

$$\left(\frac{V}{2d} - \frac{2d}{V}|\nu_n|\right)\sin\left(\sqrt{\nu_n}L\right) = -2\sqrt{\nu_n}\cos\left(\sqrt{\nu_n}L\right).$$

The case $V^2 = 4d^2\nu_n$ leads to the equation $\cos\frac{V}{2d}L = 0$ from which it follows that $\nu_n = \left(\frac{V}{2d}\right)^2$ is a solution if $\left(\frac{V}{2\pi d}L + \frac{1}{2}\right)$ is an integer. In the case $V^2 \neq 4d^2\nu_n$, using a notation of Péclet number and a designation $\sqrt{\zeta_n} = \sqrt{\nu_n}L$, the equation passes to the form

$$\tan\sqrt{\zeta_n} = \frac{\sqrt{\zeta_n}}{\frac{\zeta_n}{\mathrm{Pe}} - \frac{\mathrm{Pe}}{4}}.$$

Since ζ_n are not explicitly expressible, this algebraic equation is used to at least estimate the eigenvalues.

From Sturm-Liouville theory we have that the eigenvalues $\lambda = d\zeta + \frac{V^2}{4d}$ of the operator $-\mathcal{L}_{dV}$ are real for Danckwert's boundary conditions; this is therefore inherited by the roots ζ. The above algebraic equation can be rewritten in a more compact form

$$\tan(\kappa\mathrm{Pe}) = \frac{\kappa}{\kappa^2 - 1/4}$$

with $\kappa := \mathrm{Pe}^{-1}\sqrt{\zeta}$. Hence we can restrict ourselves to the cases where κ is either real or pure imaginary, focusing on the latter first so that we introduce $\tilde{\kappa} = \sqrt{-\zeta}d/V = i\kappa$, with $\zeta < 0$. Then the above algebraic relation transforms into

$$\tanh(\tilde{\kappa}\mathrm{Pe}) = \frac{-\tilde{\kappa}}{\tilde{\kappa}^2 + 1/4}$$

which does not posses a solution as $\mathrm{Pe} = LV/d > 0$ and the hyperbolic tangent functions is positive for positive $\tilde{\kappa}$, while the fraction on the right-hand side is always negative in this range with the exception of $\tilde{\kappa} = 0$, as covered elsewhere in the real case.

We now consider the case with $\zeta \geq 0$. Clearly there is a solution with $\zeta = 0 = \kappa$ but it is not associated with a non-zero eigenfunction and hence it is not an eigenvalue. Further, for large positive ζ, we may approximate

$$\tan(\kappa \mathrm{Pe}) = \frac{\kappa}{\kappa^2 - 1/4} \sim \frac{1}{\kappa}.$$

Therefore $|\kappa \mathrm{Pe} - n\pi| \ll 1$ and

$$\tan(\kappa \mathrm{Pe}) \sim (\kappa \mathrm{Pe} - n\pi) \sim \frac{1}{\kappa}.$$

Taking just the larger root, which is consistent with the requirement of large κ, we have that

$$\kappa \sim \frac{n\pi}{\mathrm{Pe}} + O(1/n)$$

and one can confirm this is an excellent approximation for the 5th and higher roots. In turn, as $\lambda_n = \left(d\zeta_n + \frac{1}{4}\frac{V^2}{d}\right)$, we find

$$\lambda_n \sim d\left(\frac{n\pi}{L}\right)^2 + \frac{1}{4}\frac{V^2}{d}. \tag{28}$$

Hence, beyond the first few modes, the eigenvalues essentially coincide with those for fixed-flux boundary conditions in the presence of advection, and analogous comments apply to the eigenmodes.

It is crucial to understand the spectrum for sufficiently small domains, and hence small Pe. Hence, we need to estimate the lowest root κ_1 of the eigenvalue problem

$$\tan(\kappa \mathrm{Pe}) = \frac{\kappa}{\kappa^2 - 1/4}$$

as $\mathrm{Pe} \to 0$. From the signs of both sides we can see that $\kappa_1 > 1/2$ while $0 < \kappa_1 < \pi/(2\mathrm{Pe})$ as otherwise the Péclet number would have to be large. For sufficiently small Pe, the first root for small Péclet number can be approximated via

$$\kappa_1 \mathrm{Pe} \sim \tan(\kappa_1 \mathrm{Pe}) = \frac{\kappa_1}{\kappa_1^2 - 1/4} \sim \frac{1}{\kappa_1}$$

yielding

$$\kappa_1 \sim \mathrm{Pe}^{-1/2}$$

and hence the spectrum has the following lower bound

$$\lambda_n \geq \lambda_1 \sim \frac{V^2}{d}\left(\mathrm{Pe}^{-1/2} + \frac{1}{4}\right) \sim \frac{d}{L^2}\mathrm{Pe}^{3/2} = \frac{V^2}{d}\mathrm{Pe}^{-1/2}.$$

In summary, Danckwert's BC yields with $n \in \mathbb{N}$

$$\lambda_n = \frac{d}{L^2}\left(\zeta_n + \frac{1}{4}\mathrm{Pe}^2\right),$$

$$\gamma_n(x) = e^{\frac{\mathrm{Pe}}{2}\frac{x}{L}}\left(\sin\left(\sqrt{\zeta_n}\frac{x}{L}\right) + \frac{2}{\mathrm{Pe}}\sqrt{\zeta_n}\cos\left(\sqrt{\zeta_n}\frac{x}{L}\right)\right),$$

with ζ_n being the roots of

$$\tan(\sqrt{\zeta_n}) = \frac{\sqrt{\zeta_n}}{\mathrm{Pe}^{-1}\zeta_n - \mathrm{Pe}/4},$$

and where the index n is used to denote the discrete nature of spectrum, and labels the above roots. Note that $\zeta_n > 0$ as $\zeta = 0$ does not correspond to an eigenvalue, since this would require $\gamma = 0$. Crucially we showed that for a sufficiently small domain, so that $\mathrm{Pe} \ll 1$, one has the following bound on eigenvalues

$$\lambda_n \geq \lambda_1 \sim \frac{V^2}{d}\left(\mathrm{Pe}^{-1/2} + \frac{1}{4}\right) = \frac{d}{L^2}\left(\mathrm{Pe}^{-1/2} + \frac{1}{4}\right)\mathrm{Pe}^2 \tag{29}$$

and one additional eigenpair

$$\lambda = \frac{d}{2L^2}\mathrm{Pe}^2, \qquad \gamma(x) = e^{\frac{\mathrm{Pe}}{2L}x}\left(\cos\left(\frac{\mathrm{Pe}}{2L}x\right) + \sin\left(\frac{\mathrm{Pe}}{2L}x\right)\right),$$

if $\mathrm{Pe}/(2\pi) - 1/2$ is an integer. Since its existence requires mathematical precision in the parameter values and thus it is not biologically relevant, we will neglect this eigenpair.

By inspection of estimate (29) we can observe that for a sufficiently small domain size, the eigenvalues tend to infinity guaranteeing stability for a small enough domain. At the same time, for a fixed, small, Péclet number one has

$$\mathrm{Re}(\sigma_\pm) = \mathrm{Re}(\mu_\pm) - \lambda_1 > 0$$

and the system is linearly unstable if reaction kinetics is unstable and the domain is sufficiently large; we thus have a domain-size-driven instability.

In summary, the spectrum of $-\mathcal{L}_{dV}$ is such that it is separated from zero, in that $\lambda = 0$ is not an eigenvalue, and hence stability of the homogeneous steady state is not required. In particular we have a lower bound $\lambda_n = d\zeta_n + \frac{1}{4}\frac{V^2}{d} \geq \frac{V^2}{d}\mathrm{Pe}^{-1/2} = \lambda_1$. Stability follows then from $\mathrm{Re}(\sigma_\pm) = \mathrm{Re}(\mu_\pm) - \lambda_n \leq \mathrm{Re}(\mu_\pm) - \lambda_1$ where $\mu_\pm$ are eigenvalues characterising the kinetics. However, instability can manifest at larger domain sizes and hence a domain-size-driven instability can occur.

For differential transport one again requires $J_{22} < 0$ to have finite number of unstable modes (stability for large enough n) and the prospect of instability appears via satisfying either $\mathrm{tr}\, J - \lambda_n > 0$ or $\det J - J_{22}\lambda_n < 0$ for the first few eigenvalues, see equation (21). The fact that instability appears always only through the first few eigenmodes (following from the noted monotonicity of $\sigma_\pm$ on λ_n) entails that the system is stable for a small enough domain (owing to the asymptotic expression for $\lambda_1 \leq \lambda_n$ when Péclet number is small enough). Similarly, for a sufficiently large domain size either $\mathrm{tr}\, J - \lambda_1 > 0$ or $\det J - J_{22}\lambda_1 < 0$ can be satisfied and hence the instability and the prospect to pattern would appear.

Hence there is a fundamental difference in the pattern forming and stability properties of reaction diffusion systems with even very small advection if Danckwert's boundary conditions are the physically relevant ones, on noting that Danckwert's boundary conditions are an approximation to zero-flux boundary conditions as $V \to 0$. In particular, this is regardless of the fact that beyond the first few eigenmodes the modes are essentially the same as those associated with fixed flux and Dirichlet boundary conditions, as can be observed from eq. (28), and crucially the stability of homogeneous steady state is not required. This also implies that there is at most a finite number of unstable modes so that salt and pepper patterning, with its ensuing breakdown of the continuum approximation, does not occur.

2.3.4 Periodic BC

Substituting the expected form of the solution (25) into the transformed periodic boundary conditions we obtain a system

$$A + B = \mathrm{e}^{\frac{V}{2d}L}\left(A\mathrm{e}^{i\sqrt{\nu_n}L} + B\mathrm{e}^{-i\sqrt{\nu_n}L}\right), \tag{30}$$

$$A - B = \mathrm{e}^{\frac{V}{2d}L}\left(A\mathrm{e}^{i\sqrt{\nu_n}L} - B\mathrm{e}^{-i\sqrt{\nu_n}L}\right). \tag{31}$$

Summing both equations we obtain an equation

$$A = A\mathrm{e}^{\frac{V}{2d}L}\mathrm{e}^{i\sqrt{\nu_n}L}.$$

Assume first that $A \neq 0$. Then applying Euler's identity $\mathrm{e}^{i\pi} + 1 = 0$ in the previous equation we get

$$\sqrt{\nu_n} = \frac{2n\pi}{L} + i\frac{V}{2d} \tag{32}$$

and thus the solution is of the form

$$\nu_n = \frac{4n^2\pi^2}{L^2} + 2i\frac{n\pi V}{dL} - \frac{V^2}{4d^2}.$$

Substituting (32) back into the equation (30) we obtain $B = 0$ and thus final form of the solution.

Assume $A = 0$ for the second case. Inserting that into equation (30) we get

$$1 = \mathrm{e}^{\frac{V}{2d}L - i\sqrt{\nu_n}L},$$

whose solution is

$$\sqrt{\nu_n} = -\frac{2n\pi}{L} - i\frac{V}{2d}.$$

This form is up to the sign equal to (32) and since arguments of the functions in (25) differ from each other in the sign, the form of the resulting eigenfunction will be same as in the case $A \neq 0$.

In summary, in the case of periodic boundary conditions the eigensystem consists of pairs of the form

$$\lambda_n = \frac{d}{L^2}\left((2n\pi)^2 + i2n\pi\mathrm{Pe}\right),$$
$$\gamma_n(x) = \mathrm{e}^{i2n\pi\frac{L}{x}}$$

for $n \in \mathbb{Z}$.

In the case of periodic boundary conditions, all the eigenvalues are complex, $\lambda_n \in \mathbb{C} \setminus \mathbb{R}$, except for the trivial eigenvalue $\lambda_0 = 0$ that corresponds to a constant eigenfunction. As the homogeneous steady state is also an eigenfunction, both the conditions for the Turing instability and the domain size controlled instability overlap and thus we are only considering differences in the details of the instability conditions.

In the case without differential transport, the system is always stable, as is the case with the Turing mechanism. When considering the differential transport situation where one species

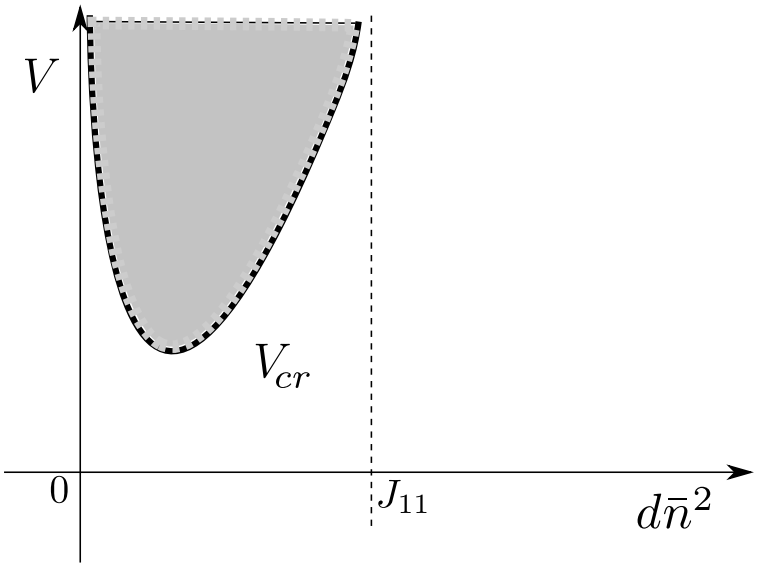

Figure 3: A qualitative illustration of the effect of constant advection for the stability of the reaction-diffusion-advection system with periodic boundary conditions when one species is diffusing and advecting while the other is fixed to a substrate. The region of instability, with an asymptote at $d\bar{n}^2 = d\left(\frac{2n\pi}{L}\right)^2 = J_{11}$, is presented in grey. For sufficiently small advection, there is negligible impact on the presence of an instability and the existence of a critical domain size below which stability of the system is always guaranteed, as follows from equation (33) and the explanation thereafter. Similarly, the cut-off for high wavenumbers is demonstrated in the figure, resulting in at most a finite number of unstable modes.

is immobile, the real part of $\sigma_\pm$ responsible for stability is, in the case of complex λ_n, given by the following

$$\mathrm{Re}(\sigma_\pm) = \frac{1}{4}\Big[2(\mathrm{tr}\,\mathbf{J} - d\bar{n}^2) \pm \sqrt{2}\sqrt{c + \sqrt{4\bar{n}^2(J_{22} - J_{11} + d\bar{n}^2)^2V^2 + c^2}}\Big],$$

as can be deduced from Eq (21), with $\bar{n} := \frac{2n\pi}{L}$ and

$$c := -4\det\mathbf{J} + d^2\bar{n}^4 + 2d\bar{n}^2(J_{22} - J_{11}) + (\mathrm{tr}\,\mathbf{J})^2 - \bar{n}^2V^2.$$

Again, the requirement of a finite number of unstable modes or alternatively the requirement that there is a critical domain length below which a system is always stable yields $J_{22} < 0$, with the equivalence of these two distinct requirements in this case arising from the fact that n appears always via the fraction n/L.

For sufficiently small advection we have

$$\mathrm{Re}(\sigma_\pm) \sim \begin{cases} \frac{1}{2}(-d\bar{n}^2 + \mathrm{tr}\,\mathbf{J} \pm \sqrt{c + \bar{n}^2V^2}), & c + \bar{n}^2V^2 > 0 \\ \frac{1}{2}(-d\bar{n}^2 + \mathrm{tr}\,\mathbf{J}), & \text{otherwise} \end{cases}. \tag{33}$$

Hence, these conditions for an instability with reaction-diffusion-advection systems are continuously transformed into instability conditions for reaction diffusion systems as v tends to zero. One can identify a critical instability from the condition $\mathrm{Re}(\sigma_-) < \mathrm{Re}(\sigma_+) = 0$ and observe that there exists a critical velocity V_{cr} that has to be surpassed in order for an instability to

appear. Further such a threshold exists only for a small enough wave number, namely $n < \frac{LJ_{11}}{d2\pi}$. Above this threshold there is a cut-off and advection no longer contributes to the instability, as clearly depicted in fig. 3 for a qualitative picture of the role of advection on instability for the differential transport scenario. Similar results, but perhaps with less detail, can be also be found in Rovinsky and Menziger [81].

2.3.5 Summary

Let us conclude this section with a brief summary of the obtained results. First we outline the computed eigenpairs for all considered BCs. Then, the summary of conclusions for particular BC can be found in table 1 where the comparison of the domain-size-driven instability with the Turing instability is provided for clarity together with the influence of advection on the systems behaviour.

Homogeneous Dirichlet : $\gamma(x=0) = 0 = \gamma(x=L)$ yields eigenpairs with $n \in \mathbb{N}$

$$\lambda_n = d\left(\frac{n\pi}{L}\right)^2 + \frac{1}{4}\frac{V^2}{d} = \frac{d}{L^2}\left((n\pi)^2 + \frac{1}{4}\mathrm{Pe}^2\right),$$

$$\gamma_n(x) = e^{\frac{V}{2d}x}\sin\left(\frac{n\pi}{L}x\right) = e^{\frac{\mathrm{Pe}}{2}\frac{x}{L}}\sin\left(n\pi\frac{x}{L}\right).$$

Zero flux : $-V\gamma(x) + d\frac{\partial}{\partial x}\gamma(x)|_{x=0,L} = 0$ yields eigenpairs with $n \in \mathbb{N}$

$$\lambda_0 = 0, \quad \lambda_n = \frac{d}{L^2}\left((n\pi)^2 + \frac{1}{4}\mathrm{Pe}^2\right),$$

$$\gamma_0(x) = e^{\mathrm{Pe}\frac{x}{L}}, \quad \gamma_n(x) = e^{\frac{\mathrm{Pe}}{2}\frac{x}{L}}\left(\sin\left(n\pi\frac{x}{L}\right) + \frac{2n\pi}{\mathrm{Pe}}\cos\left(n\pi\frac{x}{L}\right)\right).$$

Periodic : $\gamma(0) = \gamma(L)$, $\frac{\partial}{\partial x}\gamma(0) = \frac{\partial}{\partial x}\gamma(L)$ yields eigenpairs with $n \in \mathbb{Z}$

$$\lambda_n = \frac{d}{L^2}\left((2n\pi)^2 + i2n\pi\mathrm{Pe}\right),$$

$$\gamma_n(x) = e^{i2n\pi\frac{L}{x}}.$$

Danckwert's : $-V\gamma(0) + d\frac{\partial}{\partial x}\gamma(0) = 0$, $\frac{\partial}{\partial x}\gamma(L) = 0$ yields eigenpairs with $n \in \mathbb{N}$

$$\lambda_n = \frac{d}{L^2}\left(\zeta_n + \frac{1}{4}\mathrm{Pe}^2\right),$$

$$\gamma_n(x) = e^{\frac{\mathrm{Pe}}{2}\frac{x}{L}}\left(\sin\left(\sqrt{\zeta_n}\frac{x}{L}\right) + \frac{2}{\mathrm{Pe}}\sqrt{\zeta_n}\cos\left(\sqrt{\zeta_n}\frac{x}{L}\right)\right),$$

with ζ_n being the roots of

$$\tan(\sqrt{\zeta_n}) = \frac{\sqrt{\zeta_n}}{\mathrm{Pe}^{-1}\zeta_n - \mathrm{Pe}/4},$$

and where the index n is used to denote the discrete nature of spectrum, and labels the above roots. Note that $\zeta_n > 0$ as $\zeta = 0$ does not correspond to an eigenvalue, since this

would require $\gamma = 0$. Crucially we showed that for a sufficiently small domain, so that $\mathrm{Pe} \ll 1$, one has the following bound on eigenvalues

$$\lambda_n \geq \lambda_1 \sim \frac{V^2}{d}\left(\mathrm{Pe}^{-1/2} + \frac{1}{4}\right) = \frac{d}{L^2}\left(\mathrm{Pe}^{-1/2} + \frac{1}{4}\right)\mathrm{Pe}^2$$

and one additional eigenpair

$$\lambda = \frac{d}{2L^2}\mathrm{Pe}^2, \qquad \gamma(x) = e^{\frac{\mathrm{Pe}}{2L}x}\left(\cos\left(\frac{\mathrm{Pe}}{2L}x\right) + \sin\left(\frac{\mathrm{Pe}}{2L}x\right)\right),$$

if $\mathrm{Pe}/(2\pi) - 1/2$ is an integer. Since its existence requires mathematical precision in the parameter values and thus it is not biologically relevant, we will neglect this eigenpair.

Table 1: Summary of the results. Note that 'DSDI=TI' refers to a situation where the conditions for TI are the same as for DSDI. Particularly, the stability of the zero eigenvalue state is required.

	Dirichlet	Fixed Flux	Periodic	Danckwert's
DSDI = TI	No	Yes	Yes	Yes for $V = 0$ No for $V \neq 0$
$V = 0$ vs. small but $0 < V$: spectrum	$\mathrm{Pe} \ll 1$	$\mathrm{Pe} \ll 1$	diff. for arbitrary $V > 0$	$\mathrm{Pe} \ll 1$
$V = 0$ vs. small but $0 < V$: eigenfunctions	$\mathrm{Pe} \ll 1$	$\mathrm{Pe} \ll 1$	identical	$\mathrm{Pe} \ll 1$
DSDI $d_1 = d_2$, $V_1 = V_2$ (single RDA for diag $\mathbf{J}$)	Yes always stable	No for unstable kinetics	No	Yes for $V > 0$ for unstable kinetics
DSDI $d_1 = 0$, $V_2 = 0$ (differential transp.)	Yes for $J_{22} < 0$ and unstab. kin.	No always stable	Yes for $V > V_{cr}$ & $n < \frac{LJ_{11}}{2\pi d}$	Yes for $V > 0$ for $J_{22} < 0$ and unstab. kin.

3 RD system with spatial dependency in kinetics

3.1 Statement of the problem

This section consists of the outline of the original author's article [47] examining an impact of a piecewise kinetic modulation on a pattern formation in a Turing system.

We consider the following RD-system

$$\begin{aligned} \partial_t u &= d_1 \partial_{xx} u + f_1(u,v) + h(x)u, \\ \partial_t v &= d_2 \partial_{xx} v + f_2(u,v), \end{aligned} \qquad x \in (0,L) \tag{34}$$

with Neumann boundary conditions

$$\begin{aligned} \frac{\partial u}{\partial n} &= 0, \quad \text{at } x = 0, L \\ \frac{\partial v}{\partial n} &= 0, \quad \text{at } x = 0, L, \end{aligned} \tag{35}$$

where $h(x)$ is a step function defined as

$$h(x) = \begin{cases} 0 & x \in [0, \xi), \\ s & x \in [\xi, L]. \end{cases} \tag{36}$$

First for reasons that shall become evident, we need to assess what will be denoted as a pattern since the standard definition is not sufficient because inhomogeneity is always present due to the forced jump s at location ξ. We illustrate the effect of the step function via numerical simulations, considering system (34) with Schnakenberg kinetics

$$\begin{aligned} f(u,v) &= a - u + u^2 v, \\ g(u,v) &= b - u^2 v, \end{aligned} \tag{37}$$

where a, b are positive parameters. Let the step, with a size $s = 0.5$, be located in the middle of the domain $\xi = L/2$ and consider the remaining parameters d_1, d_2, a, b to be outside ($b \in \{0.01, 0.25\}$) or inside ($b \in \{1, 2\}$) the Turing space for $s = 0$.

As we can see in fig. 4 (blue wavy line), a spatial inhomogeneity occurs in each of the solutions. Note i) the different amplitudes of the pattern in the two parts of the domain (as already observed, e.g., in [71]) and ii) the different periods (see fig. 4C). Characterising such patterning behaviour in fig. 4C, within the context of emergent Turing self-organisation from a linearised system with spatial heterogeneity in the form of a step function premultiplying a linear term, constitutes the overarching aim of this study.

As mentioned above, not all the inhomogeneous solutions displayed in fig. 4 correspond to a pattern however. To represent genuine self-organisation, rather than being passively slave to the step function, such stationary solutions should have spatial oscillations extending to the domain edge on at least one side of the step even as the domain size is increased, for sufficiently large domain sizes. This requirement follows from an observation that a Turing pattern is characterised by a finite number of frequencies that appear in the pattern. Thus an increase in the domain size should result in pattern repetition over the whole domain once a critical domain size is surpassed. Therefore we plot stationary solutions to the system with the same parameters except a larger domain size, $L = 1000$, in fig. 5. By comparison, we can deduce

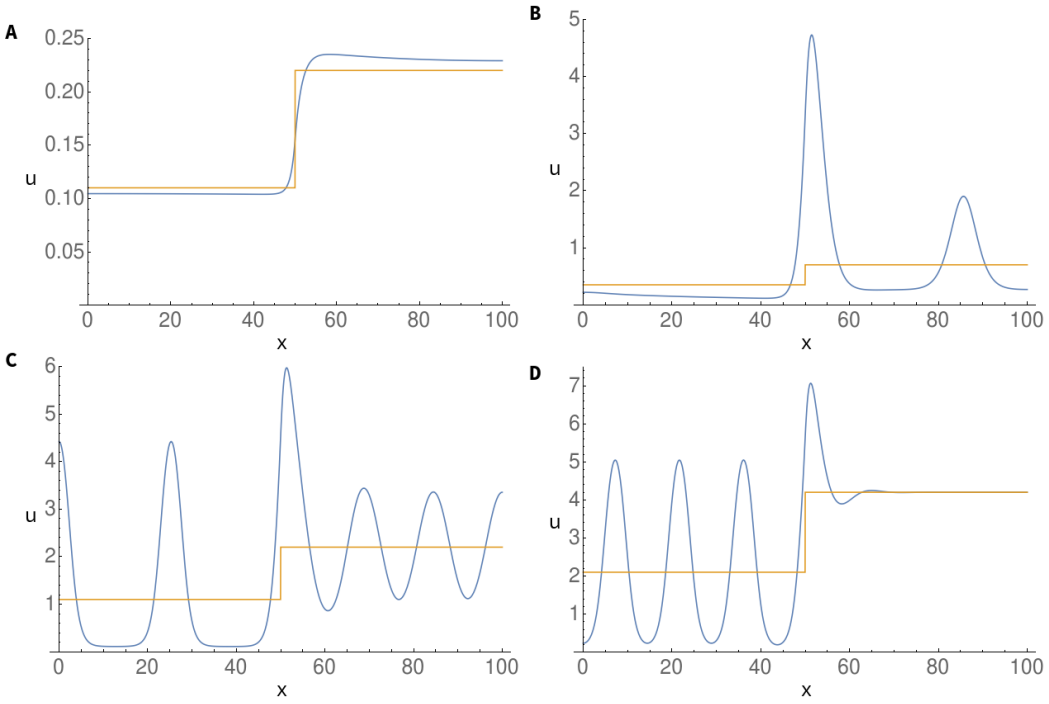

Figure 4: Plot of the long-time (close to steady state) activator concentration $u(x)$ from simulations of system (34) with Schnakenberg kinetics (37), on the domain $[0, 100]$ with zero-flux boundary conditions, and parameters: $d_1 = 1$, $d_2 = 100$, $s = 0.5$, $a = 0.1$ and A) $b = 0.01$, B) $b = 0.25$ (both outside the Turing space for $s = 0$), C) $b = 1$, D) $b = 2$ (both inside the Turing space for $s = 0$). These have been solved by Mathematica (for more details see below). Note the different vertical scales in the above plots.

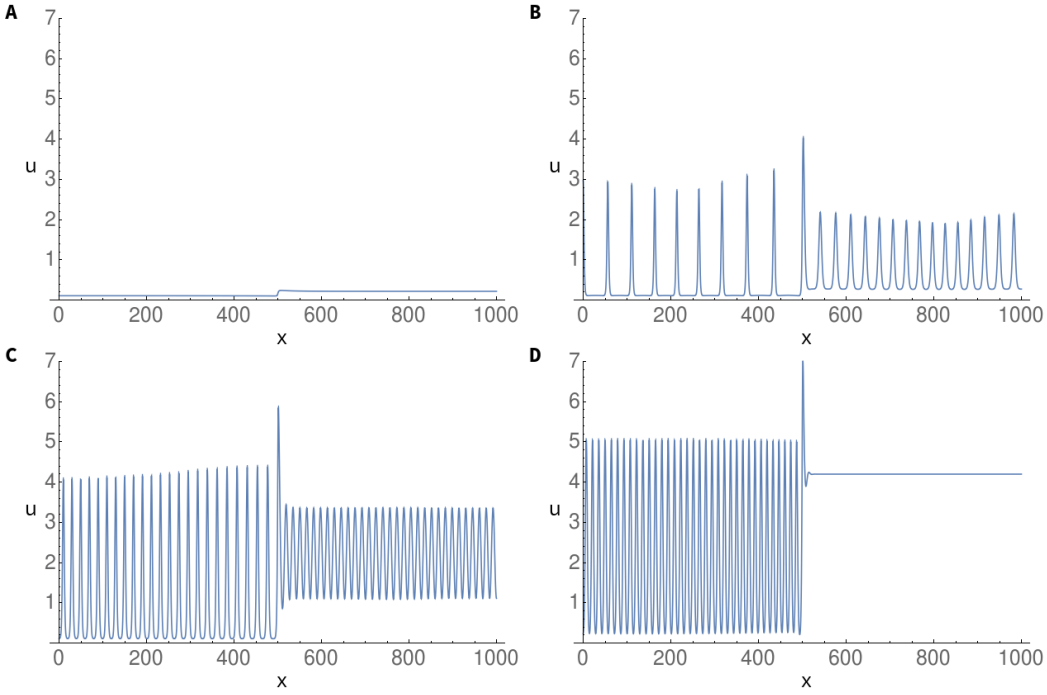

Figure 5: Plot of the long-time (close to steady state) activator concentration $u(x)$ from simulations of system (34) with the same values as in fig. 4 apart from $L = 1000$. The vertical axis is chosen equal for all plots. This figure illustrates the effect of larger L which is key for discussion of what a "pattern" should mean in systems with heterogeneous kinetics.

that the case A is not a pattern as the inhomogeneity is localised only around the point of the step ξ while being of the order of the step s. Hence we disregard such cases in the context of pattern. On the contrary, in the other examples the inhomogeneity perseveres on the whole domain; thus such cases are denoted as a pattern.

Hence our detailed objectives are: (i) to determine if a pattern emerges or not; (ii) to undertake a more specific pattern classification examining the parameter spaces for when the system will exhibit each prototype of a stationary solution represented by the plots in fig. 4 – A) no-pattern, B) right-sided pattern, C) global pattern, D) left-sided pattern[4].

Let us further make the following interesting observation. We consider step functions $\bar{u}(x), \bar{v}(x)$ defined as

$$\bar{u}(x) = \begin{cases} \bar{u}^L & x \in (0, \xi) \\ \bar{u}^R & x \in (\xi, L) \end{cases}, \qquad \bar{v}(x) = \begin{cases} \bar{v}^L & x \in (0, \xi) \\ \bar{v}^R & x \in (\xi, L) \end{cases}, \tag{38}$$

where

$$f(\bar{u}^L, \bar{v}^L) = 0 = g(\bar{u}^L, \bar{v}^L),$$
$$f(\bar{u}^R, \bar{v}^R) + s\bar{u}^R = 0 = g(\bar{u}^R, \bar{v}^R).$$

[4]Note the discrepancy between plots in fig. 4B and fig. 5B: the former case is denoted as a right-sided pattern whereas the latter patterns globally. The only change is in the value of parameter L and it seems, roughly speaking, L should be large enough and cases where pattern cannot form solely because of domain are generally classified as patterning systems nonetheless. Please note that this is analogous to the classical Turing approach where a pattern appears only once a certain minimal domain size is reached so that the first eigenmode fits within the domain and can be excited.

Note that in Turing-like problems the existence of a homogeneous steady state is assumed, guaranteeing existence of the step functions (38). The long-time solution for the variable, u, seems to be either approaching $\bar{u}(x)$ in the case without pattern, or oscillating around $\bar{u}(x)$ in the case of pattern. This leads us to a hypothesis that the behaviour of the long-time solution could be deduced from attracting properties of the system around $\bar{u}(x)$ and therefore the system characterisations could be similar to the conditions of diffusion-driven instability evaluated for the system (with a constant coefficient) considered separately on intervals $(0, \xi)$ and (ξ, L). In particular, such prospects will be considered more precisely and systematically below.

The procedure is outlined in the following section. After that, the spectral part of the following approach is complemented by a boundary layer analysis which further suggests that conditions for one-sided pattern are related to Turing conditions considered separately on each subinterval. In addition, this boundary layer analysis indicates that spatial frequency of emerging pattern is determined independently in the two subintervals while the boundary layer highlights how the patterns match in the interval around the step at $x = \xi$ of the step functions.

3.2 Brief summary of procedure

Let us follow the classical approach for a Turing model, which was reminded in section 1.1.1, and summarize it in the following paragraph with highlighted essential steps, which will coincide with the structure of this section.

Let us consider nonlinear RD system (1), we find 1) a ground (homogeneous) steady-state, the existence of which we assume due to the essence of the problem. Consider 2) a system with linear kinetics having the same qualitative behaviour to the non-linear one, which results from Taylor expansion about the ground steady-state. We perform 3) a stability analysis of that steady state with respect to the linear system and then we obtain 4) conditions for diffusion-driven instability for the linear system. At the end, as a summary of the procedure, we obtain 5) an approximate knowledge of the behaviour of a system with non-linear kinetics.

3.2.1 Steady state

As has been noted above, since the kinetics contains a non-trivial spatial dependency, a constant function cannot be a solution to system (34). Instead of the homogenous steady state, we take a heterogeneous steady state of the no-pattern type as a ground steady state. Nevertheless, such solution is difficult to find since this problem is governed by a system of two elliptic equations. Moreover, even if we managed to express the ground state, for instance in the case of very particular choice of kinetics, the coefficient of linearization about this steady state would be strongly spatially dependent, and thus such linear system would be practically analytically unusable.

Nevertheless, similarly to the classical Turing assumptions, we suppose the existence of the ground steady state of the no-pattern type and we will estimate a tool to recognize the conditions under which the Turing effect occurs.

3.2.2 Linear system

From the previous subsection follows that linearization using Taylor expansion of the kinetics about the ground state is not usable for analysis, thus a clear method to obtain a representative linear system is missing. We deal with this by adding an intermediate step, a system with similar

behaviour as the non-linear one, but with approximated kinetics more suitable for analytical methods of stability analysis. According to the reason that our task is to capture the behaviour of the system around the no-pattern, we also want to approximate the kinetics with simpler functions in such way that they exhibit the same behaviour as the nonlinear system around the no-pattern as narrowly as possible. Due to the designation of the term no-pattern we assume that this neighbourhood overlaps the neighbourhood of the step function $\bar{u}, \bar{v}$ defined in (38), and therefore we will approximate the kinetics with respect to the latter neighbourhood.

In conclusion, take approximations of reaction kinetics as Taylor expansions evaluated separately on both intervals ($\tilde{u} = u - \bar{u}$):

$$\begin{array}{lll} L: & f(u,v) = f(\bar{u}^L, \bar{v}^L) + J^L_{11}\tilde{u} + J^L_{12}\tilde{v} + \dots & g(u,v) = g(\bar{u}^L, \bar{v}^L) + J^L_{21}\tilde{u} + J^L_{22}\tilde{v} + \dots \\ R: & f(u,v) + su = f(\bar{u}^R, \bar{v}^R) + s\bar{u}^R + J^R_{11}\tilde{u} + J^R_{12}\tilde{v} + \dots & g(u,v) = g(\bar{u}^R, \bar{v}^R) + J^R_{21}\tilde{u} + J^R_{22}\tilde{v} + \dots \end{array},$$

where J^L_{ij} (resp. J^R_{ij}) denote the elements of Jacobian matrix of the map (f, g) at $(\bar{u}^L, \bar{v}^L)$ (resp. $(f + su, g)$ at $(\bar{u}^R, \bar{v}^R)$). Using notation (38) together with

$$s_{ij} = J^R_{ij} - J^L_{ij}, \quad J_{ij}(x) = \begin{cases} J^L_{ij} & x \in (0, \xi) \\ J^R_{ij} & x \in (\xi, L), \end{cases}$$

we can write down the intermediate system, an affine system describing evolution near $(\bar{u}(x), \bar{v}(x))$ while approximating the original system with non-linear kinetics, as

$$\begin{aligned} \partial_t u &= d_1 \partial_{xx} u + J_{11}(x)u + J_{12}(x)v + c_1(x) \\ \partial_t v &= d_2 \partial_{xx} v + J_{21}(x)u + J_{22}(x)v + c_2(x) \end{aligned} \quad \text{on } (0, L) \tag{39}$$

with the step functions

$$c_1(x) = -J_{11}(x)\bar{u}(x) - J_{12}(x)\bar{v}(x), \quad c_2(x) = -J_{21}(x)\bar{u}(x) - J_{22}(x)\bar{v}(x)$$

and with Neumann boundary conditions (35).

The advantage of system with affine kinetics (39) lies in the fact that the steady state is explicitly calculable, let us denote it as $(\hat{u}, \hat{v})$. Its calculation can be seen in appendix A.2, where a process familiarly called "diagonalization" is used (this approach is presented in appendix A.1) on behalf of [71]. Since the final explicit form of the analytic solution is quite complicated and the knowledge of its explicit form is not beneficial for us, it is sufficient to note an interesting issue that the resulting form of the solution to each subsystem depends on the sign of two particular conditions remarkably similar to those for the classical Turing diffusion-driven instability evaluated on both subsystems separately. This observation supports our hypothesis at the end of section 3.1 about the relation between diffusion-driven instability in the studied case and DDI conditions for patterns on $(0, \xi)$ and (ξ, L).

Note that the same qualitative behaviour (with the same long-time behaviour) is obtained when studying a perturbation of the piece-wise constant solution (38) in a generalised function sense, see appendix A.3.

Now, the linear system can be obtained from the one with affine kinetics straightforwardly using classical approach.

3.2.3 Linear stability

With the steady state $(\hat{u}, \hat{v})$ of system (39), we can analyse its stability. We focus only on the long-time behaviour of the system, which can be obtained from spectral analysis, assuming that the transient behaviour is not essential as shown for the classical Turing instability [104].

With a redefinition of $\tilde{u}, \tilde{v}$ to the time dependent perturbed solution, $\tilde{u} = u - \hat{u}$, $\tilde{v} = v - \hat{v}$ let us expand the evolution equations about the steady state to find

$$\begin{aligned} \partial_t \tilde{u} &= d_1 \partial_{xx} \tilde{u} + J_{11}(x)\tilde{u} + J_{12}(x)\tilde{v} \\ \partial_t \tilde{v} &= d_2 \partial_{xx} \tilde{v} + J_{21}(x)\tilde{u} + J_{22}(x)\tilde{v}. \end{aligned} \tag{40}$$

Since we consider Neumann boundary conditions, we have a complete orthogonal basis $y_n(x)$, $n \in \mathbb{N}_0$ of $L^2(0, L)$ and eigenvalues $\kappa_n = (n\pi/L)^2$ for the negative Laplacian (which satisfy $-\Delta y_n = \kappa_n y_n$). Now we rewrite functions $\tilde{u}$ and $\tilde{v}$ in terms of the series

$$\tilde{u}(t, x) = \sum_{n=0}^{\infty} A_n(t) y_n(x), \quad \tilde{v}(t, x) = \sum_{n=0}^{\infty} B_n(t) y_n(x). \tag{41}$$

Thus system (40) can be rewritten into the form

$$\sum_{n=0}^{\infty} \begin{pmatrix} \partial_t A_n \\ \partial_t B_n \end{pmatrix} y_n(x) + \mathbf{D} \begin{pmatrix} A_n \\ B_n \end{pmatrix} \kappa_n y_n(x) - \mathbf{J}(x) \begin{pmatrix} A_n \\ B_n \end{pmatrix} y_n(x) = 0, \tag{42}$$

where we have introduced the standard notation

$$\mathbf{D} = \begin{pmatrix} d_1 & 0 \\ 0 & d_2 \end{pmatrix}, \quad \mathbf{J}(x) = \begin{pmatrix} J_{11}(x) & J_{12}(x) \\ J_{21}(x) & J_{22}(x) \end{pmatrix}. \tag{43}$$

The difference from the standard Turing system analysis for a homogeneous system emerges from the spatial dependence of $\mathbf{J}(x)$ preventing the decoupling of individual eigenmodes and hence preventing a straightforward solution. However, we can take the advantage of the fact that $\mathbf{J}(x)$ contains only constants and step functions, all satisfying Neumann boundary conditions and hence within the span of the eigenfunctions $\{y_k\}$

$$\mathbf{J}(x) = \sum_{k=0}^{\infty} \underbrace{\begin{pmatrix} J_{11}^{(k)} & J_{12}^{(k)} \\ J_{21}^{(k)} & J_{22}^{(k)} \end{pmatrix}}_{\mathbf{J}^{(k)}} y_k(x). \tag{44}$$

The system can be rewritten as

$$\sum_{n=0}^{\infty} \left[\begin{pmatrix} \partial_t A_n \\ \partial_t B_n \end{pmatrix} y_n(x) + \mathbf{D} \begin{pmatrix} A_n \\ B_n \end{pmatrix} \kappa_n y_n(x) - \sum_{k=0}^{\infty} \underbrace{\begin{pmatrix} J_{11}^{(k)} & J_{12}^{(k)} \\ J_{21}^{(k)} & J_{22}^{(k)} \end{pmatrix} \begin{pmatrix} A_n \\ B_n \end{pmatrix}}_{=:\mathbf{C}_{k,n}} y_k(x) y_n(x) \right] = 0. \tag{45}$$

The eigenfunctions of the negative Laplacian on a one-dimensional interval are of the well-known form $y_n(x) = \cos(n\pi x/L)$ and hence we have

$$\begin{aligned} y_k(x) y_n(x) &= \frac{1}{2} \left(\cos \frac{(n+k)\pi x}{L} + \cos \frac{(n-k)\pi x}{L} \right) = \frac{1}{2} \left(\cos \frac{(n+k)\pi x}{L} + \cos \frac{|n-k|\pi x}{L} \right) = \\ &= \frac{y_{n+k}(x) + y_{|n-k|}(x)}{2}, \end{aligned} \tag{46}$$

which are again functions from the orthogonal basis. To obtain the dispersion relation we need to reorder the second sum to be able to factor out the function $y_n(x)$ and then invoke orthogonality of the orthogonal basis to transform the problem into an infinite system of ordinary differential equations. Denoting the coefficients in the internal sum by $\mathbf{C}_{k,n} \in \mathbb{R}^2$ we obtain the following form of the system:

$$\begin{aligned}\sum_{m=0}^{\infty} \begin{pmatrix}\partial_t A_m \\ \partial_t B_m\end{pmatrix} y_m(x) + \mathbf{D}\begin{pmatrix}A_m \\ B_m\end{pmatrix}\kappa_m y_m(x) = \\ = \frac{1}{2}\sum_{m=0}^{\infty}\left(\sum_{n=0}^{m}\mathbf{C}_{m-n,n} + \sum_{n=m}^{\infty}\mathbf{C}_{n-m,n}\right) y_m(x) + \frac{1}{2}\sum_{m=1}^{\infty}\sum_{n=0}^{\infty}\mathbf{C}_{n+m,n} y_m(x).\end{aligned} \tag{47}$$

The coupled evolution equations for the eigenmodes are then of the form:

$$\begin{aligned}0 &= \begin{pmatrix}\partial_t A_m \\ \partial_t B_m\end{pmatrix} + \mathbf{D}\begin{pmatrix}A_m \\ B_m\end{pmatrix}\kappa_m - \frac{1}{2}\sum_{n=0}^{\infty}\mathbf{C}_{|m-n|,n} - \frac{1}{2}\sum_{n=0}^{\infty}\mathbf{C}_{m+n,n} - \frac{1}{2}\mathbf{C}_{0,m}, \quad \text{for } m \geq 1, \\ 0 &= \begin{pmatrix}\partial_t A_0 \\ \partial_t B_0\end{pmatrix} + \mathbf{D}\begin{pmatrix}A_0 \\ B_0\end{pmatrix}\kappa_0 - \frac{1}{2}\sum_{n=0}^{\infty}\mathbf{C}_{n,n} - \frac{1}{2}\mathbf{C}_{0,0}.\end{aligned} \tag{48}$$

In our case, the elements of matrices $\mathbf{J}^{(k)}$ can be computed as:

$$\begin{aligned}J_{ij}^{(k)} &= \frac{\langle s_{ij}\Theta_\xi(x), y_k(x)\rangle}{\|y_k(x)\|^2} = \frac{2}{L}\int_\xi^L s_{ij}\cos\frac{k\pi x}{L}\mathrm{x} = -\frac{2s_{ij}}{k\pi}\sin\frac{k\pi\xi}{L}, \\ J_{ij}^{(0)} &= \frac{\langle J_{ij}(x), y_0(x)\rangle}{\|y_0(x)\|^2} = J_{ij}^{L} + \frac{s_{ij}(L-\xi)}{L}.\end{aligned} \tag{49}$$

While in the case of spatial homogeneity, the spectrum and dispersion relation for the system rate of growth in terms of wavenumber is given by the solvability condition for the eigenmodes, the analogous information is not analytically accessible in this framework for spatially heterogeneous functions.

Nevertheless, system (48) is linear and hence the solution can be written in terms of an exponential of a linear operator. Since we are not able to calculate the spectrum of the infinite matrix (for more illustrative form see appendix A.3 in [47], the case of only one parameter $J_{11}(x)$ as a step function)

$$\begin{pmatrix}
J_{11}^{(0)} - d_1\kappa_0 & J_{12}^{(0)} & \frac{J_{11}^{(1)}}{2} & \frac{J_{12}^{(1)}}{2} & \dots \\
J_{21}^{(0)} & J_{22}^{(0)} - d_2\kappa_0 & \frac{J_{21}^{(1)}}{2} & \frac{J_{22}^{(1)}}{2} & \dots \\
J_{11}^{(1)} & J_{12}^{(1)} & J_{11}^{(0)} + \frac{J_{11}^{(2)}}{2} - d_1\kappa_1 & J_{12}^{(0)} + \frac{J_{12}^{(2)}}{2} & \dots \\
J_{21}^{(1)} & J_{22}^{(1)} & J_{21}^{(0)} + \frac{J_{21}^{(2)}}{2} & J_{22}^{(0)} + \frac{J_{22}^{(2)}}{2} - d_2\kappa_1 & \dots \\
J_{11}^{(2)} & J_{12}^{(2)} & \frac{J_{11}^{(1)}+J_{11}^{(3)}}{2} & \frac{J_{12}^{(1)}+J_{12}^{(3)}}{2} & \dots \\
J_{21}^{(2)} & J_{22}^{(2)} & \frac{J_{21}^{(1)}+J_{21}^{(3)}}{2} & \frac{J_{22}^{(1)}+J_{22}^{(3)}}{2} & \dots \\
J_{11}^{(3)} & J_{12}^{(3)} & \frac{J_{11}^{(2)}+J_{11}^{(4)}}{2} & \frac{J_{12}^{(2)}+J_{12}^{(4)}}{2} & \dots \\
J_{21}^{(3)} & J_{22}^{(3)} & \frac{J_{21}^{(2)}+J_{21}^{(4)}}{2} & \frac{J_{22}^{(2)}+J_{22}^{(4)}}{2} & \dots \\
\vdots & \vdots & \vdots & \vdots & \ddots
\end{pmatrix} \tag{50}$$

we will use MATLAB to estimate it by calculating spectrum of its truncated principal submatrix $\mathbf{M}_n \in \mathbb{C}^{2n,2n}$. First let us explore some properties of the infinite matrix. It can be rewritten via the following synoptic sum of two matrices

$$\begin{pmatrix} 0 & \frac{\mathbf{J}^{(1)}}{2} & \frac{\mathbf{J}^{(2)}}{2} & \frac{\mathbf{J}^{(3)}}{2} & \frac{\mathbf{J}^{(4)}}{2} & \cdots \\ \mathbf{J}^{(1)} & \frac{\mathbf{J}^{(2)}}{2} & \frac{\mathbf{J}^{(1)}+\mathbf{J}^{(3)}}{2} & \frac{\mathbf{J}^{(2)}+\mathbf{J}^{(4)}}{2} & \frac{\mathbf{J}^{(3)}+\mathbf{J}^{(5)}}{2} & \cdots \\ \mathbf{J}^{(2)} & \frac{\mathbf{J}^{(1)}+\mathbf{J}^{(3)}}{2} & \frac{\mathbf{J}^{(4)}}{2} & \frac{\mathbf{J}^{(1)}+\mathbf{J}^{(5)}}{2} & \frac{\mathbf{J}^{(2)}+\mathbf{J}^{(6)}}{2} & \cdots \\ \mathbf{J}^{(3)} & \frac{\mathbf{J}^{(2)}+\mathbf{J}^{(4)}}{2} & \frac{\mathbf{J}^{(1)}+\mathbf{J}^{(5)}}{2} & \frac{\mathbf{J}^{(6)}}{2} & \frac{\mathbf{J}^{(1)}+\mathbf{J}^{(7)}}{2} & \cdots \\ \mathbf{J}^{(4)} & \frac{\mathbf{J}^{(3)}+\mathbf{J}^{(5)}}{2} & \frac{\mathbf{J}^{(2)}+\mathbf{J}^{(6)}}{2} & \frac{\mathbf{J}^{(1)}+\mathbf{J}^{(7)}}{2} & \frac{\mathbf{J}^{(8)}}{2} & \cdots \\ \vdots & \vdots & \vdots & \vdots & \vdots & \ddots \end{pmatrix} + \bigoplus_{k=0}^{\infty} \begin{pmatrix} J_{11}^{(0)} - d_1\kappa_k & J_{12}^{(0)} \\ J_{21}^{(0)} & J_{22}^{(0)} - d_2\kappa_k \end{pmatrix} \quad (51)$$

where $\otimes$ stands for the Kronecker product and $\oplus$ denotes a direct sum.

Since $J_{ij}^{(k)}$ denotes a Fourier coefficient and its norm vanishes for $k \to \infty$, the first matrix is bounded, compact and has a high degree of symmetry and therefore can be intuitively understood as a small perturbation of the second matrix which is unbounded since κ_k grows to infinity as $k \to \infty$. We will not be able to show that the spectrum of the infinite matrix is a limit of the spectrum of the truncated matrices but we shall show that the stability of the truncated linear system is determined by spectrum of a matrix of a relatively small dimension. Further we may justify truncating the matrix due to the continuum approximation, which is behind the formulation of the model itself.

At the end of this subsection, we shall show that with $\sigma(\mathbf{M}_{N+1})$ denoting the spectrum of the truncated matrix $\mathbf{M}_{N+1}$

$$\begin{pmatrix} 0 & \frac{\mathbf{J}^{(1)}}{2} & \frac{\mathbf{J}^{(2)}}{2} & \cdots & \frac{\mathbf{J}^{(N)}}{2} \\ \mathbf{J}^{(1)} & \frac{\mathbf{J}^{(2)}}{2} & \frac{\mathbf{J}^{(1)}+\mathbf{J}^{(3)}}{2} & \cdots & \frac{\mathbf{J}^{(N-1)}+\mathbf{J}^{(N+1)}}{2} \\ \mathbf{J}^{(2)} & \frac{\mathbf{J}^{(1)}+\mathbf{J}^{(3)}}{2} & \frac{\mathbf{J}^{(4)}}{2} & \cdots & \frac{\mathbf{J}^{(N-2)}+\mathbf{J}^{(N+2)}}{2} \\ \mathbf{J}^{(3)} & \frac{\mathbf{J}^{(2)}+\mathbf{J}^{(4)}}{2} & \frac{\mathbf{J}^{(1)}+\mathbf{J}^{(5)}}{2} & \cdots & \frac{\mathbf{J}^{(N-3)}+\mathbf{J}^{(N+3)}}{2} \\ \vdots & \vdots & \vdots & \ddots & \vdots \\ \mathbf{J}^{(N)} & \frac{\mathbf{J}^{(N-1)}+\mathbf{J}^{(N+1)}}{2} & \frac{\mathbf{J}^{(N-2)}+\mathbf{J}^{(N+2)}}{2} & \cdots & \frac{\mathbf{J}^{(2N)}}{2} \end{pmatrix} + \bigoplus_{k=0}^{N} \begin{pmatrix} J_{11}^{(0)} - d_1\kappa_k & J_{12}^{(0)} \\ J_{21}^{(0)} & J_{22}^{(0)} - d_2\kappa_k \end{pmatrix}$$

it holds that $\sigma(\mathbf{M}_{N+1}) \approx \sigma(\mathbf{M}_N) \cup \{-d_1\kappa_N + O(1), -d_2\kappa_N + O(1)\}$ as $N \to \infty$.

In particular, we shall show that with N large enough, two eigenvalues are of the order κ_N (which grows to infinity as $N \to \infty$). With $\lambda = \mu\kappa_N$, $\mu = O(1)$ as $N \to \infty$ we have that

$$\begin{aligned} \det(\mathbf{M}_{N+1} - \lambda\mathbf{I}) = \kappa_N^2 \Bigg\{ \left[\det(\mathbf{M}_N - \lambda\mathbf{I}) \left(\frac{1}{\kappa_N}(J_{11}^{(0)} + J_{11}^{(2N)}/2) - d_1 - \mu \right) + O(\kappa_N)^{2N-1} \right] \\ \times \left(\frac{2J_{22}^{(0)} + J_{22}^{(2N)}}{2\kappa_N} - d_2 - \mu \right) + \frac{(2J_{12}^{(0)} + J_{12}^{(2N)})(2J_{21}^{(0)} + J_{21}^{(2N)})}{4\kappa_N} O(\kappa_N)^{2N} \Bigg\} = \\ = \det(\mathbf{M}_N - \lambda\mathbf{I}) \left(J_{22}^{(0)} + \frac{J_{22}^{(2N)}}{2} - \kappa_N(d_2 + \mu) \right) \left(J_{11}^{(0)} + \frac{J_{11}^{(2N)}}{2} - \kappa_N(d_1 + \mu) \right) + O(\kappa_N)^{2N+1}, \end{aligned}$$

where we note that the $\det(\mathbf{M}_N)$ is a polynomial of $2N$-th order. Therefore two eigenvalues are indeed of the order κ_N, in particular $\lambda_1 = -d_1\kappa_N + O(1)$ and $\lambda_2 = -d_2\kappa_N + O(1)$, while the remaining $2N$ eigenvalues are (in the leading order) the eigenvalues of $\mathbf{M}_N$. Hence the information about the stability associated with an arbitrarily large truncated matrix can be

deduced from a smaller matrix $\mathbf{M}_N$ (in practice the choice of $N = 50$ seems to be good enough). In addition, we anticipate that this characteristic of the spectrum will translate even into case with the arbitrarily large N and which seems to be confirmed by the numerical calculations.

3.2.4 Formulation and numerical verification of DDI conditions for linear case

Spectral theory as detailed in the previous subsection yields a plausible approach to stability analysis but its practical use seems to be limited as the algebraic complexity even after truncation requires a numerical approach and provides neither information about one-sided patterns nor the effect of spatial heterogeneity on the spatial frequency variation in the resulting pattern. The asymptotes, on the other hand, can be used to estimate conditions for Turing pattern emergence and its classification.

As a summary of all the above partial results suggests that the conjectured conditions are of the form of conditions for Turing's diffusively driven instability evaluated for the system with constant coefficients considered separately on intervals $(0, \xi)$ and (ξ, L). Therefore, let us denote the following conditions for the latter interval:

$$\begin{aligned}
T1^R &:= J_{11}^L + s_{11} + J_{22}^L + s_{22} < 0,\\
T2^R &:= (J_{11}^L + s_{11})(J_{22}^L + s_{22}) - (J_{12}^L + s_{12})(J_{21}^L + s_{21}) > 0,\\
T3^R &:= (J_{11}^L + s_{11})d_2 + (J_{22}^L + s_{22})d_1 > 0,\\
T4^R &:= ((J_{11}^L + s_{11})d_2 + (J_{22}^L + s_{22})d_1)^2 - 4d_1d_2((J_{11}^L + s_{11})(J_{22}^L + s_{22}) -\\
&\qquad - (J_{12}^L + s_{12})(J_{21}^L + s_{21})) > 0,
\end{aligned} \tag{52}$$

and analogously for the former interval $T1^L$-$T4^L$ (particularly noting that $Ti^L \equiv Ti^R$, $i \in \{1, \ldots, 4\}$ with all $s_{ij} = 0$).

Now, we have eight conditions (52) and hence 256 combinations to be analysed. Such number is too large to be analysed one by one, therefore we deduce some additional assumptions. Since we are interested in a phenomenon similar to Turing's self-organisation, we disregard the case when the kinetics themselves induce instability. In classical Turing patterning two of the DDI conditions are equivalent to a requirement of a stable homogeneous steady state in the absence of diffusion [41]. Therefore, in our case we assume that $T1^L \wedge T2^L \wedge T1^R \wedge T2^R$ holds (corresponding to a stable homogeneous steady state on both parts of $(0, L)$) and we focus on the remaining 16 combinations.

The sets corresponding to each combination are denoted by distinct regions, see table 2. For all parameters in each region we want to know if a pattern can emerge or not (that means particularly in the case of linear kinetics: whether a small perturbation exponentially increases or decays in time). This crucially includes an assessment of whether one can assign this property of pattern existence to every point in each region, independent of further details. As it was noted in the previous analysis of linear system stability, we use two tools: (i) calculating the largest real part of eigenvalues of the truncated matrix (50), using MATLAB and (ii) solving the evolution problem (39) using Mathematica (for more details on computational approaches see appendix A.4).

In both approaches we take large sets of parameter values sampling each region. Other parameters are fixed for every numerical experiment if it is not stated otherwise. The step location is at $\xi = 120$, with $L = 400$, where the latter has been chosen to be sufficiently large so as not to prevent a possible pattern due to insufficient room in the domain (as checked by confirming the results are unchanged with $\xi = 300$, $L = 1000$ and $\xi = 30$, $L = 100$ for example,

$T1^L \wedge T1^R \wedge T2^L \wedge T2^R$				
	$T3^L \wedge T3^R$	$\neg T3^L \wedge T3^R$	$T3^L \wedge \neg T3^R$	$\neg T3^L \wedge \neg T3^R$
$T4^L \wedge T4^R$	(U,+)	(U,+)	(U,+)	(0,-)
$\neg T4^L \wedge T4^R$	(U,+)	(U,+)	(0,-)	(0,-)
$T4^L \wedge \neg T4^R$	(U,+)	(0,-)	(U,+)	(0,-)
$\neg T4^L \wedge \neg T4^R$	(0,-)	(0,-)	(0,-)	(0,-)
$\neg(T1^L \wedge T1^R \wedge T2^L \wedge T2^R)$				
(U,+)				

Table 2: The table summarising the results for the regions, i.e. the sets of the parameters satisfying combinations of the conditions (52) in the explored parameter space. All parameters in each region exhibit the same behaviour. We impose the following designation: U and 0 denote unbounded and zero long-time solutions of the evolution problem, $+$ and $-$ denote signs of the largest real part of eigenvalues of the matrix (50).

not shown). Further, to reduce the seven (not considering L) dimensional parameter space we fix diffusion coefficients with a sufficiently large ratio $d_1 = 1, d_2 = 100$ and also fix $s \in (-1, 1)$. The remaining parametric space was discretized and the comparison between the identified conditions and computations was examined in 2D slices of this parameter space and the slices with varying J_{11}^L, J_{12}^L have been presented in fig. 6.

Before we present the relation between conditions (52) and pattern formation, we compare the numerical and spectral approaches based on computational results. First, the results from the spectral approach concur with those from solving the evolution problem. In particular, with the possible exception of the very near vicinity of the parameter space boundaries between differing stability behaviours, the largest real part of eigenvalues is negative if and only if the supremum norm of the solution to the evolution problem is smaller than the initial norm. Due to the conformity of the results from both methods while being very different conceptually the conclusions from either approximation are inferred to be generally accurate.

Second, the character of pattern emergence is indeed the same within each region from table 2. Particularly, if two regions express an opposite behaviour, the change is located exactly on the border of the regions (with negligible imperfection due to numerical imprecision). Hence, these observations entail a justification of the chosen conditions (52).

The results are outlined in table 2 and fig. 6 which can be summarised as: a Turing pattern will emerge for a large enough $\min(\xi, L-\xi)$ with unstable eigenmodes that satisfy the boundary conditions if and only if

$$\left(T1^L \wedge T2^L \wedge T1^R \wedge T2^R\right) \wedge \left(\left(T3^L \wedge T4^L\right) \vee \left(T3^R \wedge T4^R\right)\right) \tag{53}$$

holds.

3.2.5 Specification and numerical verification of DDI conditions for nonlinear case

From the spectral analysis and numerical verification we obtained condition (53) for determining whether the non-linear system exhibits Turing pattern or not. Nevertheless, it does not give us a direct answer to our second task to distinguish among all the one-sided pattern and both-sided pattern in the case of non-linear kinetics, which is clearly beyond the scope of the spectral

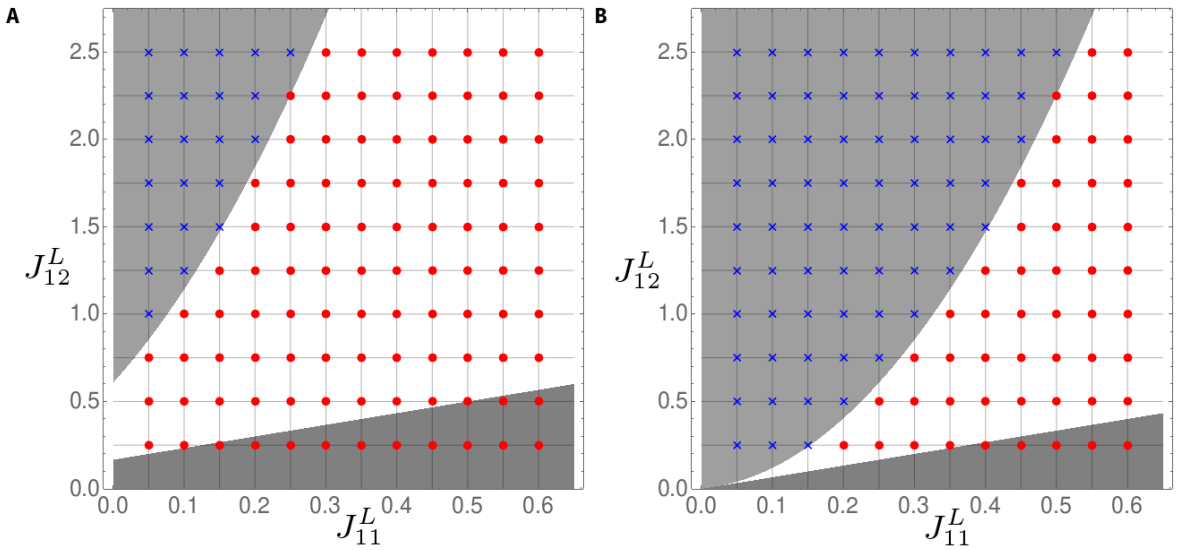

Figure 6: An illustration of the match between the identified Turing instability conditions for affine kinetics, Eqn. (53), and the results from the evolution of system (40) with $c_1(x) = 1$, $c_2(x) = 3$, $J_{21}(x) = -3$, $J_{22}(x) = -2$, $s_{12} = 0$, $L = 100$, $\xi = 30$, $d_1 = 1$, $d_2 = 100$ and: A) $s_{11} = 0.25$, B) $s_{11} = -0.25$. The remaining two parameters, J_{11}^L, J_{12}^L, are considered as parameters for exploring stability properties and are on the x and y axes. In the background the conditions (53) are plotted in the grayscale, which, in increasing grayscale intensity, highlight regions with an unbounded solution indicating the existence of pattern (white), decaying solution indicating no-pattern and the region where $T1^L \wedge T2^L \wedge T1^R \wedge T2^R$ does not hold (the darkest grey). The spots denote the resulting pattern type based on numerical solution to the evolution problem: an unbounded solution indicating a pattern (a red disk) and decaying solutions corresponding to no-pattern (a blue cross).

analysis in the previous section. However, from the current approach we can observe a strong indication for the hypothesis, in what form such tool should be composed from conditions (52).

In particular assuming $T1^L \wedge T2^L \wedge T1^R \wedge T2^R$ it could be expected that a pattern on the left will emerge only if $T3^L \wedge T4^L$ holds and the pattern on the right will emerge only if $T3^R \wedge T4^R$ holds. Therefore we propose and will subsequently numerically verify the following conditions:

$$\begin{aligned}
&T1^L \wedge T2^L \wedge T1^R \wedge T2^R \wedge \quad (T3^L \wedge T4^L) \wedge \quad (T3^R \wedge T4^R) && \text{pattern on both sides,}\\
&T1^L \wedge T2^L \wedge T1^R \wedge T2^R \wedge \quad (T3^L \wedge T4^L) \wedge \neg(T3^R \wedge T4^R) && \text{pattern on the left side,}\\
&T1^L \wedge T2^L \wedge T1^R \wedge T2^R \wedge \neg(T3^L \wedge T4^L) \wedge \quad (T3^R \wedge T4^R) && \text{pattern on the right side,}\\
&T1^L \wedge T2^L \wedge T1^R \wedge T2^R \wedge \neg(T3^L \wedge T4^L) \wedge \neg(T3^R \wedge T4^R) && \text{no-pattern.}
\end{aligned} \tag{54}$$

and we shall use both the spectral approach and numerical solution of the full system to verify these conditions. The former can be used just for the assessment of (in)stability while the latter will be employed to check these conditions for the existence of one-sided pattern.

black!25 We proceed to test this, considering Schnakenberg kinetics

$$f(u,v) = a - u + u^2 v, \quad g(u,v) = b - u^2 v, \tag{55}$$

and Gierer-Meinhardt kinetics

$$f(u,v) = a - bu + \frac{u^2}{v}, \quad g(u,v) = u^2 - v, \tag{56}$$

with a,b positive constants as two exemplars for reaction kinetics in Turing models.

Numerical experiments have been implemented using Wolfram Mathematica as in the linear case (see appendix A.4). The terminal time is $\tau = 10^3$. This choice was sufficient to distinguish the non-existence of pattern from its presence, where in the latter case the convergence of a norm was clearly observed suggesting a convergence of the long-time solutions to stationary patterns. The initial condition was set to be small random noise around the stationary solution $(\bar{u}(x), \bar{v}(x))$. For both choices of kinetics we take $L = 400$, $\xi = 120$, $d_1 = 1$, $d_2 = 100$; this parameter selection follows the reasoning from the linear case. Large sets of the remaining parameters a, b, s are considered to capture the rich behaviour sufficiently to illustrate the legitimacy of the instability conditions (54).

In particular, the types of pattern resulting from simulations agree well with the predictions given by conditions (54) as depicted in fig. 7. The degree of correspondence seems to be very high at least in the tested scenarios (kinetics and parameters selection) giving merit to the approach and the resulting conditions, despite the absence of rigour.

3.3 Boundary layer analysis

To proceed with the analysis for general kinetics and to facilitate a boundary layer analysis we regularise the Heaviside replacing $h(x)$ with

$$h_\delta(x) = \frac{s}{2}\left[1 + g\left(\frac{x-\xi}{\delta}\right)\right], \qquad \text{with } g \in C^\infty(R), \lim_{x\to\pm\infty} g(x) = \pm 1,\ g' \geq 0$$

where one can think of, for example,

$$h_\delta(x) = \frac{s}{2}\left[1 + \tanh\left(\frac{x-\xi}{\delta}\right)\right]$$

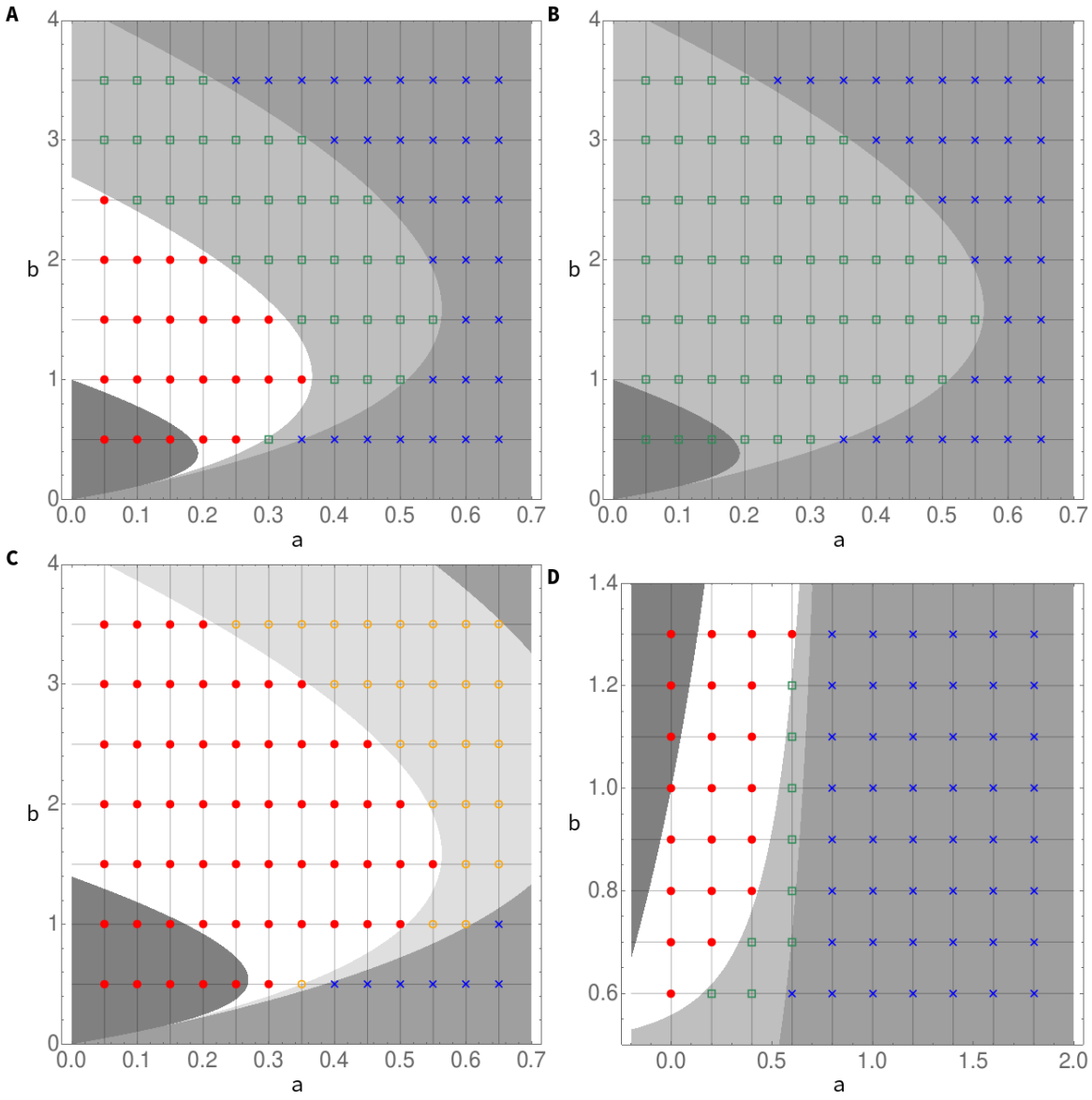

Figure 7: An illustration of the match between the identified Turing instability conditions, Eqn. (54), and the results from the evolution of system (34) with Schnakenberg kinetics: A) $s = 0.25$, B) $s = 0.75$, C) $s = -0.25$; and Gierer-Meinhardt kinetics: D) $s = 0.5$. In the background the conditions (54) are plotted in the grayscale, which, in increasing grayscale intensity, highlight regions with a both-sided pattern (white), a right-sided pattern, left-sided pattern, no-pattern and the region where $T1^L \wedge T2^L \wedge T1^R \wedge T2^R$ does not hold (the darkest grey). The spots denote the resulting pattern type based on numerical solution to the evolution problem: a both-sided pattern (a red disk), a left-sided pattern (a green square), a right-sided pattern (an orange circle) and no-pattern (a blue cross).

and consider small values of $\delta > 0$. Then the steady state (assuming it exists), (u_s, v_s), satisfies

$$\begin{aligned} 0 &= d_1 \partial_{xx} u_s + f(u_s, v_s) + h_\delta(x) u_s \\ 0 &= d_2 \partial_{xx} v_s + g(u_s, v_s) \end{aligned} \quad \text{on } (0, L). \tag{57}$$

Expanding about the steady state that is not designated to be a pattern, as described earlier, we have

$$u = u_s + \tilde{u}, \qquad v = v_s + \tilde{v},$$

with

$$\begin{aligned} \tilde{u}_t &= d_1 \partial_{xx} \tilde{u} + J_{11}(u_s, v_s)\tilde{u} + J_{12}(u_s, v_s)\tilde{v} + h_\delta(x)\tilde{u} \\ \tilde{v}_t &= d_2 \partial_{xx} \tilde{v} + J_{21}(u_s, v_s)\tilde{u} + J_{22}(u_s, v_s)\tilde{v} \end{aligned} \quad \text{on } (0, L), \tag{58}$$

where $\mathbf{J}(u_s, v_s)$ is the Jacobian of the kinetics about the steady solution (u_s, v_s).

We proceed with a boundary layer analysis. Based on the continuity of solution on data we argue that for small enough jump s the steady state solution that does not correspond to a pattern will be approximately $(\bar{u}^L, \bar{v}^L)$ sufficiently to the left of $x = \xi$ and approximately $(\bar{u}^R, \bar{v}^R)$ sufficiently to the right, where

$$\begin{aligned} f(\bar{u}^L, \bar{v}^L) = 0 &= g(\bar{u}^L, \bar{v}^L) \\ f(\bar{u}^R, \bar{v}^R) + s\bar{u}^R = 0 &= g(\bar{u}^R, \bar{v}^R). \end{aligned}$$

Hence for $x < \xi$, $|x - \xi| \gg \delta$ we anticipate the approximation

$$\tilde{u}_t = d_1 \partial_{xx} \tilde{u} + J_{11}(\bar{u}^L, \bar{v}^L)\tilde{u} + J_{12}(\bar{u}^L, \bar{v}^L)\tilde{v}, \qquad \tilde{v}_t = d_2 \partial_{xx} \tilde{v} + J_{21}(\bar{u}^L, \bar{v}^L)\tilde{u} + J_{22}(\bar{u}^L, \bar{v}^L)\tilde{v} \tag{59}$$

and similarly

$$\tilde{u}_t = d_1 \partial_{xx} \tilde{u} + J_{11}(\bar{u}^R, \bar{v}^R)\tilde{u} + J_{12}(\bar{u}^R, \bar{v}^R)\tilde{v} + s\tilde{u}, \qquad \tilde{v}_t = d_2 \partial_{xx} \tilde{v} + J_{21}(\bar{u}^R, \bar{v}^R)\tilde{u} + J_{22}(\bar{u}^R, \bar{v}^R)\tilde{v} \tag{60}$$

for $x > \xi$, $|x - \xi| \gg \delta$. These can be considered as the outer problems for a leading order boundary layer approximation.

We proceed to consider the prospects of an internal boundary layer near $x \approx \xi$. Indeed noting the form of $h_\delta(x)$, which drives hetergeneous behaviour near $x = \xi$, one can rescale the spatial component via

$$X = (x - \xi)/\delta.$$

This will lead to the absence of a dominant balance for an inner expansion with $\tilde{u} \sim u_{in}(X, t) + o(1)$, which instead yields $d_1 \partial_{XX} u_{in} = 0$ at leading order, with an analogous observation for $\tilde{v} \sim v_{in}(X, t) + o(1)$. The resulting linear solution behaviour is divergent as $|X| \to \infty$ unless u_{in} and v_{in} are constant, indicating no boundary layer, but instead a matching of the left and right outer solutions, via a nominal but constant inner layer solution. Given the kinetics are assumed to be order unity as δ is decreased, a dominant balance at leading order, and thus more complex dynamics, is only conceivable with the concomitant temporal rescaling, $T = t/\delta^2$. Then, at leading order

$$\partial_T u_{in} = d_1 \partial_{XX} u_{in}, \qquad \partial_T v_{in} = d_2 \partial_{XX} v_{in},$$

with the kinetics subdued by a factor of δ^2. The resulting dynamics is very fast and, more importantly, pure diffusion. Thus it will not drive patterning within the inner region but

instead instigate diffusion on a very fast timescale, acting to homogenise across the inner region, whereby for $T \gg 1$, i.e. $t \gg \delta^2$, one will expect an inner solution which is approximately constant after transients have relaxed even if the initial conditions are highly varying in the vicinity of $x \approx \xi$.

Hence, considering the impact of $\delta \ll 1$, with the limit of zero δ corresponding to the Heaviside function of interest in the kinetics, the evidence is that the inner solution of a boundary layer analysis does not induce patterning but has a rather trivial dynamics. Instead, the behaviour of the outer solutions, i.e. Eqns. (59), (60), is indicated as governing the propensity of system patterning. Proceeding, this allows one to infer that if both outer solutions are unstable, then instability on both sides of $x = \xi$ is expected. In contrast, if one outer solution is unstable and the other stable, we expect an instability on one side of $x = \xi$. Analogous reasoning suggests stability if the outer solution dynamics either side of $x = \xi$ is stable. Finally, due to this local nature of the result we expect that the spatial frequency of the emerging patterns is also related locally to the Turing conditions and hence with the prospect of a change in spatial frequency of patterning across the domain.

4 Conclusion

This thesis dealt with the robustness of the Turing system, one of the possible mechanism of pattern formation. At first, this mechanism with its stability analysis was reminded and some difficulties of such simple model were mentioned. Then, in section 1.2 it was indicated by the list of possible generalizations of the original Turing system that this mechanism is widely used for a description of large amount of phenomena in various fields. The main focus of this work was the investigation of two such generalizations – to explore the Turing's pattern formation in the system with small advection in section 2 and the system with a small spatial dependency in the linear term of kinetics in section 3. In both cases, slightly modified mechanisms of the Turing's original one were employed and the influence of small added phenomena was emphasised to obtain conclusions on the question, whether these added phenomena change the behaviour of the appropriate system decisively and hence, if the Turing system is robust with respect to them. The discussion of these results follows separately for both cases with the final conclusion about the robustness of the Turing system at the end of this section.

RD system with advection In section 2 we have explored alternative mechanisms for domain-size-driven instabilities, considering the presence of advection and a number of associated boundary conditions. In particular, the need for stability of the homogeneous steady state is generally relaxed, resulting in less stringent constraints for domain-size-driven self-organisation. Additionally, Sturm-Liouville theory has been utilised in section 1.2.3 to provide a general theoretical framework that is applicable to systems on bounded domains and has allowed a more extensive study than previously presented, as illustrated for example with the further details on stability conditions for systems with differential transport and periodic boundary conditions. Furthermore, the differences in spectral analysis on finite and infinite domains [80] are anticipated to be responsible for differences in the presented results here and those associated with classical stability studies of reaction diffusion advection systems on infinite domains [81, 82, 83, 87, 88, 86, 66, 67, 95]. Finally note that a recent study about a domain-dependent driven instability [85] also generalises the idea of instability occurrence outside of the Turing mechanism.

A summary of the presented results can be found in table 1, details can be found in the corresponding subsections of section 2.3. In particular, we have found that domain-size-driven instabilities, distinct from the Turing mechanism and without the requirements of stability to homogeneous perturbations, can exist (i) in reaction diffusion systems with Dirichlet boundary conditions and (ii) in the presence of advection with Dirichlet, periodica and Danckwert's with no mass externally added for any of the species.

Patterning resulting from domain-size-driven instabilities in these cases has been shown to occur for both equal transport coefficients and when one species is immobile. Provided the matrix of linearised kinetics $\mathbf{J}$ is diagonalisable, the former case of equal transport coefficients can be rewritten into a single reaction-diffusion-advection problem and hence reveals the prospect of self-organisation due to domain size even for a single species. In addition, with equal transport of the species, no further constraints are required to ensure the absence of salt-and-pepper patterning, that is self-organisation at arbitrarily small wavelengths, which in turn induces a breakdown of the continuum approximation. In presence of one immobile species there is, in contrast, an additional requirement on the kinetics, summarised by $J_{22} < 0$, so that the immobile species is required to inhibit its own production. However this simple constraint is sufficient to entail that the observed Edar receptor dynamics in hair follicle formation is also inconsistent

with the instability mechanisms presented here [63, 35]. Note that the above analysis reveals that in both cases only the first few eigenmodes are unstable and that the first eigenmode has the largest real part of eigenvalue, and hence is the fastest growing mode. Further for large Péclet number, $\mathrm{Pe} \gg 2n\pi$ from eq. (61), the first few eigenvalues are similar in size and hence the emergent pattern can be expected to depend on initial data.

We have also shown that with Danckwert's boundary conditions, the system's stability is dependent on domain size, demonstrating a singular dependence on advection whenever Danckwert's boundary conditions are physically appropriate. This is due to the behaviour of the first mode, λ_1, and thus applies despite the fact that beyond the first few modes the Danckwert's modes are essentially the same as those due to fixed flux boundary conditions for instance. These observations emphasise the physical importance of the boundary conditions in self-organisation and highlight the prospect that extreme sensitivity to even weak advection can exist for reaction-diffusion-advection patterning dynamics.

A second objective has also been to consider the possibility of a distinguishing signature of domain-size-driven instabilities. This is enabled by the identification of explicit forms for eigenfunctions of the spatial transport operator $-\mathcal{L}_{dV}$ when there is a domain driven instability, that is for Dirichlet, Danckwert's, periodic and fixed flux boundary conditions. In particular these eigenmodes are not simply harmonics in the presence of advection, which entails that one possible signature is the spatial modulation of pattern amplitude across the domain without the need for complex feedbacks. This is even more likely in the case of spatially varying advection, though we have not considered examples of the latter in detail. However with Dirichlet boundary conditions in the absence of advection, which also exhibits a domain-size-driven instability, there is in contrast no clear distinction of the pattern from that of a standard Turing mechanism, emphasising that the observation of patterning is not sufficient in isolation to conclude that a Turing mechanism is present.

In summary, the proposed domain-size-driven instabilities induced by advection or boundary conditions introduce an alternative, less constrained, mechanism for self-organisation that still induces patterning as a domain size increases beyond a critical value. Such a patterning mechanism is not slave to the concept of short-range activation and long-range inhibition intrinsic in the Turing instability and, in the case of advection, there is a ready distinction from the Turing instability via a spatial modulation of the pattern without complex feedback. Finally, the fact domain-size-driven instability is contingent on the boundary conditions emphasises the need to consider edge effects very carefully in relating modelling to experiment and additionally highlights how the local regulation on domain boundaries can have a fundamental influence over a very long-range.

RD system with spatial dependency in kinetics In section 3 we considered a reaction diffusion system with a spatial dependence via a linear kinetic term with a coefficient in the form of a spatial step function and we analysed the resulting impact on conditions for pattern formation. First we defined a pattern as a steady solution with an inhomogeneity persevering throughout a large enough domain. Using an analytical-numerical approach we examined a case of affine kinetics and deduced conditions for pattern emergence in a very simple form, Eqn. (52). For the case of non-linear kinetics we took conditions inherited from a suitable linearisation, generalising the previous conditions to those stated in (54), with a verification for two choices of kinetics and a range of parameter values. Further note that conditions (54) and their agreement with numerics also match the intuition of at least some experimentalists in the field, e.g. [20], and suggests further analytical progress may be feasible at least for step

function behaviours in the kinetics.

If we compare our results with the previously studied system with an additive spatial step function independent of the morphogen concentrations [71], the patterns in our case have not only different amplitudes on the two sides of the step but also different frequencies. This highlights that patterning with sharp changes in spatial frequency may be a signature of kinetic heterogeneity characterised by rapid transitions in kinetics.

One interesting point is whether there is any restriction on the size of the step s. Although the final conditions (54) are well defined for any value of s, a restriction arises from our definition of a pattern in section 3.1. We need that the eventual pattern should be more significant in comparison to the inhomogeneity localised around ξ, which is expected to be true for sufficiently small s, by appeal to continuity with respect to parameters. For larger s the localised inhomogeneity will also be larger, which can be easily seen even in the linear case due to the larger gap between $\bar{u}(x)$ (resp. $\bar{v}(x)$) at the point ξ and thus has every potential to invalidate our findings for sufficiently large s.

The conditions (54) are necessary diffusion-driven instability (DDI) conditions and depend directly on the diffusion coefficients, kinetics and the size of the step. As well as in the classical Turing system, if DDI conditions hold, a large enough domain is necessary for pattern to emerge; thus the intervals $(0, \xi)$ and (ξ, L) are also required to be sufficiently large. Moreover, sufficiently large intervals are necessary for a pattern to be correctly identifiable, as seen in the comparison of fig. 4B and fig. 5B where both systems are predicted to exhibit patterning on the left of the step, but only the latter does, since the subdomain $[0, \xi)$ is smaller than the emergent pattern period in fig. 4B. Finally, note that differences in spatial frequencies are observed to be independent of both interval lengths and hence independent of both ξ and L. However, as the boundary layer analysis suggests, the spatial frequency can be different in the two parts of the domain as it is evaluated independently on the two subintervals.

Section 3 is concerned with a special case of heterogeneity in the kinetics though this can be easily generalised to a certain extent. Firstly, it is easy to see that the particular choice of a spatially dependent linear term in the kinetics is not important for the analysis even in the case of non-linear kinetics. Further, the same approach as well as the results, will be valid for a step function $h(x)$ with finitely many steps. A limitation arises, however, due to the note from the previous paragraphs – the sizes of the steps should be small enough in comparison to the surrounding intervals so that the localised inhomogeneity due to the step does not exceed the emerging pattern in magnitude/amplitude. Further, the discreteness of eigenmodes results in a lower bound on the size of the supporting intervals of each step.

The question of a generalisation to a spatial dependency is expected for slowly varying function $h(x)$. In such a case we can take an approximation of $h(x)$ using a simple function and take the advantage of conclusions of this approximative system. In the case of a more general dependency it may be difficult to show similar conclusions. Actually, as a recent study shows [48] even shallow gradients coupled to non-linear kinetics may lead to an unexpected and complex behaviour but finding a clear cut distinction between these cases is beyond the scope of this paper. Furthermore, how and where the present intuitive analysis fails also remains to be explored as do higher dimensional domains and curved geometries, which may allow ready generalisation.

We could also consider a higher-dimensional space. The presented approach is easily extendable to domains in the form of higher-dimensional rectangles. For example, one might readily find conditions yielding the emergence of a pattern with spots on one part and stripes on the other part of a higher dimensional domain.

Finally, let us finish with a summary of the identified hypothetical DDI conditions: (in)stability in the Turing model analysed here appears to be a local property and can be analysed as such, with the local assessment of whether parameters are within the Turing space providing a strong indication for an unstable eigenmode excitation, at least on a sufficiently large domain with concomitant spatial frequency heterogeneity.

Contribution to the robustness problem The robustness of the pattern formation is connected to an influence of an arbitrarily small advection, or spatial dependency respectively, to the original Turing system, i.e. system without the effect of these phenomena. These conclusions can be already obtained from the results of main parts of this thesis.

In the case of the system with advection, let us recapitulate the results summarized in section 2.3.5 comparing the systems with zero advection and with arbitrarily small, characterized by $\mathrm{Pe} \ll 1$.

The zero flux Robin boundary conditions for small advection $0 < \mathrm{Pe} \ll 1$ become Neumann for $V = 0$. The eigenvalues are

$$\lambda_0 = 0, \quad \lambda_n = \frac{d}{L^2}\left((n\pi)^2 + \frac{1}{4}\mathrm{Pe}^2\right), \quad n \in \mathbb{N} \tag{61}$$

with the corresponding eigefunctions

$$\gamma_0 = e^{\mathrm{Pe}\frac{x}{L}}, \quad \gamma_n = c(V, L, d, n)e^{\frac{\mathrm{Pe}}{2}\frac{x}{L}}\left(\frac{\mathrm{Pe}}{2n\pi}\sin\left(\frac{n\pi}{L}x\right) + \cos\left(\frac{n\pi}{L}x\right)\right).$$

Therefore we may conclude that the spectrum for $V = 0$ is close to that of $0 < \mathrm{Pe} \ll 1$, whilst the eigenfunctions are continuously transformed into the eigenfunctions of a reaction diffusion system as the Péclet number vanishes.

Similarly for Dirichlet boundary condition, which are independent of Pe, one has that the distance between the spectra is proportional to Pe^2 while the difference in the eigenfunctions is also on the scale of Pe. For the periodic boundary condition (being again identical in both cases) the spectra consist of a countable set of points located on a line parallel to real axis, with its distance to the spectrum of the associated reaction diffusion problem proportional to $i2n\pi\mathrm{Pe}$. As the distance depends on the wavenumber, n, the spectra are always different with significant differences appearing for large wavenumbers not affecting the stability properties of the system due to the above mentioned cut-off. Finally, Danckwert's boundary conditions, which collapse to a zero-flux reaction diffusion system for $V = 0$, have a very different spectrum as it is always separated from zero. For $0 < \mathrm{Pe} \ll 1$, the first few eigenvalues determine the system's behaviour as $\lambda_1 \sim \frac{d}{L^2}\mathrm{Pe}^{3/2}$ which can be arbitrarily large for sufficiently small L. In contrast for $V = 0$ one always has stability, as follows from standard Turing analysis [64, 35, 104]. To have similar spectra one would have to require $\mathrm{Pe} \ll 1$ but still the effects on stability properties for arbitrarily small but non-zero Péclet number are profound.

Finally note that for constant advection we may denote by τ the time required for a species to be advected from one boundary to the other. Then $\mathrm{Pe} = LV/d = \tau L^2/d$, while in developmental and cell biology applications one typically considers $d \sim 10^{-9}\mathrm{m}^2\mathrm{s}^{-1}$ with $L \sim 10^{-3}\mathrm{m}$, which suggests in this situation that $\mathrm{Pe} \leq 1$ requires $V \leq 10^{-6}\mathrm{m\ s}^{-1}$. Hence the Péclet number may have a significant effect on systems behaviour as discussed above, even for the small scales of advective velocity in cellular physiology.

For the case of spatial dependency, the conclusions follow directly from obtained results. From its form (52) folows that the conditions (54) are contionuous in s for s around zero and therefore the emergence of Turing patterns occurs for $s = 0$ and $s \ll 1$ in the same cases. Moreover, this continuity of the system behaviour with respect to s preserves in the whole problem – the homogeneous steady state is smoothly transformed into steady state of the type no-pattern; from numerical experiments we can deduced that the period in patterns (in the sence of section 3) changes according to changes in s; and finally the whole procedure of stability analysis outlined in section 3.2 become standard if we suppose special choice $s = 0$. As a summary of these observations, we can conclude that the standard the Turing system, if its main idea is expanded in same way as it is presented in section 3.1, is robust with respect to small effects of such spatial dependency in kinetics.

Acknowledgment

I would like to express my deepest gratitude to my supervisor Václav Klika for his endless patience with which he constantly helped me to reshape my thoughts into the legible academic form, spend lots of time discussing on crucial difficulties, and for all the opportunities aiding me in the research that he provided me throughout my doctoral studies.

I would also like to thank all the colleagues from Mathematical and biological seminar and from MAFIA, the working group at the Department of Mathematics, for the inspirational discussions and valuable advice.

V neposlední řadě děkuji celé své rodině za důvěru a neutuchající podporu, a to i přesto, že jsem nebyl schopen dostatečně vysvětlit, čemu se to vlastně věnuji.

Presented work was partially supported by the Student Grant Agency of the Czech Technical University in Prague No. SGS12/198/OHK4/3T/14 and SGS15/215/OHK4/3T/14, and partially within the CENTEM project, reg. no. CZ.1.05/2.1.00/03.0088.

A Appendix

A.1 Diagonalization

This section outlines a method, which we call diagonalization, to easily compute an analytical solution of the system composed of two elliptic equations with linear kinetics. This procedure will be used in appendix A.2 to compute analytic solution to system (39), i.e. the system with affine kinetics and step functions as coefficients. This procedure follows [71].

We consider a linear elliptic system with the trivial solution

$$\begin{aligned} -\Delta u &= a_{11}u + a_{12}v, \\ -\Delta v &= a_{21}u + a_{22}v \end{aligned} \tag{62}$$

on some interval. The boundary conditions are not specified, yet. Our purpose is to obtain a particular solution via a diagonalization principle.

Adding the first equation to the r-th multiple of the second one and supposing $r \neq -a_{11}/a_{21}$ gives

$$-(\Delta u + r\Delta v) = (a_{11} + ra_{21})\left(u + \frac{a_{12} + ra_{22}}{a_{11} + ra_{21}}v\right).$$

To obtain an equation only in the variable $w = u + rv$, it suffices to hold

$$\frac{a_{12} + ra_{22}}{a_{11} + ra_{21}} = r. \tag{63}$$

The roots of the quadratic equation are of the form

$$r_{1,2} = \frac{a_{22} - a_{11} \pm \sqrt{D}}{2a_{21}}, \qquad D = \operatorname{tr}^2 \mathbf{A} - 4 \det \mathbf{A}. \tag{64}$$

Several possibilities can occur governed by the sign of the discriminant D:

Positive discriminant

Since D is positive, there exists a pair of distinct real roots. Using designation $\lambda_i = a_{11} + r_i a_{21}$, system (62) can be rewritten into a system containing two independent equations:

$$-\Delta w_i = \lambda_i w_i, \quad i = 1, 2 \tag{65}$$

Moreover, it is an easy computation that for $i = 1, 2$ the number λ_i is an eigenvalue of the matrix $\mathbf{A}$ and $(-r_{3-i}, 1)^\top$ is the corresponding eigenvector. The solution to system (65) are of the form

$$w_i = c_{i1}\cos\left(\sqrt{\lambda_i}x\right) + c_{i2}\sin\left(\sqrt{\lambda_i}x\right), \tag{66}$$

where $\mathbf{C} \in \mathbb{R}^{2\times 2}$ will be determined by boundary conditions, and hence we have the original variables

$$\begin{aligned} u &= \frac{r_1 c_{21}\cos\left(\sqrt{\lambda_2}x\right) + r_1 c_{22}\sin\left(\sqrt{\lambda_2}x\right) - r_2 c_{11}\cos\left(\sqrt{\lambda_1}x\right) - r_2 c_{12}\sin\left(\sqrt{\lambda_1}x\right)}{r_1 - r_2}, \\ v &= \frac{c_{11}\cos\left(\sqrt{\lambda_1}x\right) + c_{12}\sin\left(\sqrt{\lambda_1}x\right) - c_{21}\cos\left(\sqrt{\lambda_2}x\right) - c_{22}\sin\left(\sqrt{\lambda_2}x\right)}{r_1 - r_2}. \end{aligned} \tag{67}$$

Negative discriminant

In the case of negative D, the roots $r_{1,2}$ are complex conjugate, the diagonalized system is again of the form (65), however λ_i and w_i are also complex. Thus we take real and complex parts of the equations, we denote the real parts by the lower index R and the complex parts by the lower index C and from the obtained four equations we get a system consisting of two independent equations:

$$\begin{aligned} -\Delta w_R &= \lambda_R w_R - \lambda_C w_C, \\ -\Delta w_C &= \lambda_C w_R + \lambda_R w_C. \end{aligned} \tag{68}$$

The system is not in a diagonalized form, however it is easilly solvable if the system is rewritten into a system of four linear differential equation of the first order. Then the solutions to the problem are of the form

$$\begin{aligned} w_R &= c_2 e^{\eta_1 x}\cos\eta_2 x - c_1 e^{\eta_1 x}\sin\eta_2 x - c_4 e^{-\eta_1 x}\cos\eta_2 x + c_3 e^{-\eta_1 x}\sin\eta_2 x, \\ w_C &= c_1 e^{\eta_1 x}\cos\eta_2 x + c_2 e^{\eta_1 x}\sin\eta_2 x + c_3 e^{-\eta_1 x}\cos\eta_2 x + c_4 e^{-\eta_1 x}\sin\eta_2 x, \end{aligned} \tag{69}$$

where c_i are real constants and η_1, η_2 denote the real and the complex part of the square root of $-\lambda_R + i\lambda_C$, i.e.

$$\begin{aligned} \eta_1 &= |\operatorname{Re}\sqrt{-\lambda_R + i\lambda_C}| = \sqrt{\frac{-\lambda_R + \sqrt{(\lambda_R)^2 + (\lambda_C)^2}}{2}}, \\ \eta_2 &= |\Im\sqrt{-\lambda_R + i\lambda_C}| = \sqrt{\frac{\lambda_R + \sqrt{(\lambda_R)^2 + (\lambda_C)^2}}{2}}. \end{aligned}$$

Note that the following holds

$$|\lambda| = \eta_1^2 + \eta_2^2, \quad \lambda_R = \eta_2^2 - \eta_1^2, \quad \lambda_C = 2\eta_1\eta_2,$$

thus (69) can be expressed only by x, η_i and c_i. The solution in the original variables is of the form

$$\begin{aligned} u &= w_R - i\frac{r_1 + r_2}{r_1 - r_2} w_C = w_R + \frac{a_{11} - \lambda_R}{\lambda_C} w_C = w_R + \frac{a_{11} - \eta_1^2 + \eta_2^2}{2\eta_1\eta_2} w_C, \\ v &= \frac{2i}{r_1 - r_2} w_C = \frac{a_{21}}{\lambda_C} w_C = \frac{a_{21}}{2\eta_1\eta_2} w_C \end{aligned} \tag{70}$$

and finally

$$\begin{pmatrix} u \\ v \end{pmatrix} = \begin{pmatrix} c_2 + \frac{a_{11}-\eta_1^2+\eta_2^2}{2\eta_1\eta_2} c_1 & -c_1 + \frac{a_{11}-\eta_1^2+\eta_2^2}{2\eta_1\eta_2} c_2 & -c_4 + \frac{a_{11}-\eta_1^2+\eta_2^2}{2\eta_1\eta_2} c_3 & c_3 + \frac{a_{11}-\eta_1^2+\eta_2^2}{2\eta_1\eta_2} c_4 \\ \frac{c_1 a_{21}}{2\eta_1\eta_2} & \frac{c_2 a_{21}}{2\eta_1\eta_2} & \frac{c_3 a_{21}}{2\eta_1\eta_2} & \frac{c_4 a_{21}}{2\eta_1\eta_2} \end{pmatrix} FS, \tag{71}$$

where FS denotes fundamental system in the vector form, ie.

$$FS = \left(e^{\eta_1 x}\cos\eta_2 x, \quad e^{\eta_1 x}\sin\eta_2 x, \quad e^{-\eta_1 x}\cos\eta_2 x, \quad c_4 e^{-\eta_1 x}\sin\eta_2 x\right)^T.$$

Trivial discriminant

Since $D = 0$ we have only one real solution $r = (a_{22} - a_{11})/2a_{21}$ and thus we cannot expect a diagonalised system. However, we can take the obtained equation in the variable $w = u + rv$

and add one equation from the original system (62). Then we obtain a system

$$\begin{aligned} -\Delta w &= \frac{a_{11}+a_{22}}{2} w, \\ -\Delta v &= \frac{a_{11}+a_{22}}{2} v + a_{21} w, \end{aligned}$$

which is easily solvable:

$$\begin{aligned} w &= c_1 e^{\sqrt{\frac{a_{11}+a_{22}}{2}}x} + c_2 e^{-\sqrt{\frac{a_{11}+a_{22}}{2}}x} \\ v &= \left(c_3 - \frac{\sqrt{2}a_{21}c_1}{\sqrt{a_{11}+a_{22}}} x \right) e^{\sqrt{\frac{a_{11}+a_{22}}{2}}x} + \left(c_4 + \frac{\sqrt{2}a_{21}c_2}{\sqrt{a_{11}+a_{22}}} x \right) e^{-\sqrt{\frac{a_{11}+a_{22}}{2}}x}, \end{aligned} \tag{72}$$

even in the original variables:

$$\begin{aligned} u = &\left(c_1 - \frac{a_{22}-a_{11}}{2a_{21}} c_3 + \frac{a_{22}-a_{11}}{\sqrt{2(a_{11}+a_{22})}} c_1 x \right) e^{\sqrt{\frac{a_{11}+a_{22}}{2}}x} + \\ &+ \left(c_2 - \frac{a_{22}-a_{11}}{2a_{21}} c_4 - \frac{a_{22}-a_{11}}{\sqrt{2(a_{11}+a_{22})}} c_2 x \right) e^{-\sqrt{\frac{a_{11}+a_{22}}{2}}x} \\ v = &\left(c_3 - \frac{\sqrt{2}a_{21}c_1}{\sqrt{a_{11}+a_{22}}} x \right) e^{\sqrt{\frac{a_{11}+a_{22}}{2}}x} + \left(c_4 + \frac{\sqrt{2}a_{21}c_2}{\sqrt{a_{11}+a_{22}}} x \right) e^{-\sqrt{\frac{a_{11}+a_{22}}{2}}x}, \end{aligned} \tag{73}$$

where c_i are constants.

It remains to discuss the case $r = -a_{11}/a_{21} =: r_1$. Since r_1 is one of the roots of equation (63), from the above we know that there has to be the second distinct real root r_2. Adding the first equation of system (62) to the r_i-multiple of the second equation for $i = 1, 2$ we obtain a system

$$\begin{aligned} -(\Delta u - \frac{a_{11}}{a_{21}} \Delta v) &= \left(a_{12} - \frac{a_{11}}{a_{21}} \right) v, \\ -(\Delta u + r_2 \Delta v) &= (a_{11} + r_2 a_{21}) \left(u + \frac{a_{12} + r_2 a_{22}}{a_{11} + r_2 a_{21}} v \right). \end{aligned} \tag{74}$$

To rewrite it into an easily solvable system we need $0 \neq a_{12} + r_2 a_{22}$ to hold. If it would not be true, then the quadratic equation for these roots r_1 and r_2 would have to be of the form

$$0 = (r - r_1)(r - r_2) = r^2 + \left(\frac{a_{11}}{a_{21}} + \frac{a_{12}}{a_{22}} \right) r + \frac{a_{11} a_{12}}{a_{21} a_{22}},$$

which contradicts to the form of the quadratic equation (63). Thus taking $w_2 = u + r_2 v$ and $\lambda_2 = a_{11} + r_2 a_{21}$ we get the following reformulation of system (74)

$$\begin{aligned} -\left(\Delta w_2 - \left(\frac{a_{11}}{a_{21}} + r_2 \right) \Delta v \right) &= \left(a_{12} - \frac{a_{11}}{a_{21}} \right) v, \\ -\Delta w_2 &= \lambda_2 w_2 \end{aligned} \tag{75}$$

and solution to this problem in the original variables is of the form

$$\begin{aligned} u &= \frac{\lambda_2 - r_2 a_{21}}{\lambda_2} \left(c_1 e^{\sqrt{\lambda_2}x} + c_2 e^{-\sqrt{\lambda_2}x} \right) - r_2 c_3 e^{\sqrt{\frac{a_{12}a_{21}-a_{11}}{\lambda_2}}x} - r_2 c_4 e^{-\sqrt{\frac{a_{12}a_{21}-a_{11}}{\lambda_2}}x}, \\ v &= \frac{a_{21}}{\lambda_2} \left(c_1 e^{\sqrt{\lambda_2}x} + c_2 e^{-\sqrt{\lambda_2}x} \right) + c_3 e^{\sqrt{\frac{a_{12}a_{21}-a_{11}}{\lambda_2}}x} + c_4 e^{-\sqrt{\frac{a_{12}a_{21}-a_{11}}{\lambda_2}}x}. \end{aligned} \tag{76}$$

A.2 Analytic solution to the stationary problem

The task of this section is to find a stationary solution to system (39), i.e. the system with affine kinetics and step functions as coefficients. We will use the method called diagonalization outlined in appendix A.1. For clarity of the presentation, we will consider a step function only in one coefficient of the affine kinetics.

We consider a following reaction-diffusion system with affine kinetics and with step function $h(x)$ defined above (36)

$$\begin{aligned} 0 &= d_1\partial_{xx}u + b_{10} + (b_{11} + h(x))u + b_{12}v \\ 0 &= d_2\partial_{xx}v + b_{20} + b_{21}u + b_{22}v \end{aligned} \quad \text{on } (0, L), \tag{77}$$

with Neumann boundary conditions (35). Our task is to find a stationary solution to the system explicitly. Let $[u_0(x), v_0(x)]^\top$ be a solution to the equation

$$b_{10} + (b_{11} + h(x))u + b_{12}v = 0 = b_{20} + b_{21}u + b_{22}v.$$

Since $h(x)$ is a step function in ξ, it is easier to consider system (77) contracted to the interval $(0, \xi)$ and (ξ, L) separately and to use an appropriate connecting conditions in ξ. From now, the upper index L will denote correspondence to system contracted to $(0, \xi)$, R to (ξ, L) respectively. Thus system (77) can be rewritten using $\tilde{u}^L = u^L - u_0^L$, $\tilde{v}^L = v^L - v_0^L$, $\tilde{u}^R = u^R - u_0^R$, $\tilde{v}^R = v^R - v_0^R$ (the tilde will be omitted) into the form

$$\begin{aligned} 0 &= d_1\partial_{xx}u^L + b_{11}u^L + b_{12}v^L, \\ 0 &= d_2\partial_{xx}v^L + b_{21}u^L + b_{22}v^L, \\ 0 &= d_1\partial_{xx}u^R + (b_{11} + s)u^R + b_{12}v^R, \\ 0 &= d_2\partial_{xx}v^R + b_{21}u^R + b_{22}v^R, \end{aligned} \quad \begin{aligned} &\text{in } (0, \xi), \\ &\\ &\text{in } (\xi, L), \\ &\end{aligned} \tag{78}$$

with the following boundary and connecting conditions

$$\begin{aligned} \frac{\partial u^L}{\partial n}(0) = \frac{\partial v^L}{\partial n}(0) = 0, \qquad & \frac{\partial u^R}{\partial n}(L) = \frac{\partial v^R}{\partial n}(L) = 0, \\ \frac{\partial u^L}{\partial n}(\xi) = \frac{\partial u^R}{\partial n}(\xi), \qquad & \frac{\partial v^L}{\partial n}(\xi) = \frac{\partial v^R}{\partial n}(\xi), \\ u^R(\xi) - u^L(\xi) = u_0^L - u_0^R, \qquad & v^R(\xi) - v^L(\xi) = v_0^L - v_0^R. \end{aligned} \tag{79}$$

Now we can solve the system via applying transformation into the diagonalized system on both subsystems separately, as it was presented in appendix A.1, and finish calculation by employing the connecting conditions.

Let us briefly present the outcome of appendix A.1. The solutions of a linear reaction diffusion system with constant coefficient

$$\begin{aligned} 0 &= \partial_{xx}u + a_{11}u + a_{12}v, \\ 0 &= \partial_{xx}v + a_{21}u + a_{22}v, \end{aligned} \tag{80}$$

with Neumann boundary condition in 0 (if condition is required in L, substitution $x \mapsto L - x$ is sufficient) and meantime with unspecified second boundary condition (regarding to the

connection condition) are of the form

$$\begin{aligned} u &= \frac{r_1 c_2 \cos\left(\sqrt{\lambda_2}x\right) - r_2 c_1 \cos\left(\sqrt{\lambda_1}x\right)}{r_1 - r_2}, \\ v &= \frac{c_1 \cos\left(\sqrt{\lambda_1}x\right) - c_2 \cos\left(\sqrt{\lambda_2}x\right)}{r_1 - r_2} \end{aligned} \tag{81}$$

if $\operatorname{tr}^2 \mathbf{A} - 4 \det \mathbf{A} > 0$ and

$$\begin{aligned} u = {} & \frac{c_1 a_{11} + 2c_2\eta_1\eta_2 + c_1(\eta_2^2 - \eta_1^2)}{2\eta_1\eta_2}(e^{\eta_1 x} + e^{-\eta_1 x})\cos\eta_2 x \\ & + \frac{c_2 a_{11} - 2c_1\eta_1\eta_2 + c_2(\eta_2^2 - \eta_1^2)}{2\eta_1\eta_2}(e^{\eta_1 x} - e^{-\eta_1 x})\sin\eta_2 x, \\ v = {} & \frac{c_1 a_{21}}{2\eta_1\eta_2}(e^{\eta_1 x} + e^{-\eta_1 x})\cos\eta_2 x + \frac{c_2 a_{21}}{2\eta_1\eta_2}(e^{\eta_1 x} - e^{-\eta_1 x})\sin\eta_2 x \end{aligned} \tag{82}$$

if $\operatorname{tr}^2 \mathbf{A} - 4 \det \mathbf{A} < 0$.

Applying on our two systems (78), we see that the form of the solutions depends on the sign of D on each sides defined in (64), i.e. on signs of the following two expressions

$$\begin{aligned} D^L &:= (d_2 b_{11} + d_1 b_{22})^2 - 4 d_1 d_2 \det \mathbf{B}, \\ D^R &:= (d_2(b_{11} + s) + d_1 b_{22})^2 - 4 d_1 d_2 (\det \mathbf{B} + s b_{22}). \end{aligned} \tag{83}$$

Thus several options can occur – for illustration, two of them are presented below; others are ommitted due to the straightforwardness of the computing and the largeness of the resulting forms.

Both discriminants are positive

For this case we obtain the system

$$\begin{aligned} 0 &= \partial_{xx}(u^L + r_i^L v^L) + \lambda_i^L (u^L + r_i^L v^L) \quad \text{in } (0, \xi), \\ 0 &= \partial_{xx}(u^R + r_i^R v^R) + \lambda_i^R (u^R + r_i^R v^R) \quad \text{in } (\xi, L) \end{aligned} \tag{84}$$

for $i = 1, 2$, where

$$\begin{aligned} r_i^L &= \frac{d_2 b_{11} - d_1 b_{22} \pm \sqrt{D^L}}{2 d_1 b_{21}}, & \lambda_i^L &= \left(\frac{b_{11}}{d_1} + r_i^L \frac{b_{21}}{d_2}\right), \\ r_i^R &= \frac{d_2(b_{11} + s) - d_1 b_{22} \pm \sqrt{D^R}}{2 d_1 b_{21}}, & \lambda_i^R &= \left(\frac{b_{11} + s}{d_1} + r_i^R \frac{b_{21}}{d_2}\right). \end{aligned} \tag{85}$$

The solution to system (84) is easily computable:

$$\begin{aligned} u^L + r_i^L v^L &= c_i^L \cos\sqrt{\lambda_i^L}x + \tilde{c}_i^L \sin\sqrt{\lambda_i^L}x, \\ u^R + r_i^R v^R &= c_i^R \cos\sqrt{\lambda_i^R}(L - x) + \tilde{c}_i^R \sin\sqrt{(\lambda_i^R}(L - x) \end{aligned} \tag{86}$$

with c_i^k, $\tilde{c}_i^k$ real constants. Since the solution (86) satisfies Neumann boundary conditions at the outer points 0 and L, the constants $\tilde{c}_i^k$ have to be zero. After this simplification we express the solution in the original variables

$$u(x) = \begin{cases} \frac{r_2^L c_1^L \cos(\sqrt{\lambda_1^L}x) - r_1^L c_2^L \cos(\sqrt{\lambda_2^L}x)}{r_2^L - r_1^L} & x \in (0,\xi] \\ \frac{r_2^R c_1^R \cos(\sqrt{\lambda_1^R}(L-x)) - r_1^R c_2^R \cos(\sqrt{\lambda_2^R}(L-x))}{r_2^R - r_1^R} & x \in (\xi, L) \end{cases},$$

$$v(x) = \begin{cases} \frac{c_1^L \cos(\sqrt{\lambda_1^L}x) - c_2^L \cos(\sqrt{\lambda_2^L}x)}{r_2^L - r_1^L} & x \in (0,\xi] \\ \frac{c_1^R \cos(\sqrt{\lambda_1^R}(L-x)) - c_2^R \cos(\sqrt{\lambda_2^R}(L-x))}{r_2^R - r_1^R} & x \in (\xi, L) \end{cases}$$

with c_i^k real constants determined by the connecting conditions at point ξ, which means that c_i^k have to be the solution to the following linear system

$$\begin{pmatrix} \frac{r_2^L \cos(\sqrt{\lambda_1^L}\xi)}{r_2^L - r_1^L} & \frac{-r_1^L \cos(\sqrt{\lambda_2^L}\xi)}{r_2^L - r_1^L} & \frac{-r_2^R \cos(\sqrt{\lambda_1^R}(L-\xi))}{r_2^R - r_1^R} & \frac{r_1^R \cos(\sqrt{\lambda_2^R}(L-\xi))}{r_2^R - r_1^R} \\ \frac{\cos(\sqrt{\lambda_1^L}\xi)}{r_2^L - r_1^L} & \frac{-\cos(\sqrt{\lambda_2^L}\xi)}{r_2^L - r_1^L} & \frac{-\cos(\sqrt{\lambda_1^R}(L-\xi))}{r_2^R - r_1^R} & \frac{\cos(\sqrt{\lambda_2^R}(L-\xi))}{r_2^R - r_1^R} \\ \frac{r_2^L \sqrt{\lambda_1^L} \sin(\sqrt{\lambda_1^L}\xi)}{r_2^L - r_1^L} & \frac{-r_1^L \sqrt{\lambda_2^L} \sin(\sqrt{\lambda_2^L}\xi)}{r_2^L - r_1^L} & \frac{r_2^R \sqrt{\lambda_1^R} \sin(\sqrt{\lambda_1^R}(L-\xi))}{r_2^R - r_1^R} & \frac{-r_1^R \sqrt{\lambda_2^R} \sin(\sqrt{\lambda_2^R}(L-\xi))}{r_2^R - r_1^R} \\ \frac{\sqrt{\lambda_1^L} \sin(\sqrt{\lambda_1^L}\xi)}{r_2^L - r_1^L} & \frac{-\sqrt{\lambda_2^L} \sin(\sqrt{\lambda_2^L}\xi)}{r_2^L - r_1^L} & \frac{\sqrt{\lambda_1^R} \sin(\sqrt{\lambda_1^R}(L-\xi))}{r_2^R - r_1^R} & \frac{-\sqrt{\lambda_2^R} \sin(\sqrt{\lambda_2^R}(L-\xi))}{r_2^R - r_1^R} \end{pmatrix} \begin{pmatrix} c_1^L \\ c_2^L \\ c_1^R \\ c_2^R \end{pmatrix} = \begin{pmatrix} s_1 \\ s_2 \\ 0 \\ 0 \end{pmatrix}$$

Both discriminants are negative

We will again use the results of appendix A.1, so we deal with the system

$$\begin{aligned} 0 &= \partial_{xx}(u^L + r_R^L v^L) + \lambda_R^L(u^L + r_R^L v^L) - \lambda_C^L(r_C^L v^L) \\ 0 &= \partial_{xx}(r_C^L v^L) + \lambda_C^L(u^L + r_R^L v^L) + \lambda_R^L(r_C^L v^L) \end{aligned} \quad \text{in } (0,\xi),$$

$$\begin{aligned} 0 &= \partial_{xx}(u^R + r_R^R v^R) + \lambda_R^R(u^R + r_R^R v^R) - \lambda_C^R(r_C^R v^R) \\ 0 &= \partial_{xx}(r_C^R v^R) + \lambda_C^R(u^R + r_R^R v^R) + \lambda_R^R(r_C^R v^R) \end{aligned} \quad \text{in } (\xi, L) \tag{87}$$

where the upper index designates correspondence to the system on the left or on the right part of the interval $[0, L]$, the lower index designates the real or the complex part of variables u, v and symbols defined (85). According to (71) we designate following

$$\eta_1^L = \frac{1}{4}\sqrt{-\lambda_R^L + \sqrt{(\lambda_R^L)^2 + (\lambda_C^L)^2}}, \quad \eta_1^R = \frac{1}{4}\sqrt{-\lambda_R^R + \sqrt{(\lambda_R^R)^2 + (\lambda_C^R)^2}},$$
$$\eta_2^L = \frac{1}{4}\sqrt{\lambda_R^L + \sqrt{(\lambda_R^L)^2 + (\lambda_C^L)^2}}, \quad \eta_2^R = \frac{1}{4}\sqrt{\lambda_R^R + \sqrt{(\lambda_R^R)^2 + (\lambda_C^R)^2}}$$

and hence the solution is of the form

$$\begin{aligned} u^L &= p_1^L e^{\eta_1^L x} \sin \eta_2^L x + p_2^L e^{\eta_1^L x} \cos \eta_2^L x + p_3^L e^{-\eta_1^L x} \sin \eta_2^L x + p_4^L e^{-\eta_1^L x} \cos \eta_2^L x, \\ v^L &= p_5^L e^{\eta_1^L x} \sin \eta_2^L x + p_6^L e^{\eta_1^L x} \cos \eta_2^L x + p_7^L e^{-\eta_1^L x} \sin \eta_2^L x + p_8^L e^{-\eta_1^L x} \cos \eta_2^L x, \\ u^R &= p_1^R e^{\eta_1^R x} \sin \eta_2^R x + p_2^R e^{\eta_1^R x} \cos \eta_2^R x + p_3^R e^{-\eta_1^R x} \sin \eta_2^R x + p_4^R e^{-\eta_1^R x} \cos \eta_2^R x, \\ v^R &= p_5^R e^{\eta_1^R x} \sin \eta_2^R x + p_6^R e^{\eta_1^R x} \cos \eta_2^R x + p_7^R e^{-\eta_1^R x} \sin \eta_2^R x + p_8^R e^{-\eta_1^R x} \cos \eta_2^R x, \end{aligned}$$

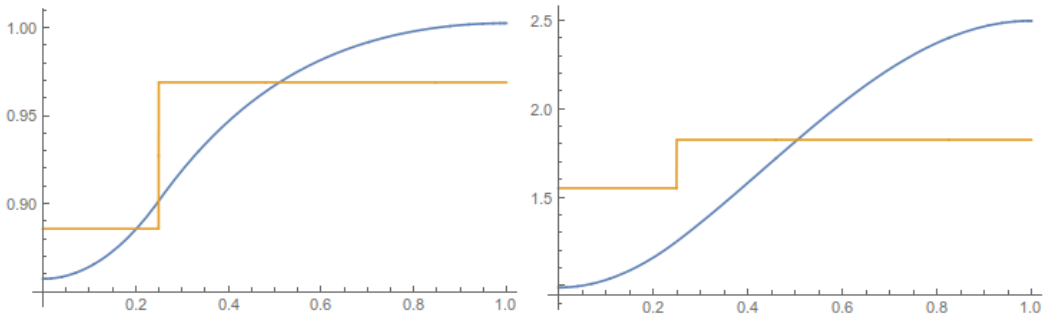

Figure 8: Plot of the stationary solution to the activator concentration $u(x)$ (blue) and semi-solution (orange), of system (77) on the domain $(0,1)$ with Neumann boundary conditions, and parameters: $d_1 = 1$, $d_2 = 1$, $s = 3$, $\xi = 0.25$, $b_{10} = 1$, $b_{12} = 20$, $b_{20} = 3$, $b_{21} = -3$, $b_{22} = -2$ and A) $b_{11} = -5$, B) $b_{11} = 10$. Case A) corresponds to decay of initial perturbations, and B) to exponential growth of perturbations suggesting the possibility of pattern formation.

where the functions p_i^j are rational in η_1, η_2, linear in constants c_i^j and depend even on b_{11}, b_{21} and s. Half of the constants c_i^j can be obtained from homogenous Neumann boundary conditions at 0 and L, the second half is determined by the conditions at ξ. The explicit formula is too cumbersome, we will illustrate the solutions in figures, only. See fig. 8.

A.3 Linearisation about a piecewise constant steady state

This is an alternative approach to analyze a stability of the RD system (39) – to linearise around step functions $(\bar{u}, \bar{v})$. If we try to proceed, we will obtain a linear system, but with terms containing a derivative of the Dirac delta function, which results from the non-trivial step in $(\bar{u}, \bar{v})$. Therefore, we are not able to obtain the linearised system following the standard approach above.

However, it is instructive to proceed further as an expansion (in generalised functions) of the delta function in the eigenfunctions $\{y_k\}$ is available and hence we can rewrite the linearised system yet again in terms of a system of equations for particular modes.

Linearisation of system (34) around step functions $(\bar{u}(x), \bar{v}(x))$ (defined in (38)) is well defined in the distributional sense and is of the form

$$\begin{aligned} \partial_t \tilde{u} &= d_1 \partial_{xx} \tilde{u} + b_{11}\tilde{u} + b_{12}\tilde{v} + s_1 d_1 \delta'(x-\xi) \\ \partial_t \tilde{v} &= d_2 \partial_{xx} \tilde{v} + b_{21}\tilde{u} + b_{22}\tilde{v} + s_2 d_2 \delta'(x-\xi) \end{aligned} \quad \text{in } (0, L), \tag{88}$$

where (s_1, s_2) denotes the sizes of the step of $(\bar{u}(x), \bar{v}(x))$ at ξ, $\delta(x)$ denotes Dirac delta function and $u(x) = \tilde{u}(x) - \bar{u}(x)$, $v(x) = \tilde{v}(x) - \bar{v}(x)$.

Since Neumann boundary conditions are considered, we expand $(\tilde{u}, \tilde{v})$ using orthonormal basis $\{y_n\}_{n\in\{0,1,..\}} = \left\{\frac{1}{L}, \frac{2}{L}\cos\left(\frac{n\pi}{L}x\right)\right\}_{n=1}^{\infty}$ as the series

$$\tilde{u} = \sum_{n=0}^{\infty} A_n y_n, \quad \tilde{v} = \sum_{n=0}^{\infty} B_n y_n \tag{89}$$

and rewrite system (88) in the form of a system of equations for each eigenmode. The Dirac delta function can be expanded in terms of any eigenfunctions of the Laplacian on any interval.

Hence we use the following expansion of Dirac delta function on $(0, L)$

$$\delta(x-\xi) = \frac{2}{L}\sum_{n=1}^{\infty} \sin\left(\frac{n\pi\xi}{L}\right)\sin\left(\frac{n\pi x}{L}\right).$$

Therefore the linearised problem has the following eigenmode expansion

$$\sum_{n=1}^{\infty} y_n \left\{ \begin{pmatrix} \dot{A}_n \\ \dot{B}_n \end{pmatrix} + \left[\begin{pmatrix} d_1 & 0 \\ 0 & d_2 \end{pmatrix} \kappa_n - \mathbf{J}(x) \right] \begin{pmatrix} A_n \\ B_n \end{pmatrix} - \underbrace{\frac{n\pi}{L}\sin\left(\frac{n\pi\xi}{L}\right) \begin{pmatrix} d_1 s_1 & 0 \\ 0 & d_2 s_2 \end{pmatrix} \begin{pmatrix} A_n \\ B_n \end{pmatrix}}_{\text{forcing}} \right\} = 0, \tag{90}$$

where $\kappa_n = \left(\frac{n\pi}{L}\right)^2$ and the matrix of linearised kinetics $\mathbf{J}(x)$ is evaluated at the piece-wise constant function $(\bar{u}(x), \bar{v}(x))$. As the $\delta'(x-\xi)$ contribution translates only into a (constant) forcing, it does not affect the (in)stability result. Thence the generalised function approach yields exactly the same problem as previously derived in eqn. (42).

A.4 Computational approaches

The spectrum of the truncated matrix (50) is computed using the Matlab inbuilt function *eig()*. When denoting N as a constant representing the size of matrix $((2N+2)\times(2N+2))$ our numerical results show that for $N > 50$ the value of the largest real part of the eigenvalues does not significantly change; larger matrices contribute to the spectrum by eigenvalues with larger negative part as we discussed above. We choose $N = 1000$. With constant M representing the truncation in eigenmode expansion of $h(x)$, i.e. we approximate

$$h(x) \approx \sum_{k=0}^{M} Z^k y_k(x), \quad \text{where} |Z^k| \lessapprox \frac{s}{k}.$$

However, the length of numerical calculation does not significantly increase with larger M, so we set $M = N$.

The solutions of the evolution system (40) are computed by Wolfram Mathematica 10 using *NDSolve()* (via the method of lines for the temporal discretisation and finite differences for space) up to time $\tau = 10^3$ or until the supremum norm of the solution exceeds 10^7. The initial condition is random noise, uniformly distributed between $(10^{-2}, 10^2)$.

Both approaches to assess stability should yield the same result as they describe the same process. However, both methods are approximate and hence small differences might occur especially close to the border of the parameter regions due to different accuracy of the approximation (truncation of the matrix versus numerical discretisation when computing the evolution problem).

References

[1] Y. Almirantis and S. Papageorgiou, *Cross-diffusion effects on chemical and biological pattern formation*, Journal of Theoretical Biology, 151 (1991), pp. 289 – 311.

[2] J. Bard and I. Lauder, *How well does Turing's theory of morphogenesis work?*, Journal of Theoretical Biology, 45 (1974), pp. 501 – 531.

[3] Benson, Debbie L and Sherratt, Jonathan A and Maini, Philip K, *Diffusion driven instability in an inhomogeneous domain*, Bulletin of mathematical biology, 55 (1993), pp. 365–384.

[4] Biancalani, Tommaso and Fanelli, Duccio and Di Patti, Francesca, *Stochastic Turing patterns in the Brusselator model*, Phys. Rev. E, 81 (2010), p. 046215.

[5] O. Bournez and A. Pouly, *A universal ordinary differential equation*, Logical Methods in Computer Science, Volume 16, Issue 1 (2020).

[6] Butler, Thomas and Goldenfeld, Nigel, *Fluctuation-driven Turing patterns*, Phys. Rev. E, 84 (2011), p. 011112.

[7] Cantini, Laura and Cianci, Claudia and Fanelli, Duccio and Massi, Emma and Barletti, Luigi and Asllani, Malbor, *Stochastic amplification of spatial modes in a system with one diffusing species*, Journal of mathematical biology, 69 (2013), pp. 1585–1608.

[8] Castets, V and Dulos, E and Boissonade, J and DeKepper, P, *Experimental-evidence of a sustained standing Turing-type nonequilibrium chemical-pattern*, Physical Review Letters, 64 (1990), pp. 2953–2956.

[9] Chaplain, Mark AJ and Ganesh, Mahadevan and Graham, Ivan G, *Spatio-temporal pattern formation on spherical surfaces: numerical simulation and application to solid tumour growth*, Journal of mathematical biology, 42 (2001), pp. 387–423.

[10] Crampin, Edmund J and Gaffney, Eamonn A and Maini, Philip K, *Reaction and diffusion on growing domains: Scenarios for robust pattern formation*, Bulletin of Mathematical Biology, 61 (1999), pp. 1093–1120.

[11] Crampin, Edmund J and Gaffney, Eamonn A and Maini, Philip K, *Mode-doubling and tripling in reaction-diffusion patterns on growing domains: A piecewise linear model*, Journal of Mathematical Biology, 44 (2002), pp. 107–128.

[12] Davies, EB, *Pseudospectra of differential operators*, Journal of Operator Theory, 43 (2000), pp. 243–262.

[13] del-Castillo-Negrete,D. and Carreras,B. A. , *Stratified shear flows in a model of turbulence-shear flow interaction*, Physics of Plasmas, 9 (2002), pp. 118–127.

[14] Di Patti, Francesca and Lavacchi, Laura and Goren, Rinat and Schein-Lubomirsky, Leora and Fanelli, Duccio and Stavans, Joel, *Robust stochastic Turing patterns in the development of a one-dimensional cyanobacterial organism*, PLOS Biology, 16 (2018), p. e2004877.

[15] Dillon, Robert and Maini, Philip and Othmer, Hans, *Pattern formation in generalized Turing systems. I: Steady-state patterns in systems with mixed boundary conditions*, Journal of Mathematical Biology, 32 (1994), p. .

[16] Duran-Nebreda, S. and Sole, R.V., *Toward synthetic spatial patterns in engineered cell populations with chemotaxis*, ACS Synth. Biol., 5 (2016), pp. 654–661.

[17] Economou, Andrew D and Green, Jeremy BA, *Thick and thin fingers point out Turing waves*, Genome biology, 14 (2013), p. 101.

[18] Ermentrout, Bard and Lewis, Mark, *Pattern formation in systems with one spatially distributed species*, Bulletin of Mathematical Biology, 59 (1997), pp. 533–549.

[19] Fanelli, Duccio and Cianci, Claudia and Di Patti, Francesca, *Turing instabilities in reaction-diffusion systems with cross diffusion*, The European Physical Journal B, 86 (2013), pp. 1–8.

[20] G. Míguez, David and Dolnik, Milos and Muñuzuri, Alberto and Kramer, Lorenz, *Effect of axial growth on Turing pattern formation*, Physical review letters, 96 (2006), p. 048304.

[21] Gaffney, E A and Monk, N A M, *Gene expression time delays and Turing pattern formation systems*, Bulletin of Mathematical Biology, 68 (2006), pp. 99–130.

[22] G. Gambino, M. Lombardo, and M. Sammartino, *Pattern formation driven by cross-diffusion in a 2d domain*, Nonlinear Analysis: Real World Applications, 14 (2013), pp. 1755 – 1779.

[23] Gambino, Gaetana and Lombardo, Maria and Sammartino, Marco, *Turing instability and traveling fronts for a nonlinear reaction–diffusion system with cross-diffusion*, Mathematics and Computers in Simulation, 82 (2012), p. 1112–1132.

[24] Garcia-Ojalvo, J and Sancho, J, *Noise in spatially extended systems*, Institute for Nonlinear Science, Springer-Verlag New York, 1999.

[25] Gierer, Alfred and Meinhardt, Hans, *A theory of biological pattern formation*, Biological Cybernetics, 12 (1972), pp. 30–39.

[26] Glimm, Tilmann and Zhang, Jianying and Shen, Yun-Qiu, *Interaction of Turing patterns with an external linear morphogen gradient*, Nonlinearity, 22 (2009), p. 2541.

[27] Glimm, Tilmann and Zhang, Jianying and Shen, Yun-Qiu, *Stability of Turing-type patterns in a reaction–diffusion system with an external gradient*, International Journal of Bifurcation and Chaos, 27 (2017), p. 1750003.

[28] Glimm, Tilmann and Zhang, Jianying and Shen, Yun-Qiu and Newman, Stuart A, *Reaction–diffusion systems and external morphogen gradients: the two-dimensional case, with an application to skeletal pattern formation*, Bulletin of mathematical biology, 74 (2012), pp. 666–687.

[29] Green, Jeremy B. A. and Sharpe, James, *Positional information and reaction-diffusion: two big ideas in developmental biology combine*, Development, 142 (2015), pp. 1203–1211.

[30] Guptasarma, Purnananda, *Does replication-induced transcription regulate synthesis of the myriad low copy number proteins of Escherichia coli?*, BioEssays, 17 (1995), pp. 987–997.

[31] Hilker, FM and Lewis, MA, *Predator-prey systems in streams and rivers*, Theoretical biology, 3 (2010), pp. 175–193.

[32] Hillen, Thomas and Painter, Kevin J, *A user's guide to PDE models for chemotaxis*, Journal of mathematical biology, 58 (2009), pp. 183–217.

[33] Iron, David and Ward, Michael, *Spike pinning for the Gierer-Meinhardt model*, Mathematics and Computers in Simulation, 55 (2000), pp. 1–15.

[34] Jou, D and Casas-Vázquez, J and Lebon, G, *Extended irreversible thermodynamics revisited (1988-98)*, Reports on Progress in Physics, 62 (1999), pp. 1035–1142.

[35] V. Klika, R. E. Baker, D. Headon, and E. A. Gaffney, *The influence of receptor-mediated interactions on reaction-diffusion mechanisms of cellular self-organisation*, Bulletin of Mathematical Biology, 74 (2012), pp. 935–957.

[36] Klika, V. and Grmela, M., *Mechano-chemical coupling in Belousov-Zhabotinskii reactions*, The Journal of Chemical Physics, 140 (2014), p. 124110.

[37] Klika, Václav, *Comparison of the effects of possible mechanical stimuli on the rate of biochemical reactions*, The Journal of Physical Chemistry B, 114 (2010), pp. 10567–10572.

[38] Klika, Václav, *A guide through available mixture theories for applications*, Critical Reviews in Solid State and Materials Sciences, 39 (2014), pp. 154–174.

[39] Klika, Václav and Grmela, Miroslav, *Coupling between chemical kinetics and mechanics that is both nonlinear and compatible with thermodynamics*, Physical Review E, 87 (2013), p. 012141.

[40] Klika, Václav and Gaffney, Eamonn A., *History dependence and the continuum approximation breakdown: the impact of domain growth on Turing's instability*, Proceedings of the Royal Society of London A: Mathematical, Physical and Engineering Sciences, 473 (2017).

[41] Klika, Václav and Kozák, Michal and Gaffney, Eamonn, *Domain size driven instability: self-organization in systems with advection*, SIAM Journal on Applied Mathematics, 78 (2018), pp. 2298–2322.

[42] Kondo, Shigeru and Miura, Takashi, *Reaction-diffusion model as a framework for understanding biological pattern formation*, Science, 329 (2010), pp. 1616–1620.

[43] K. Korvasová, E. Gaffney, P. Maini, M. Ferreira, and V. Klika, *Investigating the turing conditions for diffusion-driven instability in the presence of a binding immobile substrate*, Journal of Theoretical Biology, 367 (2015), pp. 286 – 295.

[44] Kovács, Sándor, *Turing bifurcation in a system with cross diffusion*, Nonlinear Analysis: Theory, Methods & Applications, 59 (2004), pp. 567–581.

[45] Kováč, J., *Turing model for self-organisation and influence of geometry*, Master's thesis, (In preparation).

[46] Kozák, Michal, *Bifurkace v matematických modelech v biologii*, Master's thesis, (2013).

[47] Kozák, Michal and Gaffney, Eamonn A. and Klika, Václav, *Pattern formation in reaction-diffusion systems with piecewise kinetic modulation: An example study of heterogeneous kinetics*, Phys. Rev. E, 100 (2019), p. 042220.

[48] Krause, Andrew L. and Klika, Václav and Woolley, Thomas E. and Gaffney, Eamonn A., *Heterogeneity induces spatiotemporal oscillations in reaction-diffusion systems*, Phys. Rev. E, 97 (2018), p. 052206.

[49] Krause, Andrew L. and Klika, Václav and Woolley, Thomas E. and Gaffney, Eamonn A. , *From one pattern into another: analysis of Turing patterns in heterogeneous domains via WKBJ*, Journal of The Royal Society Interface, 17 (2020), p. 20190621.

[50] P. Kulesa, G. Cruywagen, S. Lubkin, P. Main, J. Sneyd, M. Ferguson, and J. Murray, *On a model mechanism for the spatial patterning of teeth primordia in the alligator*, Journal of Theoretical Biology, 180 (1996), pp. 287 – 296.

[51] Kumar, Niraj and Horsthemke, Werner, *Effects of cross diffusion on Turing bifurcations in two-species reaction-transport systems*, Phys. Rev. E, 83 (2011), p. 036105.

[52] M. Kučera, *Reaction-diffusion systems: stabilizing effect of conditions described by quasivariational inequalities*, Czechoslovak Mathematical Journal, 47 (1997), pp. 469–486.

[53] M. Kučera and M. Väth, *Bifurcation for a reaction–diffusion system with unilateral and neumann boundary conditions*, Journal of Differential Equations, 252 (2012), pp. 2951–2982.

[54] Lebon, Georgy and Jou, David and Casas-Vázquez, José, *Understanding non-equilibrium thermodynamics*, Springer, 2008.

[55] Lengyel, I and Epstein, IR, *A chemical approach to designing Turing patterns in reaction-diffusion systems*, PNAS, 89 (1992), pp. 3977–3979.

[56] Liu, R.T. and Liaw, S.S. and Maini, P.K., *Two-stage Turing model for generating pigment patterns on the leopard and the jaguar*, Phys. Rew. E, E74 (2006).

[57] Madzvamuse, Anotida and Gaffney, Eamonn A and Maini, Philip K, *Stability analysis of non-autonomous reaction-diffusion systems: the effects of growing domains*, Journal of mathematical biology, 61 (2010), pp. 133–164.

[58] Maini, Philip and Woolley, Thomas and Baker, Ruth and Gaffney, Eamonn and Seirin Lee, Sungrim, *Turing's model for biological pattern formation and the robustness problem*, Interface focus, 2 (2012), pp. 487–96.

[59] Marciniak-Czochra, Anna and Kimmel, Marek, *Dynamics of growth and signaling along linear and surface structures in very early tumors*, Computational and Mathematical Methods in Medicine, 7 (2006), pp. 189–213.

[60] Marcon, Luciano and Diego, Xavier and Sharpe, James and Müller, Patrick, *High-throughput mathematical analysis identifies Turing networks for patterning with equally diffusing signals*, eLife, 5 (2016), p. e14022.

[61] Mau, Yair and Hagberg, Aric and Meron, Ehud, *Spatial periodic forcing can displace patterns it is intended to control*, Physical review letters, 109 (2012), p. 034102.

[62] Miura, T, *Turing and wopert work together during limb development*, Science Signaling, 6 (2013), pp. 1–3.

[63] Mou, C. and Jackson, B. and Schneider, P. and Overbeek, P.A. and Headon, D.J., *Generation of the primary hair follicle pattern*, Proc Natl Acad Sci, 103 (2006), pp. 9075–9080.

[64] Murray, James D, *Mathematical biology. II Spatial models and biomedical applications*, Springer-Verlag New York Incorporated, 2001.

[65] Murray, Sean and Sourjik, Victor, *Self-organisation and positioning of bacterial protein clusters*, Nature Physics, 13 (2017), pp. 1–10.

[66] Nekhamkina, Olga and Rubinstein, Boris Y and Sheintuch, Moshe, *Spatiotemporal patterns in thermokinetic models of cross-flow reactors*, AIChE journal, 46 (2000), pp. 1632–1640.

[67] Nekhamkina, Olga and Sheintuch, Moshe, *Asymptotic solutions of stationary patterns in convection-reaction-diffusion systems*, Physical Review E, 68 (2003), p. 036207.

[68] Ni, Wei-Ming and Tang, Moxun, *Turing patterns in the Lengyel-Epstein system for the CIMA reaction*, Transactions of the American Mathematical Society, 357 (2005), pp. 3953–3969.

[69] Ouyang, Q and Swinney, HL, *Transition from a uniform state to hexagonal and striped Turing patterns*, Nature, 352 (1991), pp. 610–612.

[70] P. Arcuri and J. D. Murray, *Pattern sensitivity to boundary and initial conditions in reaction-diffusion models*, J. Math. Biol. , 24 (1986), pp. 141–165.

[71] Page, Karen and Maini, Philip K and Monk, Nicholas AM, *Pattern formation in spatially heterogeneous Turing reaction-diffusion models*, Physica D: Nonlinear Phenomena, 181 (2003), pp. 80–101.

[72] Page, Karen M and Maini, Philip K and Monk, Nicholas AM, *Complex pattern formation in reaction–diffusion systems with spatially varying parameters*, Physica D: Nonlinear Phenomena, 202 (2005), pp. 95–115.

[73] Painter, K. J. and Maini, P. K. and Othmer, H. G., *Stripe formation in juvenile Pomacanthus explained by a generalized Turing mechanism with chemotaxis*, Proceedings of the National Academy of Sciences, 96 (1999), pp. 5549–5554.

[74] Painter, KJ and Hunt, GS and Wells, KL and Johansson, JA and Headon, DJ, *Towards an integrated experimental–theoretical approach for assessing the mechanistic basis of hair and feather morphogenesis*, Interface Focus, 2 (2012), pp. 433–450.

[75] Pavelka, M. and Maršík, F. and Klika, V., *Consistent theory of mixtures on different levels of description*, International Journal of Engineering Science, 78 (2014), pp. 192–217.

[76] Pearson, JRA, *A note on the "Danckwerts" boundary conditions for continuous flow reactors*, Chemical Engineering Science, 10 (1959), pp. 281–284.

[77] Pickett, S. T. A. and Cadenasso, M. L., *Landscape ecology: Spatial heterogeneity in ecological systems*, Science, 269 (1995), pp. 331–334.

[78] P. H. Rabinowitz, *Some global results for nonlinear eigenvalue problems*, Journal of Functional Analysis, 7 (1971), pp. 487 – 513.

[79] Raspopovic, J and Marcon, L and Russo, L and Sharpe, J, *Digit patterning is controlled by a bmp-sox9-wnt Turing network modulated by morphogen gradients*, Science, 345 (2014), pp. 266–570.

[80] Reddy, Satish C and Trefethen, Lloyd N, *Pseudospectra of the convection-diffusion operator*, SIAM Journal on Applied Mathematics, 54 (1994), pp. 1634–1649.

[81] Rovinsky, A.B. and Menzinger, M., *Chemical instability induced by a differential flow*, Phys rev lett, 69 (1992), pp. 1193–1196.

[82] Rovinsky, A.B. and Menzinger, M., *Self-organization induced by the differential flow of activator and inhibitor*, Phys rev lett, 70 (1993), pp. 778–781.

[83] Rovinsky, A.B. and Menzinger, M., *Differential flow instability in dynamical systems without an unstable (activator) subsystem*, Phys rev lett, 72 (1994), pp. 2017–2020.

[84] S. Chandrasekhar, *Hydrodynamic and hydromagnetic stability*, International Series of Monographs on Physics Oxford, England ., Dover Publications, Dover Ed ed., 1981.

[85] Sarfaraz, Wakil and Madzvamuse, Anotida, *Classification of parameter spaces for a reaction-diffusion model on stationary domains*, Chaos, Solitons & Fractals, 103 (2017), pp. 33–51.

[86] Satnoianu, R.A. and Maini, P.K. and Menzinger, M., *Parameter space analysis, pattern sensitivity and model comparison for Turing and stationary flow-distributed waves (FDS)*, Physica D: Nonlinear Phenom, 160 (2001), pp. 79–102.

[87] Satnoianu, R.A. and Merkin, J.H. and Scott, S.K., *Spatio-temporal structures in a differential flow reactor with cubic autocatalator kinetics*, Phys D: Nonlinear Phenomena, 124 (1998), pp. 345–367.

[88] Satnoianu, Razvan A. and Menzinger, Michael, *Non-Turing stationary patterns in flow-distributed oscillators with general diffusion and flow rates*, Phys. Rev. E, 62 (2000), pp. 113–119.

[89] Schnakenberg, J, *Simple chemical reaction systems with limit cycle behaviour*, Journal of theoretical biology, 81 (1979), pp. 389–400.

[90] Scott, Matthew and Poulin, Francis J. and Tang, Herbert , *Approximating intrinsic noise in continuous multispecies models*, Proceedings of the Royal Society A: Mathematical, Physical and Engineering Sciences, 467 (2011), pp. 718–737.

[91] Seirin Lee, Sungrim and Gaffney, Eamonn, *Aberrant behaviours of reaction diffusion self-organisation models on growing domains in the presence of gene expression time delays*, Bulletin of mathematical biology, 72 (2010), pp. 2161–79.

[92] Seirin Lee, Sungrim and Gaffney, Eamonn and Baker, Ruth, *The dynamics of Turing patterns for morphogen-regulated growing domains with cellular response delays*, Bulletin of mathematical biology, 73 (2011), pp. 2527–51.

[93] Seirin Lee, Sungrim and Gaffney, Eamonn and Monk, N., *The influence of gene expression time delays on Gierer-Meinhardt pattern formation systems*, Bulletin of Mathematical Biology, 72 (2010), pp. 2139–2160.

[94] Shachak, Moshe and Boeken, Bertrand and Groner, Elli and Kadmon, Ronen and Lubin, Yael and Meron, Ehud and Ne'Eman, Gidi and Perevolotsky, Avi and Shkedy, Yehoshua and Ungar, Eugene David, *Woody species as landscape modulators and their effect on biodiversity patterns*, BioScience, 58 (2008), pp. 209–221.

[95] Sheintuch, Moshe and Smagina, Yelena, *Stabilizing the absolutely or convectively unstable homogeneous solutions of reaction-convection-diffusion systems*, Physical Review E, 70 (2004), p. 026221.

[96] Sherratt, Jonathan A. and Dagbovie, Ayawoa S. and Hilker, Frank M., *A mathematical biologist's guide to absolute and convective instability*, Bull. Math. Bio, 76 (2014), pp. 1–26.

[97] Thomas, D., *Artifical enzyme membranes, transport, memory and oscillatory phenomena, in: Analysis and control of immobilized enzyme systems*, Amsterdam : North-Holland ; New York : American Elsevier, c1976, (1975), pp. 115–150.

[98] C. Tian, Z. Lin, and M. Pedersen, *Instability induced by cross-diffusion in reaction-diffusion systems*, Nonlinear Analysis: Real World Applications, 11 (2010), pp. 1036–1045.

[99] Tompkins, Nathan and Li, Ning and Girabawe, Camille and Heymann, Michael and Ermentrout, G. Bard and Epstein, Irving R. and Fraden, Seth, *Testing Turing's theory of morphogenesis in chemical cells*, PNAS, 111 (2014), pp. 4397–4402.

[100] Tso, Wung-Wai and Adler, Julius, *Negative chemotaxis in escherichia coli*, Journal of Bacteriology, 118 (1974), pp. 560–576.

[101] Turing, Alan Mathison, *The chemical basis of morphogenesis*, Philosophical Transactions of the Royal Society of London B: Biological Sciences, 237 (1952), pp. 37–72.

[102] Van Kampen, N.G., *Stochastic Processes in Physics and Chemistry*, North-Holland Personal Library, Elsevier Science, 2011.

[103] Vanag, Vladimir and Epstein, Irving, *Cross-diffusion and pattern formation in reaction–diffusion systems*, Physical chemistry chemical physics : PCCP, 11 (2009), pp. 897–912.

[104] Václav Klika, *Significance of non-normality-induced patterns: Transient growth versus asymptotic stability*, Chaos: An Interdisciplinary Journal of Nonlinear Science, 27 (2017), p. 073120.

[105] Väth, Martin, *Global solution branches and a topological implicit function theorem*, Annali di Matematica Pura ed Applicata, 186 (2007), pp. 199–227.

[106] Ward, Michael J and McInerney, Darragh and Houston, Paul and Gavaghan, David and Maini, Philip, *The dynamics and pinning of a spike for a reaction-diffusion system*, SIAM Journal on Applied Mathematics, 62 (2002), pp. 1297–1328.

[107] Wei, Juncheng and Winter, Matthias, *Spikes for the Gierer–Meinhardt system with discontinuous diffusion coefficients*, Journal of Nonlinear Science, 19 (2009), pp. 301–339.

[108] Werner, Steffen and Stückemann, Tom and Beirán Amigo, Manuel and Rink, Jochen C. and Jülicher, Frank and Friedrich, Benjamin M., *Scaling and regeneration of self-organized patterns*, Phys. Rev. Lett., 114 (2015), p. 138101.

[109] Wolpert, L, *Positional infromation and the spatial pattern of cellular differentiation*, J. Theoret. Biol, 25 (1969), pp. 1–47.

[110] Woolley, Thomas and Baker, Ruth and Gaffney, Eamonn and Maini, Philip, *Stochastic reaction and diffusion on growing domains: Understanding the breakdown of robust pattern formation*, Physical review. E, Statistical, nonlinear, and soft matter physics, 84 (2011), p. 046216.

[111] Woolley, Thomas and Baker, Ruth and Maini, Philip, *Turing's theory of morphogenesis: Where we started, where we are and where we want to go*, Springer, 05 2017, pp. 219–235.

[112] Woolley, Thomas E. and Baker, Ruth E. and Gaffney, Eamonn A. and Maini, Philip K., *Influence of stochastic domain growth on pattern nucleation for diffusive systems with internal noise*, Phys. Rev. E, 84 (2011), p. 041905.

[113] Woolley, Thomas E. and Baker, Ruth E. and Gaffney, Eamonn A. and Maini, Philip K., *Power spectra methods for a stochastic description of diffusion on deterministically growing domains*, Phys. Rev. E, 84 (2011), p. 021915.

[114] Woolley, Thomas E. and Baker, Ruth E. and Gaffney, Eamonn A. and Maini, Philip K. and Seirin-Lee, Sungrim, *Effects of intrinsic stochasticity on delayed reaction-diffusion patterning systems*, Phys. Rev. E, 85 (2012), p. 051914.

[115] Y. Hori and S. Hara, *Noise-induced spatial pattern formation in stochastic reaction-diffusion systems*, in 2012 IEEE 51st IEEE Conference on Decision and Control (CDC), 2012, pp. 1053–1058.

[116] Yi, Fengqi and Gaffney, Eamonn and Seirin Lee, Sungrim, *The bifurcation analysis of Turing pattern formation induced by delay and diffusion in the Schnakenberg system*, Discrete and Continuous Dynamical Systems - Series B, 22 (2017), pp. 647–668.